HEINRICH HEINE
UNIVERSITÄT DÜSSELDORF

The role of the metalloprotease ADAMTS4 in Aβ peptide generation and Alzheimer's disease

Inaugural-Dissertation

zur Erlangung des Doktorgrades
der Mathematisch-Naturwissenschaftlichen Fakultät
der Heinrich-Heine-Universität Düsseldorf

vorgelegt von

Susanne Walter
aus Offenbach

Düsseldorf, September 2017

aus dem Institut für Neuropathologie

der Heinrich-Heine-Universität Düsseldorf

Gedruckt mit der Genehmigung der
Mathematisch-Naturwissenschaftlichen Fakultät der

Heinrich-Heine-Universität Düsseldorf

Berichterstatter:

1. Prof. Dr. Sascha Weggen

2. Prof. Dr. Lutz Schmitt

Tag der mündlichen Prüfung:

Ich versichere an Eides Statt, dass die vorgelegte Dissertation

The role of the metalloprotease ADAMTS4 in Aβ peptide generation and Alzheimer's disease

von mir selbständig und ohne unzulässige fremde Hilfe unter Beachtung der „Grundsätze zur Sicherung guter wissenschaftlicher Praxis an der Heinrich-Heine-Universität Düsseldorf" erstellt worden ist.

Des Weiteren versichere ich, dass die Dissertation zuvor keiner anderen Universität oder Fakultät vorgelegt wurde und ich bislang keinerlei andere Promotionsversuche getätigt habe.

Düsseldorf, den 15.09.2017

_____	_____
Ort, Datum	Susanne Walter

Contents

Summary

Alzheimer's disease (AD) is the most common neurodegenerative disorder responsible for 60 - 80% of all dementia cases. The disease process starts with the accumulation of amyloid-β (Aβ) peptides in the brain, which form neurotoxic protein aggregates and trigger synaptic and neuronal loss. Aβ peptides (e.g., Aβ1-40 and Aβ1-42) are generated through sequential cleavage of the amyloid precursor protein (APP) by the proteases β- and γ-secretase. However, earlier studies had shown that the majority of insoluble Aβ peptides are truncated at the N-terminus with Aβ4-x peptides as the most abundant species. These N-truncated Aβ peptides could have an important role in the pathogenesis of AD, but their origins are unknown. We found that the Aβ peptide sequence contains putative cleavage sites for the secreted metalloprotease ADAMTS4 (a disintegrin and metalloprotease with thrombospondin motifs 4), and the central objective of this thesis was to determine the effects of ADAMTS4 on APP processing and Aβ generation *in vitro* and *in vivo*. Inducible overexpression of ADAMTS4 in HEK293 cells resulted in the secretion of Aβ4-40 but unchanged Aβ1-x peptide levels as measured by mass spectrometry and ELISA. Co-immunoprecipitation studies provided evidence that APP and ADAMTS4 might interact in the early secretory pathway, and ADAMTS4 overexpression reduced mature APP levels and secretion of the soluble APP ectodomain APPs. Aβ4-x production was not dependent on prior cleavage of APP by β-secretase, and purified ADAMTS4 was able to convert Aβ1-40 into Aβ4-40, indicating that Aβ4-x peptides might be generated both within the cell and in the extracellular space. For *in vivo* analysis, ADAMTS4$^{-/-}$ knockout mice were crossed to the 5xFAD model of AD. Aβ4-40 levels were reduced by 50% and APPs levels were increased by 30% in the brains of 12-month-old 5xFAD / ADAMTS4$^{-/-}$ mice, confirming core findings of the *in vitro* studies. Surprisingly, in the adult murine brain ADAMTS4 was exclusively expressed in cells of the oligodendrocyte lineage. Cultured oligodendrocytes secreted a variety of Aβ species but Aβ4-40 peptides were absent in oligodendrocytes prepared from ADAMTS4$^{-/-}$ knockout mice, proving that ADAMTS4 is essential for Aβ4-x generation in this cell type. Finally, white matter structures in 5xFAD mice showed punctate deposits of Aβ4-x peptides, which were reduced in 5xFAD / ADAMTS4$^{-/-}$ mice. Taken together, the studies conducted in this thesis project established that N-truncated Aβ4-x peptides can be generated by the metalloprotease ADAMTS4. Importantly, they implicate oligodendrocytes as a novel pro-amyloidogenic effector in the pathogenesis of AD.

Zusammenfassung

Die Alzheimer-Krankheit ist eine neurodegenerative Erkrankung und die häufigste Form der Demenz. Der Krankheitsverlauf beginnt mit der Anhäufung von Amyloid-β (Aβ) Peptiden im Gehirn, welche neurotoxische Proteinaggregate bilden und den Verlust von Synapsen und Neuronen einleiten. Aβ Peptide werden durch die sequentielle Spaltung des Amyloid Precursor Protein (APP) von den Proteasen β-Sekretase und γ-Sekretase gebildet. Vorherige Studien zeigten, dass die Mehrheit der unlöslichen Aβ Peptide am N-Terminus trunkiert sind und Aβ4-x dabei die vorwiegende Spezies ist. Aβ4-x Peptide spielen eine wichtige Rolle in der Pathogenese der Alzheimer-Krankheit, ihre Herkunft ist jedoch unbekannt. Die Aβ-Sequenz enthält potentielle Schnittstellen der sekretierten Metalloprotease ADAMTS4 (a disintegrin and metalloprotease with thrombospondin motifs 4) und die zentrale Zielsetzung dieser Dissertation war es, die Effekte von ADAMTS4 auf die APP-Prozessierung und die Aβ-Produktion *in vitro* und *in vivo* zu ermitteln. Induzierbare Überexpression von ADAMTS4 in HEK293 Zellen führte zur Sekretion von Aβ4-40, beeinflusste aber nicht den Aβ1-x Spiegel. Zudem reduzierte ADAMTS4 die Levels des reifen APP und die Sekretion der löslichen APPs Ektodomäne. Co-Immunopräzipitation zeigte, dass APP und ADAMTS4 im frühen sekretorischen Weg interagieren könnten. Die Aβ4-x Produktion war unabhängig von der vorherigen APP-Spaltung durch die β-Sekretase und ADAMTS4 konnte zudem Aβ1-40 in Aβ4-40 verwandeln, was zeigt, dass Aβ4-x Peptide sowohl in der Zelle als auch im extrazellulären Raum hergestellt werden könnten. Für *in vivo* Versuche wurden ADAMTS4$^{-/-}$ Knockout-Mäuse mit dem 5xFAD Mausmodell gekreuzt. In Gehirnen von 12 Monate alten 5xFAD / ADAMTS4$^{-/-}$ Mäusen war Aβ4-40 um 50% reduziert und die APPs Levels waren um 30% erhöht, welches die Haupterkenntnisse der *in vitro* Studien bestätigte. Überraschenderweise war ADAMTS4 im adulten Mäusehirn ausschließlich in Oligodendrozyten exprimiert. Primäre Oligodendrozyten sekretierten eine Vielfalt an Aβ-Spezies, jedoch produzierten Oligodendrozyten von ADAMTS4$^{-/-}$ Knockout-Mäusen keine Aβ4-40 Peptide, welches beweist, dass ADAMTS4 essentiell für die Aβ4-x Produktion in diesem Zelltyp ist. Schließlich zeigte die weiße Substanz in Gehirnen von 5xFAD Mäusen punktförmige Ablagerungen von Aβ4-x Peptiden, welche in 5xFAD / ADAMTS4$^{-/-}$ Mäusen reduziert waren. Zusammengefasst zeigten die Untersuchungen dieser Dissertation, dass N-trunkierte Aβ Peptide durch die Metalloprotease ADAMTS4 produziert werden können und deuten darauf hin, dass Oligodendrozyten ein neuer pro-amyloidogener Faktor in der Pathogenese der Alzheimer-Krankheit sein könnten.

Abbreviations

°C	Degree Celsius
AA	Amino Acid
ACE	Angiotensin-Converting Enzyme
ACH	Amyloid Cascade Hypothesis
AD	Alzheimer's Disease
ADAM	A Disintegrin And Metalloprotease
ADAMTS	A Disintegrin and Metalloproteinase with Thrombospondin motifs
AEP	Asparagine Endopeptidase
AICD	APP Intracellular Domain
ALS	Amyotrophic Lateral Sclerosis
APOE	Apolipoprotein E
APP	Amyloid Precursor Protein
APPs	soluble APP
APS	Ammonium persulfate
ARF-1	Adenosyl Ribosylation Factor-1
Aβ	Amyloid-β
BACE1	β-site APP-cleaving Enzyme 1
BCA	Bicinchoninic Acid
BSA	Bovine Serum Albumin
cDNA	complementary DNA
CNPase	Cyclic Nucleotide Phosphodiesterase
CNS	Central Nervous System
CSF	Cerebrospinal Fluid
CTF	C-terminal Fragment
d	day
DAPI	4',6-diamidino-2-phenylindole
ddH_2O	double-distilled water
DMEM	Dulbecco's Modified Eagle's Medium

DMSO	Dimethyl Sulfoxide
DNA	Deoxyribonucleic Acid
DOX	Doxycycline
DTT	Dithiothreitol
ECM	Extracellular Matrix
E. coli	*Escherichia coli*
EDTA	Ethylenediaminetetraacetic Acid
ELISA	Enzyme-linked Immunosorbent Assay
ER	Endoplasmic Reticulum
et al.	and others
FA	Formic Acid
FAD	Familial AD
FCS	Fetal Calf Serum
FGF	Fibroblast Growth Factor
g	gram
GAPDH	Glyceraldehyde 3-phosphate Dehydrogenase
GFAP	Glial Fibrillary Acidic Protein
h	hour
HRP	Horseradish Peroxidase
i.e.	that is
Iba1	Ionized calcium-binding adapter molecule 1
IgG	Immunoglobulin G
IP	Immunoprecipitation
kDa	kilodalton
l	liter
LB	Lysogeny Broth
LRP1	Low-density lipoprotein Receptor-related Protein 1
LTP	Long-term Potentiation
m	meter
M	molar

mA	milliampere
mAb	monoclonal Antibody
MBP	Myelin Basic Protein
MES	2-(N-morpholino)ethanesulfonic acid
min	minute
MMP	Matrix Metalloprotease
MRI	Magnetic Resonance Imaging
mRNA	messenger RNA
MS	Multiple Sclerosis
MT5-MMP	Membrane-type 5 MMP
MW	Molecular Weight
NBB	Netherlands Brain Bank
NDC	Non-demented Control
NP-40	Nonidet P-40
Ntg	No-transgene
OA	Osteoarthritis
OPC	Oligodendrocyte Progenitor Cell
P	Postnatal day
pAb	polyclonal Antibody
PBS	Phosphate Buffered Saline
PCR	Polymerase Chain Reaction
PDGF	Platelet-derived Growth Factor
PET	Positron Emission Tomography
PFA	Paraformaldehyde
PG	Proteoglycan
pGlu-Aβ	Pyroglutamated Aβ
PI	Protease Inhibitor
PNN	Perineuronal Net
PSEN	Presenilin
PVDF	Polyvinylidene difluoride

qPCR	quantitative real-time PCR
RA	Rheumatoid Arthritis
RNA	Ribonucleic Acid
rpm	revolutions per minute
RT	Room Temperature
rtTA3	reverse tetracycline-controlled Transactivator 3
s	second
SAD	Sporadic AD
sAPP	soluble APP
SCI	Spinal Cord Injury
SD	Standard Deviation
SDS	Sodium Dodecyl Sulfate
SDS-PAGE	SDS-Polyacrylamide Gel Electrophoresis
sw	Swedish mutation
T3	Triiodo-L-Thyronine
T4	L-Thyroxine
TAE	TRIS-Acetic acid-EDTA
TBS	TRIS Buffered Saline
TEMED	Tetramethylethylenediamine
Thy-1	Thymocyte differentiation antigen-1
TRIS	Tris(hydroxymethyl)aminomethane
TSR	Thrombospondin type 1 Sequence Repeat
UV	Ultraviolet
V	Volt
v/v	volume/volume
w/v	weight/volume
wt	wild type
x g	times gravity
β-gal	β-galactosidase

Amino acids

A	Ala	Alanine
C	Cys	Cysteine
D	Asp	Aspartic acid
E	Glu	Glutamic acid
F	Phe	Phenylalanine
G	Gly	Glycine
I	Ile	Isoleucine
K	Lys	Lysine
L	Leu	Leucine
M	Met	Methionine
N	Asn	Asparagine
P	Pro	Proline
Q	Gln	Glutamine
R	Arg	Arginine
S	Ser	Serine
T	Thr	Threonine
V	Val	Valine
W	Trp	Tryptophan
Y	Tyr	Tyrosine

1. Introduction

1.1 Alzheimer's disease

1.1.1 Alzheimer's disease pathology and clinical features

Alzheimer's disease (AD) is a neurodegenerative disorder of the central nervous system (CNS) and the most common cause of dementia (McKhann *et al.* 2011). It was first described by Alois Alzheimer and is defined by its neuropathological hallmarks of extracellular amyloid plaques and intracellular neurofibrillary tangles (Alzheimer 1907, Schellenberg & Montine 2012) [Figure 1]. The extracellular plaques are formed by aggregates of amyloid-β (Aβ) peptides and the neurofibrillary tangles are composed of hyperphosphorylated tau, a microtubule-associated protein (Glenner & Wong 1984, Grundke-Iqbal *et al.* 1986). These histopathological features are accompanied by synaptic loss and neuronal degeneration, which results in cerebral atrophy in the hippocampus and cortical areas (Fox *et al.* 1996, Rossor *et al.* 1996, Mattson 2004).

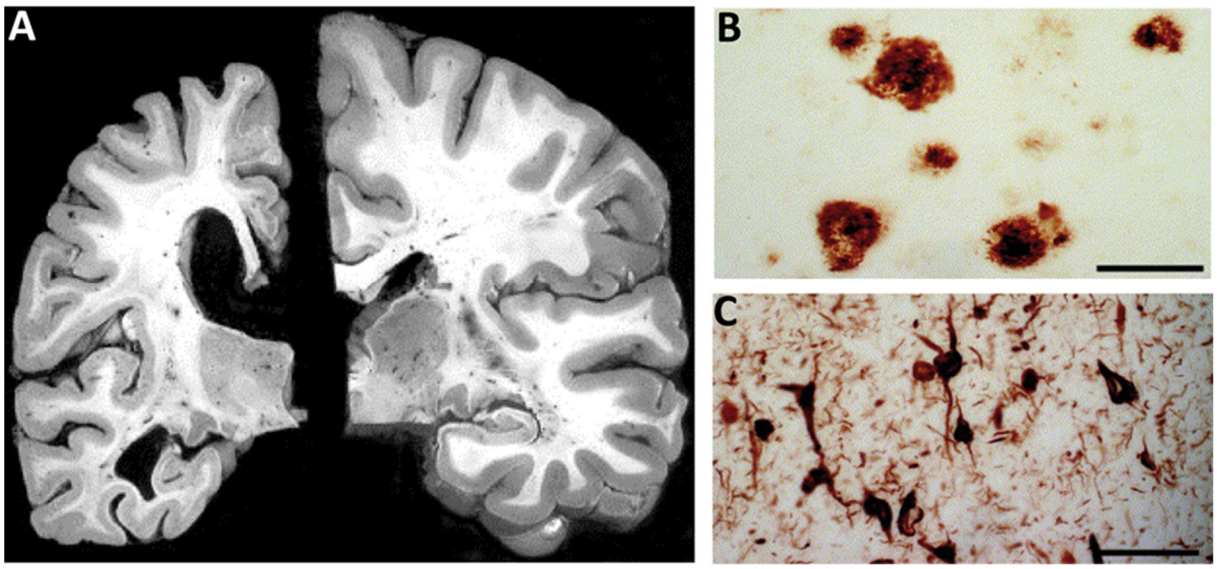

Figure 1: Neuropathological hallmarks of AD. (**A**) Comparison of coronal slices of the hemi-brains from a 70-year-old AD patient (left slice) and a healthy age-matched individual (right slice). The AD brain shows gross brain atrophy, enlarged ventricles, narrowed gyri, hippocampal atrophy, and white matter reduction (adopted from (Cairns 2009). (**B**) Immunostained extracellular amyloid plaques. Scale bar 125 µm. (**C**) Immunostained intracellular neurofibrillary tangles. Scale bar 62.5 µm. (figures B and C were modified after (LaFerla & Oddo 2005)).

The clinical manifestations of AD include symptoms of memory impairment and cognitive dysfunction, such as language, visual, and motor deficits. Additionally, patients present with confusion, impaired judgement, apathy, and depression (Barnes *et al.* 2015). A definite AD diagnosis is only possible by postmortem neuropathological analysis of brain sections, but living patients with symptoms of AD can be diagnosed based upon neuropsychological testing as well as AD biomarkers in the cerebrospinal fluid (CSF) and pathological results in magnetic resonance imaging (MRI) and positron emission tomography (PET) imaging (Dubois *et al.* 2007). Biomarkers and brain imaging techniques are also used to detect brain alterations in presymptomatic individuals since AD pathology is believed to develop over decades in the absence of any symptoms owing to the compensatory capacity of the brain (Villemagne *et al.* 2011). AD cases can be divided into two groups based on their age of onset and their genetic predispositions. Importantly, both forms are nearly indistinguishable in brain pathology and clinical manifestations (Hampel *et al.* 2015). The predominant late-onset and sporadic form of AD (SAD) usually starts after 65 years of age and involves complex but weak genetic influences (Corder *et al.* 1993, Bettens *et al.* 2013). In contrast, early-onset forms of AD usually occur between 30 and 60 years of age and are mostly inherited in an autosomal-dominant fashion. In these patients, mutations in AD relevant genes have been found and this form is referred to as familial AD (FAD). Carriers of these mutations have a 95% risk to develop AD during their lifetime but FAD only accounts for less than 1% of all AD cases (Goate *et al.* 1991, Schellenberg *et al.* 1992, Ballard *et al.* 2011, Bateman *et al.* 2011, Loy *et al.* 2014). So far, no treatments to prevent or cure the symptoms of AD are available. Currently available symptomatic treatments consist mostly of cholinesterase inhibitors to counter the loss of cholinergic neurons, but they only stabilize cognitive abilities for a limited time span and lose their effectiveness when the disease progresses (Hampel et al. 2015).

1.1.2 The amyloid cascade hypothesis

The amyloid cascade hypothesis (ACH) posits that the accumulation and aggregation of Aβ peptides in the brain is the critical step in initiating and propagating AD pathology. Subsequently, this triggers secondary events like neurofibrillary tangle formation, synapse and neuron loss, gross brain atrophy, neuroinflammation, vascular damage, and ultimately

symptoms of dementia (Beyreuther & Masters 1991, Selkoe 1991, Hardy & Higgins 1992) [Figure 2].

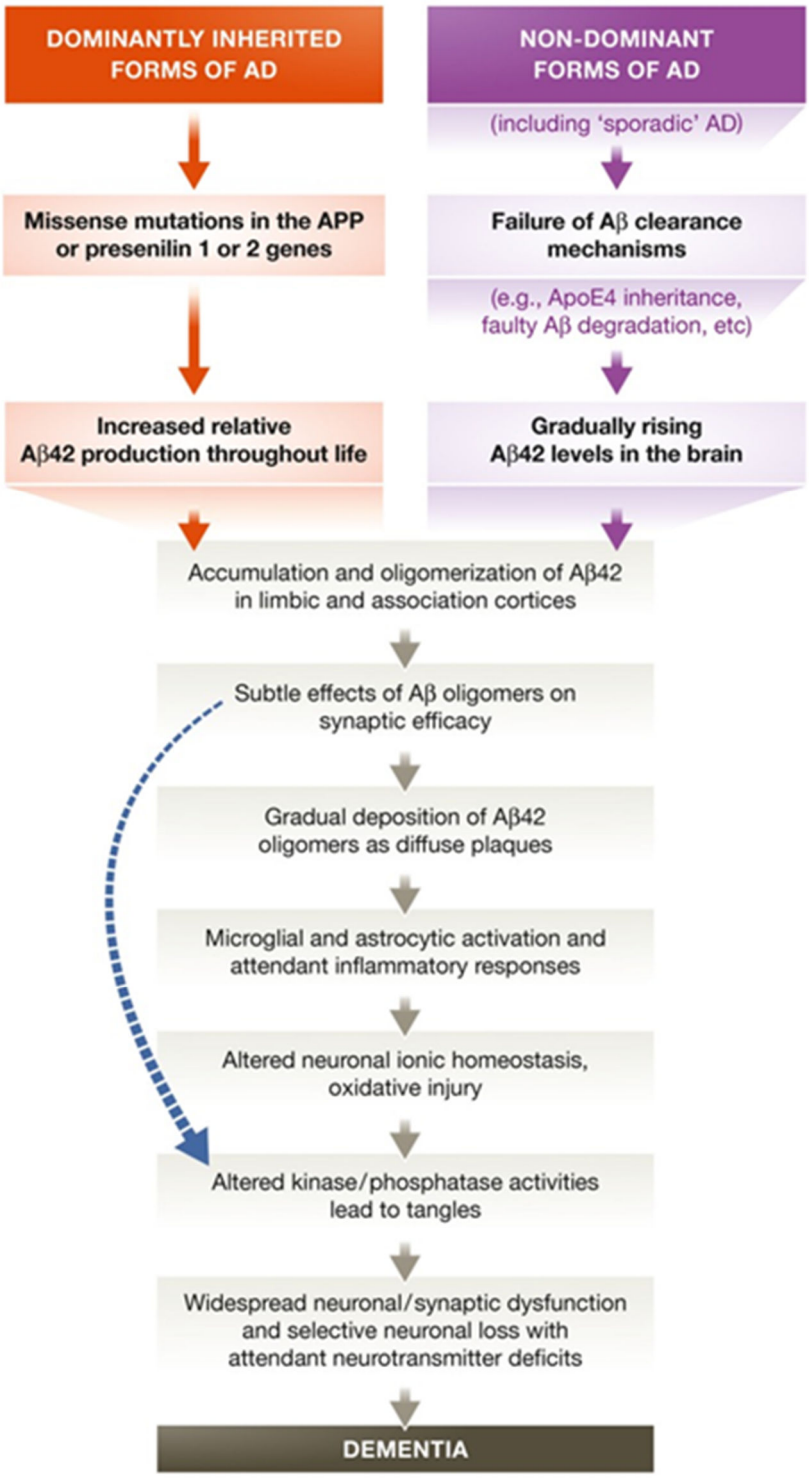

Figure 2: The amyloid cascade hypothesis. The sequence of major pathogenic events leading to AD according to the ACH. Aβ oligomers may directly affect synaptic integrity and cause neuronal loss (curved blue arrow). In addition, Aβ aggregates cause inflammation by activating microglia and astrocytes and promote the formation of neurofibrillary tangles as secondary events (adopted from (Selkoe & Hardy 2016)).

Initially, Aβ peptides were purified and sequenced from amyloid plaques in the brains of AD patients, which led to the identification of the amyloid precursor protein (APP) from which Aβ is released by sequential proteolytic cleavage of the β-secretase and the γ-secretase (Glenner & Wong 1984, Masters *et al.* 1985, Kang *et al.* 1987, De Strooper *et al.* 1998, Sinha & Lieberburg 1999, Vassar *et al.* 1999). The γ-secretase is a complex of four proteins, presenilin 1 or 2 (PSEN1 or PSEN2), anterior pharynx-defective 1 (APH-1), presenilin enhancer 2 (PEN2), and nicastrin (Wolfe *et al.* 1999, De Strooper 2003). Early support for the ACH was provided by the identification of a mutation in the APP gene that led to FAD with identical pathology to the sporadic form of AD (Goate et al. 1991). By now, over 300 mutations that cause FAD have been found and they are all located in three genes involved in Aβ production, namely APP, PSEN1, and PSEN2, which emphasizes the importance of Aβ in the pathology of AD (Levy-Lahad *et al.* 1995, Sherrington *et al.* 1995, Karran *et al.* 2011). These mutations either increase the amount of total Aβ production or shift the production to longer forms of Aβ with higher propensity for aggregation (Citron *et al.* 1992, Jarrett *et al.* 1993, Suzuki *et al.* 1994, Borchelt *et al.* 1996, Duff *et al.* 1996, Scheuner *et al.* 1996). Interestingly, mutations in tau cause frontotemporal dementia and do not lead to AD, which argues that tau aggregation is a secondary event in AD pathology (Goedert & Jakes 2005). Furthermore, patients with Down's syndrome (Trisomy 21) develop the same Aβ deposits as AD patients, which is due to three copies of the APP gene located on chromosome 21 and which causes lifelong overproduction of Aβ (Wisniewski *et al.* 1985). The only strong genetic risk factor for SAD that also lowers the age of onset is the APOE gene. APOE occurs in three alleles, APOE2, APOE3, and APOE4 and is involved in the transport and metabolism of cholesterol and triglycerides (Mahley & Rall 2000, Nickerson *et al.* 2000). Carriers of the ε4 allele have an increased risk to develop AD, four-fold in heterozygous carriers and up to 12-fold with two copies of ε4 when compared to the other APOE genotypes. APOE2 is associated with the lowest risk for developing AD but is also the least common isoform (Verghese *et al.* 2011). APOE binds Aβ, which affects its clearance, and the ε4 allele slows down its transport out of the brain causing toxic Aβ accumulation and aggregation (Deane *et al.* 2008, Castellano *et al.* 2011). Additionally, more than 20 other genetic risk factors for SAD have been identified in recent years, which have only weak effects and are involved in cholesterol metabolism, inflammation, and the microglial immune response (Jones *et al.* 2010).

1.1.3 APP processing and functional APP metabolites

APP is a type-1 transmembrane glycoprotein and part of a family with two other homologs, APP-like protein 1 and 2 (APLP1 and APLP2). However, only APP has the Aβ sequence, which can give rise to AD (Nicolas & Hassan 2014). APP occurs in three alternatively spliced isoforms APP695, APP751, and APP770 (Goate et al. 1991). While APP695 is predominantly expressed in neurons, the other two longer isoforms, which possess a Kunitz protease inhibitor domain, can be found in glial cells and other tissues in the human body (Kitaguchi *et al.* 1988, Ponte *et al.* 1988, De Strooper & Annaert 2000).

APP proteolysis can proceed in two distinct pathways [Figure 3]. The amyloidogenic pathway starts with cleavage of APP within the ectodomain by the β-secretase β-site APP-cleaving enzyme 1 (BACE1), which produces a soluble APPβ (sAPPβ) fragment (Hussain *et al.* 1999). The C-terminal membrane-bound fragment CTFβ (C99) is subsequently cleaved by the γ-secretase multiprotein complex, which releases Aβ peptides into the extracellular space and the APP intracellular domain (AICD) into the cytosol (Lichtenthaler *et al.* 2011). The γ-secretase initially cleaves APP close to the cytosolic border of its transmembrane domain and then trims this long Aβ fragment multiple times to produce Aβ peptides with progressively shorter C-termini (Takami *et al.* 2009). The non-amyloidogenic pathway is initiated by cleavage of APP within the Aβ domain from the α-secretase ADAM10 (a disintegrin and metalloprotease 10) to release sAPPα, which precludes the generation of Aβ (Sisodia 1992, Lammich *et al.* 1999). The remaining CTFα (C83) fragment is also further processed by the γ-secretase complex to generate the smaller, non-pathogenic peptide p3 and the AICD (Lichtenthaler et al. 2011).

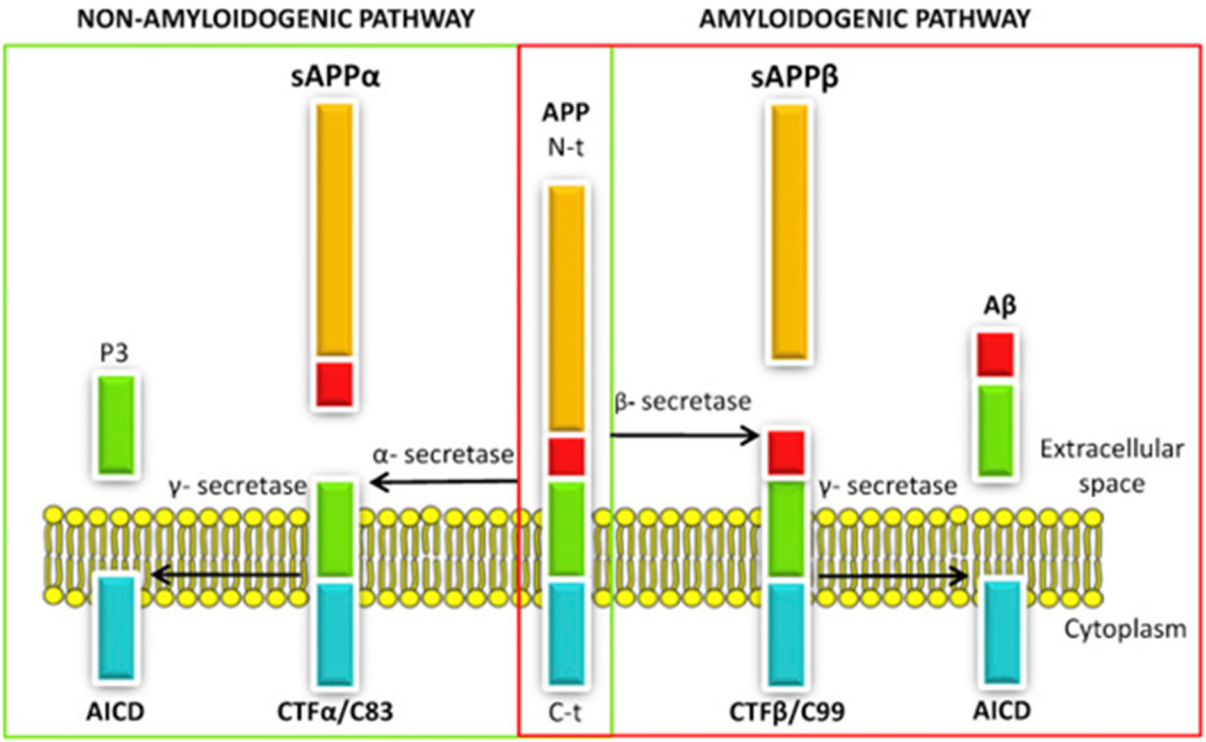

Figure 3: APP processing. APP proteolysis can occur in two different pathways. In the non-amyloidogenic pathway that prevents the toxic Aβ production (left), APP is cleaved by the α-secretase ADAM10, which releases the sAPPα ectodomain and generates a membrane-bound CTFα/C83 fragment. C83 is subsequently cleaved by the γ-secretase complex into a p3 and AICD fragment. In the amyloidogenic pathway (right), β-secretase cleavage of APP by BACE1 generates sAPPβ and CTFβ/C99, which is further processed by the γ-secretase to produce Aβ peptides of varying length at the C-terminus and the AICD fragment (adopted from (Montoliu-Gaya & Villegas 2015)).

During its transport through the secretory pathway, APP undergoes various post-translational modifications including N- and O-glycosylation, sulfation, and phosphorylation (Weidemann *et al.* 1989, Walter *et al.* 1997). The β-secretase is mainly active in endocytic compartments whereas cleavage by α-secretase takes place at the cell surface (Capell *et al.* 2002). APP is believed to be important for neuronal development and homeostasis through its involvement in establishing functional synapses (Nicolas & Hassan 2014). Various other physiological functions of APP have been proposed including regulation of gene transcription, receptor function, and cell-cell interactions (Hoefgen *et al.* 2015). APP metabolites generated by both pathways might also have important functions in the brain. The soluble fragment sAPPα seems to have neuroprotective properties and was shown to increase long-term potentiation (LTP) and to stimulate neurite outgrowth, whereas sAPPβ might be involved in axonal sprouting and

was shown to induce neuronal differentiation of human embryonic stem cells (Chasseigneaux & Allinquant 2012, Nhan *et al.* 2015). The AICD released by both pathways might be important for gene regulation. It was shown to control the expression of APP itself and of other genes involved in APP metabolism such as the low-density lipoprotein receptor-related protein 1 (LRP1) and neprilysin (Belyaev *et al.* 2010, Beckett *et al.* 2012).

1.1.4 Properties of Aβ peptides and pathological mechanisms

Aβ peptides are produced by most cell types throughout life in healthy individuals, and some studies point to a physiological function in neurite outgrowth, learning, and cell survival (Haass *et al.* 1992, Koo *et al.* 1993, Abramov *et al.* 2009, Morley & Farr 2014). Aβ might only become neurotoxic through a conformational shift of its structure and subsequent aberrant accumulation and aggregation (Walsh & Teplow 2012). Aβ peptides spontaneously aggregate into soluble oligomers and can further deposit into fibrils and eventually form insoluble plaques. Aβ aggregates have been shown to induce inflammation, oxidative stress, and altered kinase/phosphatase activity, which might initiate tau hyperphosphorylation and subsequent neuronal death (Musiek & Holtzman 2015). The main neurotoxic form seems to be the soluble oligomers, while insoluble fibrils and plaques might serve as a source and reservoir for Aβ oligomers (Knowles *et al.* 2014). Amyloid oligomers appear to interact with various membrane receptors, such as glutamate receptors and the cellular prion protein, and were shown to inhibit LTP and reduce dendritic spine density (Walsh *et al.* 2002, Zhao *et al.* 2008, Lauren *et al.* 2009, Ferreira & Klein 2011, Benilova & De Strooper 2013). They were able to disrupt synaptic plasticity and to impair learning and memory when injected into the brain of animal models (Walsh et al. 2002, Cleary *et al.* 2005). Aβ oligomers accumulated in AD brains and were specifically found in association with excitatory synapses near Aβ plaques (Lacor *et al.* 2004, Spires *et al.* 2005). They were also reported to impair neuronal insulin signaling, which is a neuroprotective signaling pathway and whose chronic inhibition could provide a possible explanation for synapse dysfunction and neuronal cell death (De Felice *et al.* 2009). Several studies have demonstrated that Aβ oligomers can induce hyperphosphorylation of tau *in vitro* and *in vivo* and that Aβ can promote the formation of neurofibrillary tangles *in vivo* (Gotz *et al.* 2001, De Felice *et al.* 2008, Braak *et al.* 2011, Chabrier *et al.* 2012). Furthermore, levels of soluble Aβ correlated better with cognitive deficits than

the actual plaque load, which can be extensive in some asymptomatic patients (Naslund *et al.* 2000, Tomic *et al.* 2009). Aβ aggregates were also shown to act as seeds and to induce pathological conformations of Aβ peptides, which might facilitate the spreading of AD across the brain (Jucker & Walker 2013, Fritschi *et al.* 2014). While γ-secretase generates numerous Aβ peptides ranging from Aβ37 to Aβ43, the most abundant Aβ peptides are Aβ40 and Aβ42. The longer Aβ42 form has two additional hydrophobic residues at the C-terminus which increases its ability to form aggregates and its neurotoxicity (Citron *et al.* 1997, Cacquevel *et al.* 2012, De Strooper & Karran 2016). The more soluble Aβ40 is the predominantly generated form, while the longer, more aggregation-prone Aβ42 peptides accumulate in AD brains and deposit first into the insoluble amyloid plaques (Burdick *et al.* 1992, Gravina *et al.* 1995, Mann *et al.* 1996). The aggregation process is facilitated by increased levels of Aβ42 peptides, either as in many forms of FAD by a higher total production of Aβ42 leading to an elevated ratio of Aβ42 to Aβ40 peptides, or as proposed for SAD by decreased Aβ clearance from the brain (Glabe 2005, Walsh & Selkoe 2007, Mawuenyega *et al.* 2010).

1.1.5 FAD mutations

Autosomal dominant mutations only account for less than 1% of all AD cases. Mutations in APP promote elevated Aβ levels either through increased processing of APP by β-secretase or through altered γ-secretase cleavage and make up around 16% of FAD cases (Hardy 1997). FAD mutations in APP are mostly located in the Aβ sequence and cluster around the β- and γ-secretase cleavage sites [Figure 4]. Located at the C-terminus where γ-secretase processing occurs is the first ever identified mutation V717I (London mutation), and other mutations like V717F (Indiana mutation) and I716V (Florida mutation), which all increase the Aβ42/Aβ40 ratio (Goate et al. 1991, Murrell *et al.* 1991, Suzuki et al. 1994, Scheuner et al. 1996, Hecimovic *et al.* 2004, Weggen & Beher 2012). The double mutation K670N/M671L (Swedish mutation) is located at the β-secretase cleavage site at the N-terminus of the Aβ sequence and leads to an elevated APP processing by BACE1 and therefore increased total Aβ production (Citron et al. 1992, Mullan *et al.* 1992, Weggen & Beher 2012). Importantly, one APP mutation (A673T, Icelandic mutation) has been found to protect against AD by decreasing the production of Aβ peptides through reduced β-secretase cleavage of APP (Jonsson *et al.* 2012, Maloney *et al.* 2014, Martiskainen *et al.* 2017).

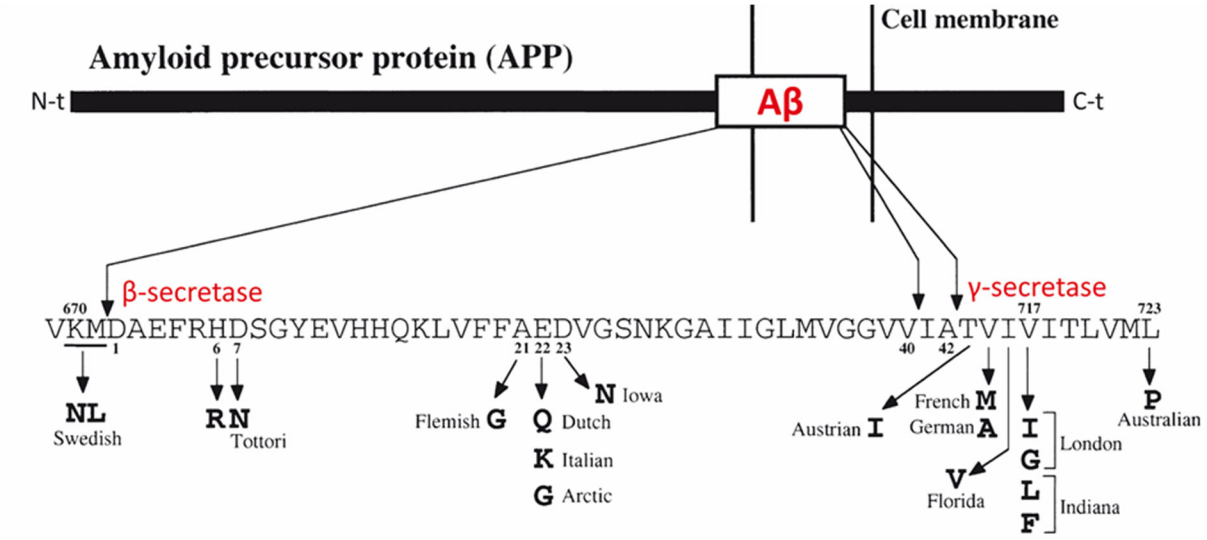

Figure 4: FAD mutations in APP. The AA sequence of Aβ (numbers below) inside the APP sequence (numbers above) and the respective AA changes of FAD mutations (modified after (Irie *et al.* 2005)). Mutations that cause AD are located at the N- or the C-terminus of the Aβ sequence. Additional mutations in APP are located in the middle of the Aβ sequence, for example the Dutch or Arctic mutations. However, these mutations do not cause AD but cerebrovascular amyloid angiopathy (CAA), which is characterized by Aβ deposition in blood vessels causing hemorrhages and strokes (Weggen & Beher 2012).

FAD mutations in the PSEN1 (around 70% of FAD) and PSEN2 genes (less than 5% of FAD) do not cluster around specific protein regions and are scattered across the whole gene sequence (Weggen & Beher 2012). As the APP mutations, the mutations in PSEN are heterozygous. All PSEN mutations affect γ-secretase activity and shift Aβ production towards the longer, more aggregation-prone Aβ42 and Aβ43 species (Hendriks *et al.* 1997, Saito *et al.* 2011, Weggen & Beher 2012).

1.1.6 Murine animal models of AD

Animal models aim to replicate the symptoms, pathological changes, and causes of AD. No single animal model fully reflects the entire complexity of human AD, but they are invaluable tools to study the underlying mechanism(s) of its pathogenesis. Murine models of AD have mostly been engineered to express human transgenes of mutant APP, PSEN, or both to mimic the genetic causes of FAD. These mouse models develop an age-dependent amyloid

pathology, neuroinflammation, and behavioral deficits (Ashe & Zahs 2010, LaFerla & Green 2012). Combined PSEN and APP mutations produce more severe and earlier amyloid plaque deposition than APP transgenes alone (Elder *et al.* 2010). While these APP-transgenic mice are good models to study the amyloid pathology and therapeutic interventions to prevent it, they have severe limitations compared to the human disease. First, APP is rarely overexpressed in FAD, and most AD cases are sporadic without any change in APP expression or mutations in the APP or PSEN genes (Rovelet-Lecrux *et al.* 2006, Robakis 2011). Second, APP-transgenic mice do not show extensive neuronal loss and they do not develop brain atrophy. Third, these models do not develop tau pathology on their own, which is why in some models a human tau transgene was incorporated as well (Ashe & Zahs 2010). Finally, while neuropathological changes are relatively easy to detect and compare between human AD cases and mouse models, recapitulating the complex changes in human higher cognitive functions that occur during AD in animal models is challenging. Changes and deficits in memory and learning, executive functions, fear conditioning, and attention have been detected in AD mouse models. Non-cognitive symptoms are a major feature of AD pathology in humans and can also be seen in some mouse models, i.e. disturbances of locomotor activity, circadian rhythm, and sleep as well as anxiety, aggression, and depression (Webster *et al.* 2014). However, whether these cognitive and behavioral changes represent fully symptomatic AD is controversial (Ashe & Zahs 2010, Jucker 2010). Nevertheless, APP-transgenic models are important to understand certain aspects of AD and are helpful to develop therapeutic strategies (Van Dam & De Deyn 2011).

The 5xFAD mouse model is one widely used AD model and expresses both human APP and PSEN1 transgenes with five FAD mutations under the control of the mouse neuron-specific Thy-1 promoter. The APP transgene contains the APP Swedish double mutation, which leads to increased total Aβ production, and the Florida and London mutations, which shift γ-secretase processing of APP to the longer, more amyloidogenic Aβ42 peptides. In addition, two mutations in PSEN1 (M146L and L286V) affect γ-secretase cleavage and promote Aβ42 production, which ultimately facilitates extensive plaque deposition (Oakley *et al.* 2006). This line was developed to greatly accelerate the onset of AD pathological changes and amyloid plaque development in mice to benefit time and cost effectiveness. 5xFAD mice have very high cerebral Aβ levels and almost exclusively generate Aβ42. Intraneuronal Aβ aggregates are already found at 1.5 months of age, and amyloid accumulation can be seen in 2-month-

old mice, which is followed by reduced expression of synaptic markers (Oakley et al. 2006, Devi & Ohno 2010, Kalinin *et al.* 2012, Wirths & Bayer 2012). This model also develops microgliosis and other signs of neuroinflammation as well as cognitive impairments like learning and memory deficits, and non-cognitive behavioral abnormalities such as motor deficits and reduced anxiety at 4 – 6 months of age (Oakley et al. 2006, Ohno *et al.* 2007). Moderate but significant neuronal loss can be detected at 9 – 12 months (Jawhar *et al.* 2012, Eimer & Vassar 2013, Girard *et al.* 2013, Richard *et al.* 2015). 5xFAD mice do not develop tau aggregation and neurofibrillary tangles. Furthermore, the Aβ42/Aβ40 ratio in 5xFAD mice is much higher than in human AD brains. 5xFAD mice have been used in numerous studies as a preclinical AD model to test the efficacy of novel therapeutic interventions (Hongpaisan *et al.* 2011, Antonios *et al.* 2015).

1.1.7 N-terminal truncation and other Aβ peptide modifications

The most abundant forms of Aβ are peptides with 40 and 42 amino acids (Aβ1-40 and Aβ1-42), but several posttranslational modifications of Aβ that can modify its aggregation behavior and promote fibril formation have been described including N-truncation, oxidation, phosphorylation, nitration, glycosylation, and pyroglutamation (Hou *et al.* 2002, Russo *et al.* 2002, Halim *et al.* 2011, Kumar *et al.* 2011, Kummer *et al.* 2011, Wittnam *et al.* 2012). The exact sequence in which different Aβ species accumulate in the human brain remains unresolved but studies indicate that Aβ1-42, pyroglutamated forms of Aβ (pGlu-Aβ), and other N-terminally truncated species form insoluble aggregates early and are even detectable in the pre-clinical phase of AD (Masters et al. 1985, Iwatsubo *et al.* 1994, Iwatsubo *et al.* 1996, Sergeant *et al.* 2003, Rijal Upadhaya *et al.* 2014). In general, N-terminal deletions enhance aggregation and fibril formation of Aβ peptides due to increased hydrophobicity, which also leads to higher neurotoxicity and could possibly initiate pathological Aβ deposition (Pike *et al.* 1995). pGlu-Aβ peptides are produced through cyclization of the N-terminal glutamate in Aβ3-x and Aβ11-x peptides by the enzyme glutaminyl cyclase. pGlu-Aβ displayed an increased propensity to form oligomeric and fibrillar assemblies that disrupted LTP and showed increased cellular toxicity (Schilling *et al.* 2006, Alexandru *et al.* 2011, Nussbaum *et al.* 2012). Studies have revealed pGlu-Aβ to be a major Aβ species in AD brains (Portelius *et al.* 2015, Thal *et al.* 2015). Aside from pGlu-Aβ3-42, another N-truncated species that appears to be a

major component of amyloid plaques in the human brain is Aβ4-42. More than 30 years ago, it was shown by N-terminal sequencing analysis of Aβ peptides purified from amyloid plaque cores that only around 10% of peptides displayed an intact N-terminus whereas more than 60% started with the phenylalanine residue in position 4 (Masters et al. 1985, Sergeant et al. 2003). Later studies using sequencing and mass spectrometry have generally supported that Aβ1-42, pGlu-Aβ3-42, and Aβ4-42 belong to the Aβ peptide species with the highest prevalence in AD brains (Masters et al. 1985, Miller *et al.* 1993, Sergeant et al. 2003, Portelius *et al.* 2010, Moore *et al.* 2012, Portelius et al. 2015). Aβ4-42 has faster aggregation kinetics than full-length Aβ species, and exposure of primary rat cortical cultures to aggregated Aβ4-x peptides induced neuron loss with the strongest effect for Aβ4-42. Furthermore, transgenic mice overexpressing Aβ4-42 (Tg4-42 line) developed severe neuronal death and memory deficits (Bouter *et al.* 2013). While N-truncated Aβ species appear to be highly abundant in the insoluble fraction of AD brains, they are substantially less abundant in APP transgenic mouse models (Kawarabayashi *et al.* 2001, Kalback *et al.* 2002, Schieb *et al.* 2011). Nevertheless, analysis of 5xFAD mouse brains revealed Aβ4-42 to be the most abundant species among the truncated Aβ forms next to Aβ5-42, pGlu-Aβ3-42, and Aβ3-42 (Wittnam et al. 2012, Antonios *et al.* 2013). These findings suggest that N-terminally truncated forms of Aβ, and in particular Aβ4-x, could be major drivers of AD pathology. However, to experimentally address the pathogenic role of Aβ4-x and other N-terminally truncated Aβ peptides *in vivo* has been difficult as it remains unresolved how these Aβ species are generated.

1.1.8 Other APP cleaving proteases

In addition to the α-, β-, and γ-secretases, several other proteases have been identified that are able to proteolytically process APP. One example is the asparagine endopeptidase (AEP) or δ-secretase, which cleaved APP at two sites in the ectodomain further N-terminal to the BACE1 cleavage site generating two alternative sAPP fragments and one CTF (Zhang *et al.* 2015). The AEP-derived CTFs acted as substrates for subsequent BACE1 proteolysis *in vitro*, and the shorter of the two sAPP fragments was toxic to primary cultured neurons. Knockout of AEP in cultured neurons and in 5xFAD mice reduced Aβ production and amyloid plaque formation (Zhang et al. 2015). Another example is the matrix metalloprotease MT5-MMP that

was identified to contribute to η-secretase cleavage of APP resulting in novel sAPP and CTF forms. η-Secretase cleavage of APP also occurred further N-terminal to the BACE1 cleavage site, and further processing of the resulting CTF (CTFη) by ADAM10 generated a novel APP peptide fragment (Aη-α) that inhibited LTP in hippocampal neurons and neuronal activity *in vivo*. Additionally, reduced plaque deposition and soluble Aβ levels were observed when MT5-MMP was knocked out in 5xFAD mice (Willem *et al.* 2015, Baranger *et al.* 2016). A few proteases that can potentially produce N-terminally truncated Aβ peptides have also been identified [Figure 5]. The best characterized is the zinc metalloprotease meprin β which produces N-truncated Aβ2-x peptides by direct cleavage of APP independent of BACE1. Membrane-bound meprin β dimers cleave APP at the cell surface and thereby compete with ADAM10 for the substrate leading to reduced sAPPα levels. Interestingly, meprin β is also inhibited by ADAM10 since it can shed the ectodomain of meprin β, which inhibits its proteolytic activity. Meprin β cleavage of APP is prevented by mutations in the first amino acids at the N-terminus of the Aβ sequence such as the double Swedish mutation and the AD-protective A673T substitution (Jefferson *et al.* 2011, Bien *et al.* 2012, Jefferson *et al.* 2013, Schonherr *et al.* 2016, Becker-Pauly & Pietrzik 2017). Levels of Aβ2-42 were increased in brains and decreased in the CSF of AD patients (Wiltfang *et al.* 2001, Bibl *et al.* 2012).

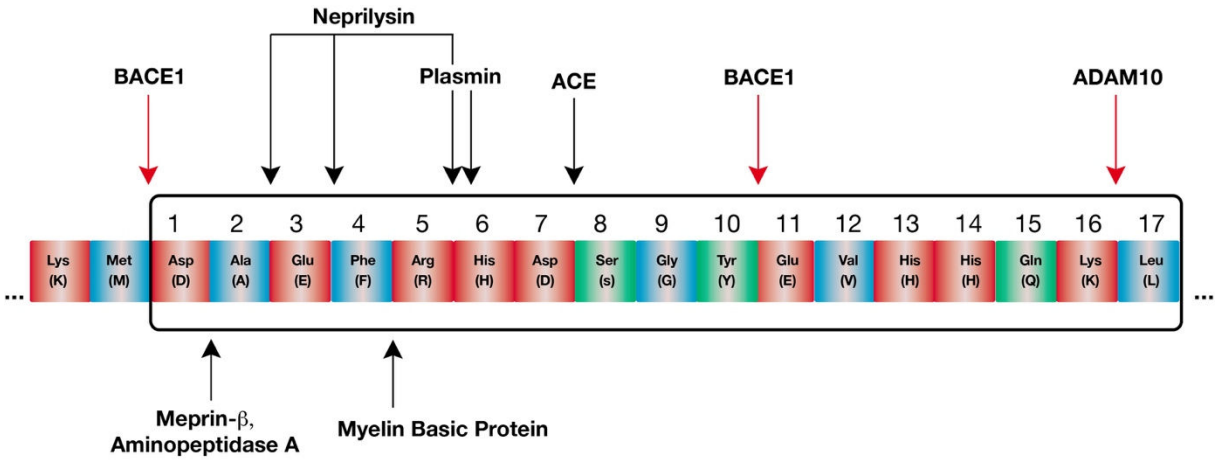

Figure 5: Cleavage sites of BACE1, meprin β, and known Aβ degrading enzymes in the Aβ sequence. The N-terminal 17 AAs of Aβ with charged polar side-chains (red), uncharged polar side-chains (green), and hydrophobic non-polar AA (blue). Cleavage sites are indicated by arrows (modified after (Bayer & Wirths 2014)).

The lysosomal cysteine protease cathepsin B was reported to act as an alternative β-secretase, but with conflicting evidence concerning its effect on Aβ pathology (Hook *et al.* 2008, Sun *et al.* 2008). Cathepsin B cleavage of APP has been proposed to enhance the production of N-truncated pyroglutamylated forms of Aβ (pGlu-Aβ), but evidence for direct cleavage of APP or Aβ by cathepsin B to generate Aβ3-x peptides has not been provided (Citron *et al.* 1995, Vassar et al. 1999, Hook *et al.* 2014). Furthermore, it was suggested that cathepsin B might generate Aβ5-x peptides in cell culture (Takeda *et al.* 2004). Alternatively, N-terminally truncated forms of Aβ could be generated by truncation of pre-existing Aβ1-x peptides by aminopeptidases or known Aβ degrading enzymes, i.e. by myelin basic protein (MBP), angiotensin-converting enzyme (ACE), and neprilysin (Sevalle *et al.* 2009, Saido & Leissring 2012, Andrew *et al.* 2016) [Figure 5]. However, these results are predominantly based on *in vitro* experiments and *in vivo* confirmation that Aβ degrading enzymes are responsible for the production of specific Aβ peptide isoforms is lacking (Bayer & Wirths 2014, Kummer & Heneka 2014).

1.1.9 The role of non-neuronal cells in Aβ generation and degradation

1.1.9.1 Astrocytes and microglia

Neurons have been suggested to be the major source of full-length as well as truncated Aβ peptides in the brain based on high APP and BACE1 expression levels and observations from cell culture models (Selkoe *et al.* 1988, LeBlanc *et al.* 1997, Vassar et al. 1999, Lee *et al.* 2003). However, expression of APP was also found in astrocytes, microglia, and oligodendrocytes (Haass *et al.* 1991, Palacios *et al.* 1992, Skaper *et al.* 2009). Interestingly, astrocytes and microglia produce both full-length Aβ and N-terminally truncated Aβ peptides (Haass et al. 1991, LeBlanc *et al.* 1996, Oberstein *et al.* 2015). Cell culture supernatants of primary human astrocytes and chicken microglia revealed N-truncated Aβ peptides starting at positions 2, 3, 4, and 5 but in the absence of pyroglutamate modifications. In contrast, primary chicken neurons predominantly secreted Aβ1-x and only small quantities of N-terminally modified peptides (Oberstein et al. 2015). Hence, Aβ peptide generation by microglia and astrocytes could have a substantial impact on amyloid levels in the brain and the abundance of specific Aβ species since the total number of glial cells in the human cerebral cortex outnumbers the amount of neurons (Herculano-Houzel 2014).

In addition, microglia cells and astrocytes affect the Aβ pool in the brain through phagocytic uptake and cellular degradation. Aggregated Aβ is a misfolded protein in the extracellular space, which activates innate immune responses by microglia and astrocytes that can act as phagocytic cells to prevent Aβ accumulation (Heneka *et al.* 2014, Meyer-Luehmann & Prinz 2015). Astrocytes were shown to internalize Aβ oligomers, which led to the release of pro-inflammatory cytokines (Nielsen *et al.* 2010, Ledo *et al.* 2013). Similarly, upon activation by insoluble Aβ aggregates, microglia released various cytokines (Lue *et al.* 2001). While pro-inflammatory cytokines were elevated in CSF and brains of AD patients, anti-inflammatory cytokines were decreased (Griffin *et al.* 1989, Cacabelos *et al.* 1991). Activated microglia were found in close association with amyloid plaques and dystrophic neurites in AD brains and AD transgenic mouse models, and microglia were able to phagocytose and degrade Aβ aggregates in culture (Paresce *et al.* 1996, Frautschy *et al.* 1998, Stalder *et al.* 2001). In AD however, the phagocytic activity of microglia and astrocytes might be reduced leading to inefficient clearance of Aβ *in vivo* and progressive amyloid accumulation (Mawuenyega et al. 2010, Krabbe *et al.* 2013, Heneka et al. 2014, Meyer-Luehmann & Prinz 2015). Furthermore, the sustained release of pro-inflammatory factors by activated microglia cells and astrocytes could promote synaptic dysfunction and brain damage (Heneka et al. 2014).

1.1.9.2 Oligodendrocytes

Oligodendrocytes are the largest group of non-neuronal cells in the brain, comprising around 75% of neocortical glial cells, whereas 20% are astrocytes and only 5% are microglia. Oligodendrocytes produce myelin that wraps around axons to facilitate neural transmission and also to provide trophic support for neurons (Funfschilling *et al.* 2012, Tognatta & Miller 2016) [Figure 6]. Oligodendrocytes were also able to produce Aβ peptides. Differentiated rat cortical oligodendrocytes released Aβ40 and Aβ42 into culture supernatants in amounts similar to those found in cultured neurons, and this production was sensitive to β- and γ-secretase inhibitors indicating that they possess both the substrate and the enzymes to generate Aβ peptides. (Skaper et al. 2009). Cell numbers of oligodendrocytes decrease with age just like neurons but those of astrocytes remain constant (Pelvig *et al.* 2008). The reason for this age-dependent decline is unknown but Aβ peptides were cytotoxic to oligodendrocytes and prevented the formation of myelin sheaths (Xu *et al.* 2001, Horiuchi *et*

al. 2012). Age-associated myelin breakdown could be seen in healthy subjects and white matter lesions were observed in AD patients (Brun & Englund 1986, Bartzokis 2011). Injection of Aβ1-42 into rat corpus callosum led to extensive white matter damage and oligodendrocyte death (Jantaratnotai *et al.* 2003). In AD patients as well as in AD transgenic mouse models, oligodendrocyte loss and demyelination occurred in the vicinity of amyloid plaques and associated with dystrophic neurites (Mitew *et al.* 2010). In addition, oligodendrocytes are the major source of iron in the brain and their damage might release it into the environment (Connor *et al.* 1990). Iron was shown to promote formation of Aβ oligomers and might thereby further enhance cytotoxicity (Huang *et al.* 2004, Liu *et al.* 2011). Oligodendrocytes derive from oligodendrocyte progenitor cells (OPCs), which in turn arise from multipotent neural stem cells in the ventricular zone (Miller 1996). Upon migration into the CNS, they differentiate into myelinating oligodendrocytes. However, proliferating OPCs remain in the adult brain and can give rise to oligodendrocytes, astrocytes, and possibly neurons throughout life (Crawford *et al.* 2014, Ettle *et al.* 2015). OPC survival and maturation *in vitro* were also negatively affected by treatment with Aβ1-42 peptides (Desai *et al.* 2010, Horiuchi et al. 2012).

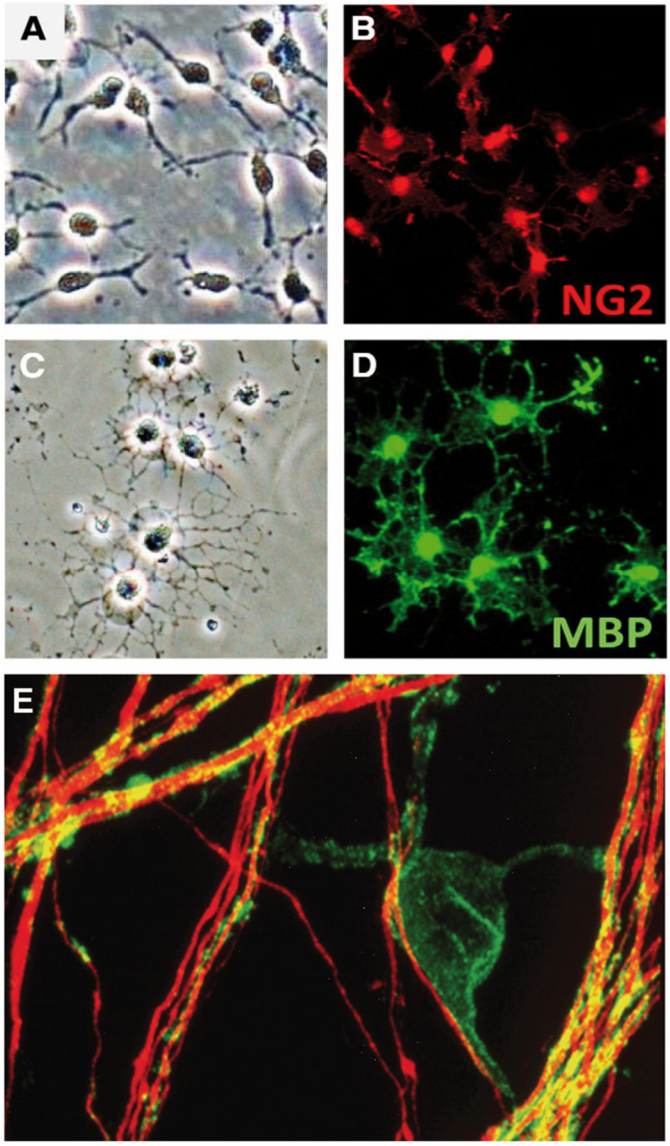

Figure 6: OPCs and mature oligodendrocytes. (**A**) Phase contrast microscopy of OPCs in culture. (**B**) OPCs display expression of neural/glial antigen 2 (NG2) as shown by immunostaining. (**C**) Phase contrast microscopy of mature oligodendrocytes in culture. (**D**) Mature oligodendrocytes express myelin basic protein (MBP) as shown by immunostaining (figures A, B, C, and D were adopted from (Kimoto *et al.* 2011). (**E**) Immunostaining of a mature oligodendrocyte (green) extending processes of myelin sheaths around axons (red) (modified after (Butt *et al.* 1997)).

1.1.10 Current AD therapeutic research

Current research into novel AD treatments is mainly focused on the amyloid pathology (Selkoe & Hardy 2016). Inhibiting β- or γ-secretases with small molecules to prevent Aβ production seems obvious. However, due to their multiple substrates, inhibition of these enzyme has the potential to cause severe side effects. While β-secretases inhibitors appear reasonably safe

and have reached late stages of clinical development, the development of γ-secretases inhibitors has been suspended (De Strooper & Chavez Gutierrez 2015, Barao *et al.* 2016). γ-Secretase modulators that shift Aβ production from Aβ42 to shorter, less neurotoxic forms but do not reduce the overall proteolytic activity of γ-secretase could be a better option but are still in early stages of clinical development (Bursavich *et al.* 2016). Active and passive immunotherapies to lower Aβ levels and remove insoluble amyloid deposits have taken the lead in the clinical development. However, several anti-Aβ antibodies have already failed in Phase 3 clinical trials (Sacks *et al.* 2017). Currently, the most promising drug candidate is aducanumab, a human monoclonal antibody that binds specifically to aggregated forms of Aβ such as amyloid plaques and oligomers but not to soluble monomers. Treatment of mild AD cases in a Phase 1b clinical trial resulted in a dose-dependent decrease in amyloid pathology as detected by amyloid imaging in living patients. Exploratory analysis further suggested less decline in cognitive and global functioning in the treated patients. A Phase 3 clinical trial is currently underway (Sevigny *et al.* 2016).

1.2 The metalloprotease ADAMTS4

1.2.1 The ADAMTS family and the extracellular matrix (ECM)

The *A Disintegrin and Metalloproteinase with Thrombospondin motifs* (ADAMTS) family includes 19 members of secreted, extracellular enzymes with a distinct domain organization (Apte 2009, Tortorella *et al.* 2009, Kelwick *et al.* 2015) [Figure 7]. The proteinase domain at the N-terminus is composed of a signal peptide followed by a pro-domain of variable length, a zinc-binding metalloproteinase domain and a disintegrin-like domain. In contrast to the disintegrin-like domains in membrane-bound ADAM proteases, in ADAMTS proteases this domain does not seem to interact with any integrins but could have a role in substrate recognition (de Groot *et al.* 2009). The pro-domain is important for proper protein folding and secretion and keeps the proteases in the latent state by preventing substrate access into the catalytic pocket. Enzymatic activity is enabled by furin or furin-like pro-protein convertase shedding of this pro-domain, either intracellularly, on the cell-surface, or in the ECM (Wang *et al.* 2004, Longpre *et al.* 2009, Kelwick et al. 2015). Further C-terminal to the central thrombospondin type 1 sequence repeat (TSR) domain lies the ancillary domain, which shows

great variability between the ADAMTS family members. Common features are the cysteine-rich domain followed by a spacer region. Subsequently, a multitude of further C-terminal modules can be found, including one or more additional TSR domains. ADAMTS4 is the only family member that does not contain additional C-terminal domains and ends after the spacer region (Kelwick et al. 2015). The ancillary domain, which can be proteolytically processed, is important for association with the ECM, regulation of enzyme activity and localization, and substrate-binding specificity. The enzymes can be further sub-grouped based on their known substrates [Figure 7]. All ADAMTS family members are predicted to be catalytically functional and contain a consensus zinc-binding HEXXHXXGXXHD active-site motif and a Met-turn in the metalloproteinase domain (Gomis-Ruth 2009, Tortorella et al. 2009). The Met-turn is a structural feature with a conserved methionine residue that is also present in the active site of other metalloproteases like matrix metalloproteases (MMPs) and reprolysins. ADAMTS genes are transcriptionally regulated by cytokines, growth factors, and hormones (Kelwick et al. 2015). The activity of ADAMTS proteases is controlled by tissue inhibitors of metalloproteinases (TIMPs) and by internalization and degradation, e.g. through interaction with LRP1 (Murphy 2011, Yamamoto *et al.* 2013). ADAMTS proteases are ubiquitously expressed in adult tissues, but ADAMTS4 expression is particularly prominent in lung, heart, and brain (Hurskainen *et al.* 1999). ADAMTS family members are involved in ECM assembly and degradation and have important functions in the development and maintenance of tissues and organs. Mutations in certain family members can give rise to inherited genetic diseases, such as the Ehlers-Danlos syndrome, thrombotic thrombocytopenic purpura, and the Weill-Marchesani syndrome, and dysregulated expression of some ADAMTS proteases is associated with various pathologies that involve ECM remodeling (Wagstaff *et al.* 2011, Kelwick et al. 2015).

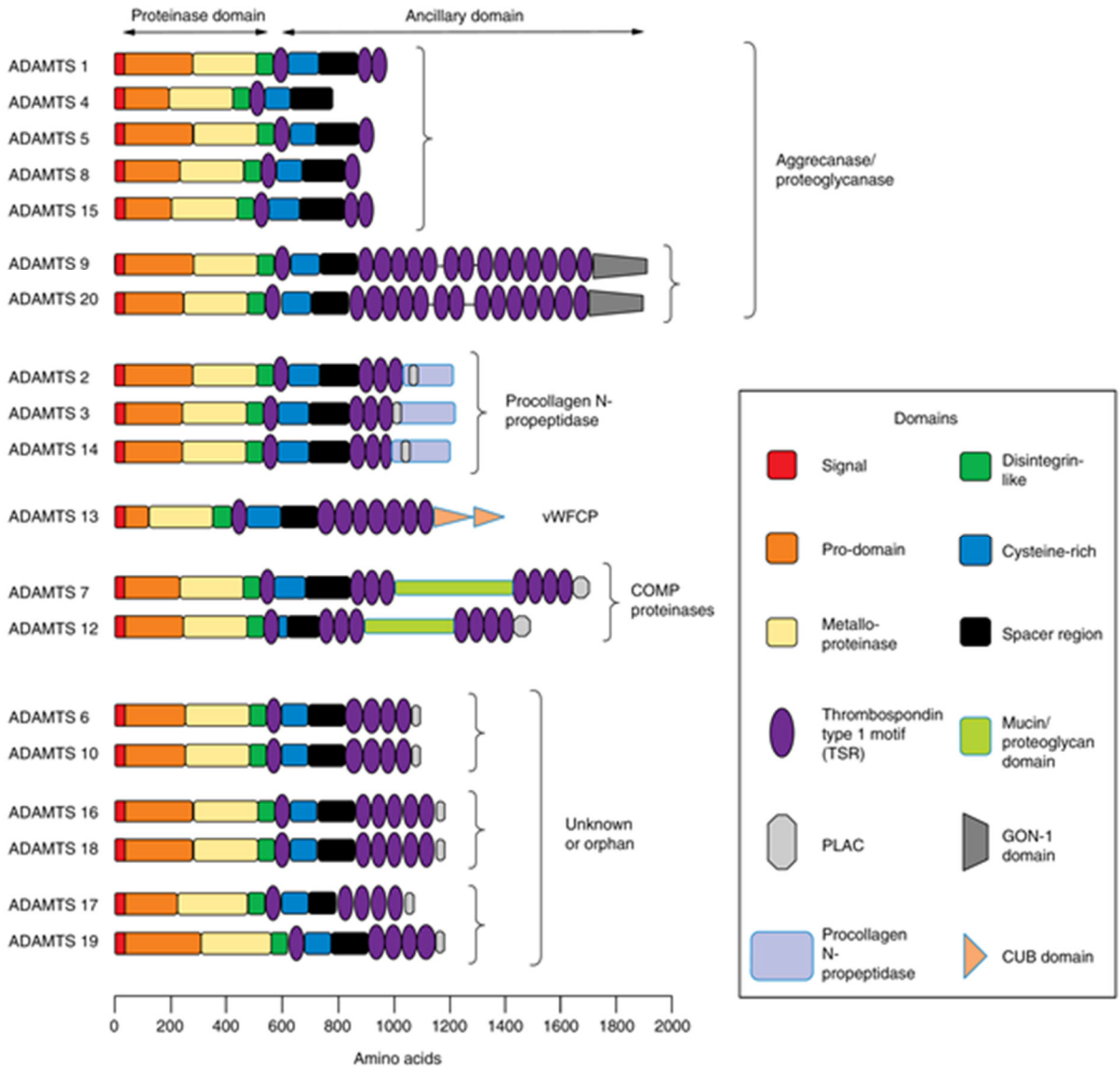

Figure 7: The ADAMTS family. The basic domain organization and major functional groups of the 19 ADAMTS family members. They are sub-grouped based on their known substrates and functions. ADAMTS proteases feature an N-terminal proteinase domain and a C-terminal ancillary domain, in which the greatest variability between family members is found. The specialized domains are listed in the key on the right (adopted from (Kelwick et al. 2015)).

The ECM is a non-cellular compartment within all tissues and organs that provides physical support as well as biochemical interaction with the cellular parts. The ECM has important functions in tissue morphogenesis, differentiation, and maintenance. Each tissue has its own unique ECM composition, but the main components are water, proteins, and polysaccharides that facilitate binding of molecular ligands and cells. The ECM is subject to constant remodeling and is a very dynamic structure to accommodate changes in tissue development,

cell migration, and intercellular interactions (Frantz *et al.* 2010). Two main classes of macromolecules are found in the ECM: proteoglycans (PGs) and fibrous proteins. Collagen is the most abundant fibrous protein within the ECM and provides tensile strength and regulates cell adhesion and migration (Rozario & DeSimone 2010). PGs fill the majority of the extracellular interstitial space and are composed of glycosaminoglycan chains linked to specific core proteins (Iozzo & Murdoch 1996). Functionally, ADAMTS proteases are proteoglycanases and degrade the core proteins of PGs including aggrecan, versican, and brevican (Stanton *et al.* 2011).

1.2.2 ADAMTS proteases in arthritis, cancer, and coronary artery disease

Arthritis describes various progressive joint diseases caused by the destruction of cartilage from articular surfaces within the joints, and includes symptoms of swelling, pain, stiffness, and a decreased range of motion (Sacitharan *et al.* 2012). Osteoarthritis (OA) is the most common form of arthritis and mainly occurs in the joints of hands, knees, and the hip. OA disease initiation is multi-factorial but the characteristic degradation of aggrecan leading to progressive loss of the whole articular cartilage is a result of uncontrolled proteolytic activity (Troeberg & Nagase 2012). Rheumatoid arthritis (RA) is a chronic autoimmune disease predominantly affecting hands, wrists, knees, and feet and is initiated by excessive production of pro-inflammatory factors in the joints which leads to cartilage destruction (Smolen & Steiner 2003). The principal enzymes involved in the pathogenesis of OA and RA are the aggrecanases ADAMTS4 (aggrecanase-1) and ADAMTS5 (aggrecanase-2) that are present in articular cartilage (Arner *et al.* 1999, Abbaszade *et al.* 1999). Articular cartilage is composed of a dense ECM with aggrecan as the major PG covalently bound to hyaluronic acid with embedded chondrocyte cells, which control ECM development, maintenance, and repair. It has viscoelastic and compressible properties and enables joint movement by providing a smooth and lubricated surface for low friction articulation and protection of underlying bones (Fox *et al.* 2009). Aggrecan degradation facilitated by ADAMTS and MMP enzymes occurs normally but is enhanced in arthritic cartilage, in which a disequilibrium of metalloproteinases and their inhibitors favors the degradation of cartilage (Lark *et al.* 1997). Aggrecan degradation is the initial crucial event leading to loss of cartilage function and is followed by essentially irreversible collagen degradation (Verma & Dalal 2011). In human OA cartilage,

chondrocytes displayed increased ADAMTS4 expression and this directly correlated with the degree of cartilage destruction. In contrast, ADAMTS5 was constitutively expressed and showed no difference between normal and OA cartilage (Naito *et al.* 2007). While ADAMTS4 and ADAMTS5 cooperate to mediate aggrecan degradation in human articular cartilage, ADAMTS5 seems to be the main aggrecanase in murine models of arthritis (Stanton *et al.* 2005, Song *et al.* 2007). Both ADAMTS4 and ADAMTS5 knockout mice are phenotypically normal and have no gross abnormalities, but only the deletion of ADAMTS5 had a protective effect on cartilage degradation in surgically induced OA (Glasson *et al.* 2004, Glasson *et al.* 2005).

ADAMTS proteases are also abundantly and differentially expressed in various types of cancer, and the TSR motif appears to have an important function in angiogenesis (Iruela-Arispe *et al.* 1999, Porter *et al.* 2004, Held-Feindt *et al.* 2006, Demircan *et al.* 2009, Minobe *et al.* 2010). Angiogenesis is required for proliferation and metastatic spreading of tumor cells and is facilitated by degradation of ECM components and modulation of endothelial cell adhesion (Mongiat *et al.* 2016). Overexpression of proteolytically active ADAMTS4 promoted melanoma tumor progression and angiogenesis, while catalytically inactive mutants showed anti-angiogenic and anti-tumorigenic activity through their TSR domain (Rao *et al.* 2013). Degradation of the ECM by ADAMTS proteases also affects the tumor microenvironment by allowing for cell migration and the release of ECM fragments that act on cancer cells influencing their viability and metastatic potential. (Wagstaff et al. 2011). The brain specific PG brevican was expressed in glioma cell lines and tumor tissue, and its proteolytic processing by ADAMTS4 and ADAMTS5 might contribute to their invasiveness (Matthews *et al.* 2000, Nakamura *et al.* 2000, Nakada *et al.* 2005).

Coronary artery diseases are caused by atherosclerosis, the hardening and narrowing of arteries due to the deposition of atherosclerotic plaques composed of cells, ECM, lipids, and debris. In advanced disease stages, plaques may rupture and form a thrombus that can dislocate into the circulation to block arteries and cause stroke or ischemia (Weber & Noels 2011). ADAMTS4 levels were elevated in human plasma of patients with both acute coronary syndromes as well as stable coronary artery disease and expression levels were associated with disease severity, which might indicate a causative role of ADAMTS4 in atherosclerosis through vascular remodeling and plaque destabilization (Zha *et al.* 2010, Chen *et al.* 2011).

Versican is an abundant component of blood vessel walls and is critical in the formation of atherosclerotic lesions. Versican fragments generated by ADAMTS4 cleavage were detected in atherosclerotic plaques, and their cleavage may weaken the structural integrity of the lesion and cause ruptures (Sandy *et al.* 2001). ADAMTS4 expression was elevated during progression of atherosclerosis in a mouse model and in human atherosclerotic plaques (Wagsater *et al.* 2008). Macrophages in atherosclerotic lesions were reported to express ADAMTS4, which stimulated the invasion of macrophages into the ECM of lesion sites (Ren *et al.* 2013). ADAMTS4 knockout in a mouse model of atherosclerosis led to more stable plaques, reduced macrophage invasion, and ultimately reduced atherosclerosis (Kumar *et al.* 2016).

1.2.3 ADAMTS proteases in the physiological CNS

ADAMTS proteoglycanases are present in several CNS structures, including cortex, hippocampus, striatum, and spinal cord (Yuan *et al.* 2002, Jungers *et al.* 2005, Miguel *et al.* 2005, Cross *et al.* 2006b, Howell *et al.* 2012, Krstic *et al.* 2012). Evidence has been provided by qPCR and immunohistochemistry that neurons, astrocytes, microglia, and oligodendrocytes express ADAMTS4 (Hamel *et al.* 2005, Tauchi *et al.* 2012, Levy *et al.* 2015). However, an *in situ* hybridization study suggested that, in the developing hippocampus and neocortex, ADAMTS4 was exclusively expressed by oligodendrocytes and might have a function in axon myelination through ECM remodeling (Levy et al. 2015). In contrast, ADAMTS5 was mainly detected in neuronal cell bodies and their processes in the rat brain (Dubey *et al.* 2017). The physiological roles of ADAMTS proteases in the CNS are unknown but studies point to a function in neuronal plasticity (Lemarchant *et al.* 2017). The ECM surrounds cell bodies and proximal dendrites in the brain and enwraps synaptic contacts. It forms a mesh-like structure termed perineuronal nets (PNNs) around neurons in the hippocampus and cortex and around motoneurons in the spinal cord, to control axon guidance and pathfinding during neural development and to regulate synaptic plasticity (Zimmermann & Dours-Zimmermann 2008, Lemarchant *et al.* 2013). The ECM stabilizes established neuronal networks and thereby inhibits structural plasticity, but ECM modulation and PG degradation in the adult brain can facilitate activity-dependent plasticity and learning (Valenzuela *et al.* 2014). PG molecules were described to inhibit neurite outgrowth and their accumulation in glial scars after CNS damage prevented axon regeneration (Davies *et al.* 1997, Carulli *et al.* 2005). ADAMTS proteoglycanases and their

cleavage products were detected in the rat hippocampus and could be involved in the plasticity of PNNs and surrounded neurons (Yuan et al. 2002). Furthermore, ADAMTS proteases were elevated in the dentate gyrus during neuritic sprouting after entorhinal cortex lesions (Mayer *et al.* 2005). Recombinant ADAMTS4 promoted neurite outgrowth of cortical neurons *in vitro* by degrading PGs, and by activating signaling pathways independent of its proteolytic activity, presumably through receptor binding (Hamel *et al.* 2008). ADAMTS4 and ADAMTS5 were also shown to cleave reelin, which is involved in synaptic plasticity in the adult brain and during neuronal development (Krstic et al. 2012). ADAMTS4 is the proteoglycanase with the highest expression in the mouse CNS with highest levels during the first weeks after birth, and it was also detected in postmortem human brains (Howell et al. 2012, Lemarchant *et al.* 2016a, Lemarchant *et al.* 2016b). The developmental upregulation of ADAMTS4 in mice coincides with several important aspects of neural development, i.e. refinement and maturation of neural circuits and myelination (Levy et al. 2015).

1.2.4 ADAMTS proteases in CNS injuries and diseases

ECM proteolysis by ADAMTS enzymes has been proposed to be both beneficial and detrimental in pathological conditions of the CNS. Changes in ADAMTS expression and activity have been described in ischemic stroke, spinal cord injury (SCI), amyotrophic lateral sclerosis (ALS), multiple sclerosis (MS) and seizures (Yuan et al. 2002, Cross *et al.* 2006a, Cross et al. 2006b, Lemarchant et al. 2016b). Cytokines have been reported to regulate ADAMTS expression outside of the CNS and in astrocyte cultures, and the cytokine-rich environment following CNS injuries could regulate ADAMTS expression and activity (Cross et al. 2006a, Mimata *et al.* 2012). A significant increase in ADAMTS4 activity was observed in spinal cord lesions after SCI (Demircan *et al.* 2014). Furthermore, treatment with recombinant human ADAMTS4 improved functional recovery by degrading accumulated PGs in the glial scar and PGs in the ECM, to facilitate axonal regeneration and sprouting (Tauchi et al. 2012, Lemarchant *et al.* 2014). Increased ADAMTS4 protein expression was detected in the ischemic core of mice and human patients after stroke, and treatment with recombinant ADAMTS4 reduced the release of pro-inflammatory cytokines in microglia and astrocyte cultures (Lemarchant et al. 2016a). In contrast, decreased expression and activity of ADAMTS4 was found in a mouse model of ALS. Treatment of ALS mice with recombinant ADAMTS4 increased

the degradation of PNNs around motoneurons and decreased the glial production of neurotrophic factors, which led to accelerated neuromuscular dysfunction and neurodegeneration (Lemarchant et al. 2016b). In human brains, ADAMTS5 mRNA and protein levels were low and even further decreased in MS white matter. In contrast, ADAMTS4 expression was unchanged between normal and MS tissue and it was approximately 50-fold higher expressed than ADAMTS5. However, ADAMTS4 protein levels were significantly higher in MS samples and were predominantly associated with astrocytes in lesions. Therefore, increased ECM turnover by ADAMTS4 could have a role in lesion development in MS (Haddock *et al.* 2006). Taken together, these findings suggest that ADAMTS proteases could promote neural plasticity and regeneration by facilitating ECM remodeling, by removing inhibitory glial scars, and by acting as an anti-inflammatory factor to reduce neuroinflammation. However, in some cases, increased ADAMTS proteolytic activity might be detrimental to neuronal networks through loss of PNNs and downregulated production of neurotrophic factors, leading to further brain injury and invasion of macrophages.

ADAMTS proteases have also been proposed to be involved in the pathophysiology of AD, but reports are conflicting and little is known about their possible contribution to the disease process. ADAMTS1 was shown to be overexpressed in AD brains compared to controls, while ADAMTS5 levels were comparable (Miguel et al. 2005). In another study, ADAMTS4 and ADAMTS5 expression was slightly decreased in human AD brains, which suggests no enhanced ECM degeneration in AD but rather accumulation of undesired ECM compounds (Pehlivan *et al.* 2016). Treatment with Aβ induced ADAMTS4 expression in primary rat astrocytes, which could promote ECM degradation and lead to the dysfunction of neural networks (Satoh *et al.* 2000). Proteolytic cleavage of brevican was diminished in a transgenic mouse model of AD, which could negatively influence neural plasticity. However, a local accumulation of ADAMTS-derived brevican fragments was detected surrounding plaques, which suggests elevated protease activity in the vicinity of dystrophic neurites (Ajmo *et al.* 2010). Finally, co-localization of ADAMTS4 and ADAMTS4-related reelin fragments was found in AD transgenic mice, and enhanced cleavage of reelin by ADAMTS4 might result in increased formation of reelin aggregates and decreased reelin-dependent signaling (Krstic et al. 2012). In APP-transgenic mice crossed to heterozygous reelin knockout mice, reduced reelin signaling has been shown to accelerate both amyloid and tau pathologies (Kocherhans *et al.* 2010).

2. Objectives

The prime objective of this thesis was to investigate how the secreted metalloprotease ADAMTS4 might affect APP processing and Aβ generation *in vitro* and *in vivo*. The Aβ sequence within APP contains two motifs that resemble the consensus protease recognition sequence of ADAMTS4 as described by Hill et al. (Hills *et al.* 2007). Cleavage of ADAMTS4 after two glutamic acid residues in positions 3 and 11 of the Aβ sequence could lead to the generation of N-terminally truncated Aβ4-x and Aβ12-x peptides. In addition, in preliminary experiments we had observed an increase in total Aβ levels when ADAMTS4 was transiently overexpressed in HEK293 cells.

Consequently, this thesis project included the following key tasks:

1. To generate a tissue culture model with inducible ADAMTS4 expression and to use this model to investigate how moderate overexpression of ADAMTS4 would affect APP processing and Aβ generation *in vitro*.
2. To cross the 5xFAD mouse model of AD to ADAMTS4$^{-/-}$ knockout mice and to explore a potential role of ADAMTS4 *in vivo* by analyzing APP processing, Aβ levels, and the extent of the amyloid pathology.
3. To use ADAMTS4$^{-/-}$ knockout reporter mice to determine the expression of ADAMTS4 in the adult murine brain.
4. To compare ADAMTS4 mRNA expression levels in brain tissues of human AD patients and age-matched, non-demented control individuals.

3. Materials

3.1 Cell lines

Name	Description	
HEK293	Human embryonic kidney cells transformed with sheared adenovirus 5 DNA	(Sagi *et al.* 2011) Gift from Dr. Edward Koo, UC San Diego, USA
HEK293FT	Fast growing HEK293F cells containing the SV40 large T-antigen	Thermo Fisher Scientific, USA
HEK293/TetOn-ADAMTS4-V5	HEK293 cells stably expressing rtTA3 and inducible ADAMTS4-V5	(Bradshaw *et al.* 2017)
HEK293-APP695sw	HEK293 cells stably expressing APP695sw	
HEK293-APP695sw/TetOn-ADAMTS4-V5	HEK293-APP695sw cells stably expressing rtTA3 and inducible ADAMTS4-V5	
HEK293-APP695wt	HEK293 cells stably expressing APP695wt	
HEK293-APP695wt/TetOn-ADAMTS4-V5	HEK293-APP695wt cells stably expressing rtTA3 and inducible ADAMTS4-V5	
SMA-560	Spontaneous murine astrocytoma cells (Serano *et al.* 1980)	(Uhl *et al.* 2004) Gift from Dr. Wolfgang Wick, University of Heidelberg
SMA-560/TetOn-ADAMTS4-V5	SMA-560 cells stably expressing rtTA3 and inducible ADAMTS4-V5	

3.2 Mouse strains

Name	Genotype	
C57Bl/6J	Wild type	The Jackson Laboratory, USA
B6.129P2-*Adamts4*^{tm1Dgen}/J (ADAMTS4$^{-/-}$ knockout)	Homozygous mutant in which the ADAMTS4 locus is replaced with the bacterial lacZ gene	The Jackson Laboratory, USA
5xFAD	Transgenic mouse model expressing human APP KM670/671NL (Swedish),	(Oakley et al. 2006)

	APP I716V (Florida), APP V717I (London), human PSEN1 M146L, and PSEN1 L286V under the control of the Thy-1 promoter	
5xFAD / ADAMTS4$^{-/-}$	5xFAD mice with ADAMTS4$^{-/-}$ knockout	

3.3 Human brain samples

Human brain samples consisted of superior frontal gyrus samples of 20 AD patients and 20 non-demented controls (NDC) obtained from the Netherlands Brain Bank (www.brainbank.nl). All material has been collected from donors from whom a written informed consent for brain autopsy and the use of the material and clinical information for research purposes had been obtained by The Netherlands Brain Bank (NBB).

	NBB internal reference	Autopsy Number	Sex	Age	Braak stage	Post-mortem delay time	Diagnosis
1	2000-042	S00/081	M	78	5	07:45	AD
2	2005-075	S05/280	M	82	5	05:05	AD
3	2001-095	S01/219	F	81	6	05:30	AD
4	2008-004	S08/005	F	82	6	04:20	AD
5	2007-079	S07/297	F	54	6	06:35	AD
6	2006-008	S06/023	F	85	2	04:40	NDC
7	2010-007	S10/023	F	85	2	05:19	NDC
8	2004-060	S04/188	M	85	1	04:15	NDC
9	2004-020	S04/053	M	96	1	05:23	NDC
10	1994-119	S94/325	F	51	0	07:40	NDC
11	2001-063	S01/145	M	85	5	04:45	AD
12	2005-010	S05/039	M	93	5	04:30	AD
13	2002-096	S02/299	F	82	6	06:00	AD
14	2003-110	S03/315	F	82	5	04:35	AD
15	2009-086	S09/280	F	84	6	04:50	AD
16	1997-045	S97/145	F	55	0	05:35	NDC
17	2010-070	S10/196	F	60	1	07:30	NDC
18	2010-015	S10/035	F	73	1	07:45	NDC
19	2009-022	S09/067	F	77	1	02:55	NDC
20	1996-084	S96/249	F	78	2	07:30	NDC
21	2009-041	S09/133	F	85	6	05:10	AD
22	2001-070	S01/161	F	86	6	05:40	AD

23	2006-006	S06/017	F	87	6	05:00	AD
24	2005-013	S05/050	F	89	6	04:30	AD
25	2001-066	S01/151	F	96	5	05:50	AD
26	2008-027	S08/083	F	80	1	06:58	NDC
27	2007-075	S07/275	F	82	2	05:10	NDC
28	2002-071	S02/209	F	82	1	07:08	NDC
29	2004-012	S04/038	F	82	1	07:00	NDC
30	2009-042	S09/134	F	84	1	06:55	NDC
31	2001-117	S01/267	F	57	6	04:05	AD
32	2000-094	S00/196	F	61	6	06:25	AD
33	1996-089	S96/266	F	74	5	06:05	AD
34	2006-079	S06/264	F	77	5	06:05	AD
35	2001-076	S01/173	F	78	6	03:45	AD
36	1997-116	S97/270	M	80	0	06:56	NDC
37	2007-082	S07/308	M	81	2	07:55	NDC
38	2004-061	S04/196	F	88	unknown	06:15	NDC
39	2006-080	S06/282	F	89	2	06:25	NDC
40	2010-062	S10/181	F	94	1	05:50	NDC

3.4 Bacterial strain

Name	**Genotype**	
Subcloning Efficiency *E. coli* DH5α	F^- Φ80*lac*ZΔM15 Δ(*lac*ZYA-*arg*F) U169 *rec*A1 *end*A1 *hsd*R17(r_k^-, m_k^+) *pho*A *sup*E44 *thi*-1 *gyr*A96 *rel*A1 λ^-	Thermo Fisher Scientific, USA

3.5 Adenoviral strain

Name	**Genotype**	
APP695sw adenovirus	pAdEasy-1 vector carrying an expression cassette for human APP695sw	(Luo *et al.* 2007)

3.6 Antibodies

3.6.1 Primary antibodies

Name	Antigen	Species	Type	
22C11	APP N-terminus (AA 66-81)	mouse	monoclonal	(Kuhn *et al.* 2010) Gift from Dr. Stefan Kins, University of Kaiserslautern
4G8	Aβ mid-region (AA 17-24)	mouse	monoclonal	BioLegend, USA
6A1	Human sAPPβ-sw C-terminus	mouse	monoclonal	IBL, Japan
Anti-Actin	Actin C-terminus	rabbit	polyclonal	Sigma-Aldrich, Munich
Anti-CNPase 11-5B	Human CNPase	mouse	monoclonal	Sigma-Aldrich, Munich
Anti-FLAG M2	FLAG-Tag	mouse	monoclonal	Sigma-Aldrich, Munich
Anti-GFAP	Full-length human GFAP	guinea pig	polyclonal	Synaptic Systems, Goettingen
Anti-Iba1	Rat Iba1 (AA 134-147)	guinea pig	polyclonal	Synaptic Systems, Goettingen
Anti-V5 Tag	V5-Tag	mouse	monoclonal	Thermo Fisher Scientific, USA
Anti-β-Galactosidase	*E. coli* β-Galactosidase	rabbit	polyclonal	Merck, Darmstadt
BAP-15	Aβ42 C-terminus	mouse	monoclonal	(Brockhaus *et al.* 1998)
BAP-24	Aβ40 C-terminus	mouse	monoclonal	(Brockhaus et al. 1998)
BAP-29	Aβ38 C-terminus	mouse	monoclonal	(Brockhaus et al. 1998)
CT-15	Human APP695 C-terminus (AA 680-695)	rabbit	polyclonal	(Soriano *et al.* 2001) Gift from Dr. Edward Koo, UC San Diego, USA
IC16	Human Aβ N-terminus (AA 1-16)	mouse	monoclonal	(Hahn *et al.* 2011)
IG7/5A3	APP ectodomain (AA 380-665)	mouse	monoclonal	(Weggen *et al.* 2001) Gift from Dr. Edward Koo, UC San Diego, USA

PSL-029-2	Aβ4-x N-terminus	guinea pig	monoclonal	(Wirths *et al.* in press) Gift from Dr. Oliver Wirths, University of Goettingen

3.6.2 Secondary antibodies

Antigen	**Conjugate**	**Species**	
Guinea pig IgG	DyLight 488	goat	Thermo Fisher Scientific, USA
Mouse IgG	Alexa Fluor 594	goat	Thermo Fisher Scientific, USA
Mouse IgG	DyLight 594	goat	Thermo Fisher Scientific, USA
Mouse IgG	IRDye 800CW	goat	LI-COR Biosciences, Bad Homburg
Rabbit IgG	Alexa Fluor 488	goat	Thermo Fisher Scientific, USA
Rabbit IgG	DyLight 488	goat	Thermo Fisher Scientific, USA
Rabbit IgG	DyLight 594	goat	Thermo Fisher Scientific, USA
Rabbit IgG	IRDye 800CW	goat	LI-COR Biosciences, Bad Homburg

3.7 Plasmids and Primers

3.7.1 Plasmids

Name	**Application**	
Gateway pDONR221	Cloning	Thermo Fisher Scientific, USA
pLenti CMVtight Hygro DEST	Cloning	Gift from Eric Campeau, Addgene, USA
pLenti CMV rtTA3 Blast	Lentiviral expression vector	Gift from Eric Campeau, Addgene, USA
pLenti CMVtight Hygro-ADAMTS4-V5	Lentiviral expression vector	

pMD2.G	Lentiviral envelope vector	Gift from Didier Trono, Addgene, USA
pMDLg/pRRE	Lentiviral packaging vector	(Dull *et al.* 1998), Addgene, USA
pRSV-Rev	Lentiviral packaging vector	(Dull et al. 1998), Addgene, USA
pcDNA3.1(+)-FE65-FLAG	Transient transfection	
pLBCX-ADAMTS4-FLAG	Transient transfection	
pLHCX-APPsw	Transient transfection	

3.7.2 Primers

Oligonucleotide primers were purchased from IDT, Belgium.

Name	**Application**	**Sequence**
attB1-ADAMTS4_For	Cloning	GGGG ACA AGT TTG TAC AAA AAA GCA GGC T ATG TCC CAG ACA GGC TCG
attB2-ADAMTS4-V5_Rev	Cloning	GGGG AC CAC TTT GTA CAA GAA AGC TGG GT CTA CGT AGA ATC GAG ACC GAG GAG AGG GTT AGG GAT AGG CTT ACC TTT CCT GCC CGC CCA
ADAMTS4_For	Mouse OPC qPCR	CCT GAC CAC TTT GAC ACA GC
ADAMTS4_Rev	Mouse OPC qPCR	CTG ACT GGA GCC CAT CAT CT
CNPase_For	Mouse OPC qPCR	TGC TGC ACT GTA CAA CCA AAT TC
CNPase_Rev	Mouse OPC qPCR	GAG AGC AGA GAT GGA CAG TTT GAA
MBP_For	Mouse OPC qPCR	CAC AGA GAC ACG GGC ATC CT
MBP_Rev	Mouse OPC qPCR	TCT GCT TTA GCC AGG GTA CCT T
GAPDH_For	Mouse OPC qPCR	CTC AAC TAC ATG GTC TAC ATG TTC CA
GAPDH_Rev	Mouse OPC qPCR	CCA TTC TCG GCC TTC ACT AT
ADAMTS4_For	Human brain qPCR	GAG CTG TGC TCT TCT GTT GGT GA
ADAMTS4_Rev	Human brain qPCR	CAG AGA AGC GAA GCG CTT GGT T
ARF1_For	Human brain qPCR	GAC CAC GAT CCT CTA CAA GC
ARF1_Rev	Human brain qPCR	TCC CAC ACA GTG AAG CTG ATG
CMVtight_For	Sequencing	TGA ACC GTC AGA TCG CCT GGA
ADAMTS4_For_1	Sequencing	ACC TCT CGC CAT GTC ATG GCC
ADAMTS4_For_2	Sequencing	CCG GAC AGC TCC TCG GTC TGT

3.8 Reagents

3.8.1 Chemicals

1-Step Ultra TMB-ELISA substrate solution Thermo Fisher Scientific, USA

30% Acrylamide 37.5:1 Bis-Acrylamide	Roth, Karlsruhe
Agar	Roth, Karlsruhe
Agarose	Bio-Budget, Krefeld
Ammonium persulfate (APS)	Sigma-Aldrich, Munich
Ampuwa Sterile Water	Fresenius Kabi, Bad Homburg
Bicine	Merck, Darmstadt
Bis-Tris	Merck, Darmstadt
Bovine Serum Albumin (BSA)	Sigma-Aldrich, Munich
Bromophenol blue	Roth, Karlsruhe
Deoxynucleotide-tri-phosphate (dNTP)	New England Biolabs, Frankfurt
Dithiothreitol (DTT)	Sigma-Aldrich, Munich
Ethanol	Roth, Karlsruhe
Ethylenediaminetetraacetic acid (EDTA)	Roth, Karlsruhe
Gelatin from cold water fish skin	Sigma-Aldrich, Munich
Glacial Acetic Acid	Merck, Darmstadt
Glycerol	VWR, Darmstadt
Glycine	Roth, Karlsruhe
Hydrochloric acid (HCl)	Sigma-Aldrich, Munich
Isopropanol	Roth, Karlsruhe
MES (2-(N-morpholino)ethanesulfonic acid)	Roth, Karlsruhe
Midori Green Advance DNA Stain	NIPPON Genetics Europe, Düren
NP-40 (Igepal)	Sigma-Aldrich, Munich
Paraformaldehyde (PFA)	Sigma-Aldrich, Munich
Potassium chloride (KCl)	Sigma-Aldrich, Munich

Potassium dihydrogen phosphate (KH_2PO_4)	Merck, Darmstadt
ProLong Gold Antifade Mountant with DAPI	Thermo Fisher Scientific, USA
Protease inhibitor cocktail tablets, EDTA-free	Roche, Mannheim
Saponin	Sigma-Aldrich, Munich
Sodium azide (NaN_3)	Merck, Darmstadt
Sodium carbonate (Na_2CO_3)	Sigma-Aldrich, Munich
Sodium chloride (NaCl)	Roth, Karlsruhe
Sodium dodecyl sulfate (SDS)	BioRad, Munich
Sodium hydrogen carbonate ($NaHCO_3$)	Merck, Darmstadt
Sodium hydroxide (NaOH)	Merck, Darmstadt
Sodium phosphate dibasic (Na_2HPO_4)	Sigma-Aldrich, Munich
Sodium phosphate monobasic (NaH_2PO_4)	Sigma-Aldrich, Munich
Sucrose	Sigma-Aldrich, Munich
Sulfuric acid 96% (H_2SO_4)	Roth, Karlsruhe
TEMED (N,N,N',N'-Tetramethylethylenediamine)	Roth, Karlsruhe
TRIS (Tris(hydroxymethyl)aminomethane)	Roth, Karlsruhe
TRIS-HCl	Roth, Karlsruhe
Triton-X 100	Pierce, Bonn
Tryptone	Roth, Karlsruhe
Tween-20	Roth, Karlsruhe
Yeast extract	Roth, Karlsruhe

3.8.2 Cell culture reagents

Accutase solution	Sigma-Aldrich, Munich

B-27 supplement	Thermo Fisher Scientific, USA
B-27 supplement, minus vitamin A	Thermo Fisher Scientific, USA
BSA Fraction V (7.5%)	Thermo Fisher Scientific, USA
DMEM	Thermo Fisher Scientific, USA
DMEM/F-12, no glutamine	Thermo Fisher Scientific, USA
DMSO (Dimethyl sulfoxide)	Roth, Karlsruhe
DPBS, no calcium, no magnesium (PBS -/-)	Thermo Fisher Scientific, USA
Fetal Bovine Serum (FBS)	Thermo Fisher Scientific, USA
GlutaMAX	Thermo Fisher Scientific, USA
Opti-MEM	Thermo Fisher Scientific, USA
Poly-L-lysine hydrobromide	Sigma-Aldrich, Munich
Recombinant mouse FGF-b	ImmunoTools, Friesoythe
Recombinant mouse PDGF-AA	ImmunoTools, Friesoythe
Sodium pyruvate 100x	Thermo Fisher Scientific, USA
T3 (Triiodo-L-Thyronine)	Sigma-Aldrich, Munich
T4 (L-Thyroxine)	Sigma-Aldrich, Munich
Trypsin-EDTA (0.5%), no phenol red	Thermo Fisher Scientific, USA

3.8.3 Antibiotics

Ampicillin	Sigma-Aldrich, Munich
Blasticidin S	AppliChem, Darmstadt
Doxycycline hydrochloride	Sigma-Aldrich, Munich
Geniticin disulfate (G418)	Roth, Karlsruhe
Hygromycin B	Roth, Karlsruhe

Kanamycin	Sigma-Aldrich, Munich
Penicillin-Streptomycin 10000 U/ml	Thermo Fisher Scientific, USA

3.8.4 Synthetic Aβ peptides

Full-length Aβ peptides (Aβ1-40, Aβ1-42, Aβ1-38)	JPT, Berlin
N-terminally truncated Aβ peptides (Aβ4-40, Aβ4-42)	PSL, Heidelberg

3.8.5 BACE1 Inhibitor

β-Secretase Inhibitor IV	Merck, Darmstadt

3.8.6 Transfection reagents

Lipofectamine 2000	Thermo Fisher Scientific, USA
Polybrene	Sigma-Aldrich, Munich

3.8.7 Beads

Anti-A2B5 Microbeads	Miltenyi Biotec, Bergisch Gladbach
Dynabeads M-280 anti-mouse IgG	Thermo Fisher Scientific, USA
Dynabeads M-280 anti-rabbit IgG	Thermo Fisher Scientific, USA

3.8.8 Size standards

PageRuler Plus Prestained Protein ladder (10 - 250 kDa)	Thermo Fisher Scientific, USA
Quick-Load 2-log DNA Ladder	New England Biolabs, Frankfurt

3.8.9 Enzymes and enzyme mixes

Benzonase 250 U/µl	Sigma-Aldrich, Munich
Gateway BP Clonase II Enzyme mix	Thermo Fisher Scientific, USA
Gateway LR Clonase II Enzyme mix	Thermo Fisher Scientific, USA
Phusion High-Fidelity DNA Polymerase	Thermo Fisher Scientific, USA
Platinum SYBR Green qPCR SuperMix-UDG	Thermo Fisher Scientific, USA

3.8.10 Kits

BCA Protein Assay Kit	Pierce, Bonn
EZ-Link Plus Activated Peroxidase Kit	Thermo Fisher Scientific, USA
E.Z.N.A. Plasmid DNA Mini Kit I	VWR, Darmstadt
Genopure Plasmid Maxi Kit	Roche, Mannheim
Neural Tissue Dissociation Kit (P)	Miltenyi Biotec, Bergisch Gladbach
PureLink Genomic DNA Mini Kit	Thermo Fisher Scientific, USA
QIAquick Gel Extraction Kit	Qiagen, Hilden
QuantaBlu Fluorogenic Peroxidase Substrate Kit	Thermo Fisher Scientific, USA

3.9 Laboratory hardware and appliances

Autoclave	Systec, Linden
Binocular microscope	Wild Heerbrugg, Switzerland
Blot containers	GenHunter, USA
Centrifuges	Eppendorf, Hamburg
	Hettich, Tuttingen
Confocal fluorescence microscope LSM-510	Zeiss, Oberkochen

Dissecting instruments	Roth, Karlsruhe
Electronic Transferpette (1 µl – 300 µl)	BRAND, Wertheim
Electrophoresis and Blotting power supply	Consort, Belgium
Electrophoresis system RunOne EP-2000	Embi Tec, USA
Freezer (-20°C)	Liebherr, Bulle
Freezer (-80°C)	Thermo Fisher Scientific, USA
Glassware	Schott, Mainz
Heating block	Eppendorf, Hamburg
Ice machine	Ziegra, Isernhagen
Incubator (tissue culture)	Binder, Tuttlingen
Incubator (bacteria)	New Brunswick Scientific, USA
Laminar Flow Hood	Clean Air Techniek, Netherlands
LI-COR ODYSSEY CLx	LI-COR Biosciences, Bad Homburg
Light-optical microscope	Wilovert, Wetzlar
MACS MultiStand Magnet	Miltenyi Biotec, Bergisch Gladbach
Magnetic particle concentrator MPC-S	Thermo Fisher Scientific, USA
Magnetic stirrer	Heidolph, Kehlheim
Microwave	Unirop, Fürth
MilliQ Water Purification System	Merck, Darmstadt
NanoDrop ND-1000 Spectrophotometer	PEQLAB, Erlangen
PARADIGM Microtiterplate reader	Beckman Coulter, Krefeld
pH meter 525	WTW, Weilheim
Pipettes 0.2 µl – 10 µl	Eppendorf, Hamburg
Pipettes 1 µl – 1000 µl	Gilson, USA

Pipettor AccuJet	VWR, Darmstadt
Plasticware	VWR, Darmstadt
Platform shaker	Heidolph, Kehlheim
Rotary shaker SB2	VWR, Darmstadt
Safire multimode microplate reader	Tecan, Crailsheim
Scale (Max = 110 g)	Sartorius, Goettingen
Scale (Max = 2000 g)	KERN, Balingen
StepOnePlus Real-Time PCR Cycler	Thermo Fisher Scientific, USA
T3 Thermocycler	Biometra, Goettingen
Tank Blotter	CBS Scientific, USA
UV Transilluminator	Vilber, Eberhardzell
Vacuum pumps	VWR, Darmstadt
Vi-CELL XR cell counter	Beckman Coulter, Krefeld
Vortex Mixer	IKA, Staufen
Water bath	Julabo, Seelbach
X-Cell SureLock Mini-Cell Electrophoresis system	Thermo Fisher Scientific, USA

3.10 Consumables

10 cm Petri dishes (bacteria)	Sarstedt, Nuembrecht
10 cm Petri dishes (cell culture)	Nunc, Wiesbaden
96-well high-binding plate	Greiner Bio-One, Frickenhausen
Cell scraper	TPP, Switzerland
Cell strainer 70 µm	Falcon, USA
Coverslips (10 mm diameter)	VWR, Darmstadt

Cryotubes	Thermo Fisher Scientific, USA
Disposable gloves	Ansell, Munich
Immobilon-FL Transfer Membrane (PVDF)	Merck, Darmstadt
Microscope slides	Engelbrecht, Edermünde
Microwell plates	Nunc, Wiesbaden
MS columns	Miltenyi Biotec, Bergisch Gladbach
Needles	Becton Dickinson, USA
Novex Empty Gel Cassettes	Thermo Fisher Scientific, USA
Optical adhesive film	STARLAB, Ahrensburg
Pasteur pipettes	Roth, Karlsruhe
Pipettes (5 ml – 25 ml)	Sigma-Aldrich, Munich
Pipet tips (10/20 µl, 20 µl, 200 µl, 1000 µl)	STARLAB, Ahrensburg
Pipetting reservoirs	VWR, Darmstadt
Reaction tubes (0.5 ml, 1.5 ml, 2ml)	Eppendorf, Hamburg
Scalpels	Feather, Japan
Slide-A-Lyzer Dialysis cassette	Thermo Fisher Scientific, USA
Sterile vacuum filter units (500 ml)	VWR, Darmstadt
Sterile syringe filter (0.45 µm)	VWR, Darmstadt
Syringes	B. Braun, Melsungen
Tubes (15 ml, 50 ml)	Greiner Bio-One, Frickenhausen
Whatman paper	Whatman, Dassel

3.11 Software

Adobe Illustrator CS3

Adobe Photoshop CS3

CLC Main Workbench 6

EndNote X7

Image Studio Software 2.1

Microsoft Office Professional Plus 2010

Prism GraphPad 5.0

StepOnePlus Software 2.0

4. Methods

4.1 Molecular Cloning

4.1.1 Polymerase chain reaction (PCR)

PCR is a technique to amplify selected segments of DNA. A thermal cycler is used to generate repeated cycles of heating and cooling to enable different temperature-dependent reactions. The first step is DNA denaturation, in which the two strands of the double-stranded DNA are separated by a high temperature. Subsequently, the temperature is lowered to allow template amplification. In the annealing step, short DNA oligonucleotides called primers bind to specific complementary target sequences on both ends of the strand to initiate the DNA synthesis. The annealing temperature is determined based on the specific melting temperature of the primers. A heat-stable DNA polymerase binds to the hybridization site and catalyzes a new DNA strand from free nucleotides during the elongations step at the optimal temperature for the enzyme and amount of time for the number of base pairs that need to be generated. This cycle is repeated multiple times and the newly generated DNA can also be used as a template which leads to exponential amplification of the target sequence. A final longer elongation step is used to ensure that every initiated synthesis was successfully completed. Afterwards, the reaction is stored at 4°C until further use. The PCR reactions were carried out using the Phusion High-Fidelity DNA Polymerase according to manufacturer's instruction.

4.1.2 Agarose gel electrophoresis and PCR product purification

After the PCR, gel electrophoresis is used to separate the mixture of DNA fragments by length in a matrix of agarose.

Materials:

TAE buffer:	80 mM TRIS
	2 mM EDTA
	0.1% Glacial acetic acid (w/v)

1% Agarose solution:	1% Agarose (w/v) in TAE buffer
6x Sample buffer:	10 mM TRIS-HCl
	60 mM EDTA
	30% Glycerol (w/v)
	0.25% Bromophenol blue (w/v)

1. Prepare the agarose solution by dissolving the agarose in TAE buffer using a microwave.
2. Stir the hot agarose solution and let it cool down for approximately 5 min.
3. Add Midori Green to the agarose solution (1:10,000).
4. Pour the agarose solution into a cassette and place a comb into the gel.
5. Let the agarose gel harden for 30 min.
6. Remove the comb and place the agarose gel into a running chamber containing TAE buffer.
7. Dilute the PCR product in 6x sample buffer to a total volume of 50 µl.
8. Load the sample and 5 µl of the DNA ladder onto the agarose gel.
8. Run the agarose gel at 100 V for approximately 30 min.
9. Expose the agarose gel to UV light and cut out the desired DNA fragment using a scalpel.
10. Purify the DNA using the QIAquick Gel Extraction Kit according to manufacturer's instructions.

4.1.3 Gateway cloning

The Gateway cloning technology employs site-specific recombination to generate expression vectors with a gene of interest. PCR products of the gene of interest are flanked with *att*B recombination sites to allow insertion into an entry vector (BP reaction). In the next step, the DNA segment of the gene of interest is transferred from the entry vector to a destination vector to create an expression clone (LR reaction). The reactions were carried out according to manufacturer's instructions.

4.1.4 Bacterial transformation and plasmid purification

Vector DNA is introduced into competent bacterial cells to replicate and amplify the plasmid.

Materials:

LB medium:	1% Tryptone (w/v)
	0.5% Yeast extract (w/v)
	1% NaCl (w/v)
	→ Autoclave and store at 4°C
LB agar:	1% Tryptone (w/v)
	0.5% Yeast extract (w/v)
	1% NaCl (w/v)
	1.5% Agar (w/v)
	→ Autoclave

While stirring, let the LB agar cool down to RT and then add ampicillin or kanamycin to a final concentration of 50 mg/ml. Pour 15 ml of LB agar + antibiotic per 10 cm dish. Incubate the plates at RT until hardening of the LB agar and store them at 4°C until further use.

1. Defrost competent Subcloning Efficiency *E. coli* DH5α on ice.
2. Add 5 µl plasmid DNA to 50 µl cell volume.
3. Mix the solution by gently pipetting.
4. Incubate on ice for 30 min.
5. Incubate for 45 s at 42°C in a heating block.
6. Incubate on ice for 2 min.
7. Add 250 µl of LB medium and mix by gently pipetting.
8. Incubate for 1 h at 37°C on a shaker.
9. Plate 100 µl cell suspension onto a LB agar plate.
10. Incubate the plate at 37°C overnight.

Plasmid DNA was isolated from single colonies using the E.Z.N.A. Plasmid DNA Mini Kit I according to manufacturer's instructions and sequenced with the appropriate primers (StarSEQ, Mainz). The correct plasmid DNA was re-transformed and purified using the Genopure Plasmid Maxi Kit according to manufacturer's instructions.

4.2 Cell culture

Cell culture experiments were performed under sterile conditions in an S1 laboratory using a cell culture laminar flow hood and sterile consumable materials. All cell culture media were stored at 4°C and pre-warmed before use in a water bath at 37°C. The cells were incubated in a humidified incubator at 37°C and 5% CO_2. Experiments involving viral particles were carried out under S2 conditions in a separate laboratory.

4.2.1 Immortalized cell lines

Immortalized cell lines were cultured in supplemented DMEM and passaged onto new 10 cm culture dishes approximately every four days. After washing with PBS, the dishes were

incubated with 1.5 ml trypsin-EDTA solution for ca. 5 min at RT to dissociate cell monolayers. Subsequently, 8.5 ml of fresh cell culture medium were added and the appropriate fraction of cells was transferred onto new 10 cm dishes. For experiments, cell numbers were measured using the Vi-CELL XR cell counter and cells were plated on poly-L-lysine treated dishes or plates to prevent cell dissociation. Therefore, dishes or plates were incubated with the poly-L-lysine solution for 15 min at RT. After removal of the solution, dishes or plates were washed with PBS. Cells were prepared for cryopreservation by completely removing the medium through centrifugation for 5 min at 1000 rpm and dissolving the cells in 1 ml of freezing medium. Afterwards, the cells were frozen at -80°C and transferred to liquid nitrogen for long-term storage.

Materials:

Cell culture medium:	DMEM
	10% FCS (v/v)
	1% Sodium pyruvate (v/v)
	5% Penicillin/Streptomycin (v/v)
Trypsin-EDTA solution:	0.05% Trypsin-EDTA (v/v) in PBS
	→ Store at 4°C
Poly-L-lysine solution:	0.01% Poly-L-lysine (w/v) in ddH_2O
	→ Sterile filtration, store at 4°C
Freezing medium:	5% DMSO (v/v) in FCS
	→ Store at -20°C

4.2.1.1 Transient transfection

Transient transfection of plasmid DNA was performed using Lipofectamine 2000 according to manufacturer's instructions. The medium was changed 4 h after transfection and cells were incubated for 72 h before testing for transgene expression. For conditioned cell culture supernatants, the medium was reduced to half of the recommended volume 24 h prior to sample collection.

4.2.1.2 Dose-response curve for antibiotic selection (Kill curve)

A kill curve is used to determine the optimal antibiotic concentration for selecting stable cell colonies. The parental cells are subjected to increasing amounts of antibiotic to determine the minimum concentration needed to kill all the cells over the course of one week. Subsequently, transfected cells are treated with this antibiotic concentration to eliminate all cells that did not incorporate the plasmid DNA containing the gene of interest and the antibiotic resistance gene. In parallel, non-transfected control cells are cultured under the same conditions to determine the timepoint when all negative cells are eliminated.

4.2.1.3 Production of lentiviral particles

Lentiviral particles were produced in 293FT cells using a third-generation lentiviral packaging system (Dull et al. 1998).

Day 1:

1. Seed $4x10^6$ cells on a poly-L-lysine coated 10 cm culture dish.
2. Incubate overnight at 37°C.

Day 2:

3. Change the medium to 7 ml Opti-MEM.
4. Incubate for 1 h at 37°C.
5. Add 4 µg of each packaging and envelope vector and 10 µg of the expression vector to 667 µl Opti-MEM in a 2 ml tube.

6. Mix by pipetting and incubate for 5 min at RT.
7. Add 26.6 µl Lipofectamine 2000 to 667 µl Opti-MEM in a 2 ml tube.
8. Mix by pipetting and incubate for 5 min at RT.
9. Add the plasmid containing solution to the solution with the transfection reagent.
10. Mix by pipetting and incubate for 20 min at RT.
11. Add the transfection mix to the cells.
12. Incubate for 24 h at 37°C.

Day 3:

13. Change the medium to 7 ml cell culture medium.
14. Incubate for 48 h at 37°C.

Day 5:

15. Remove the supernatant using a sterile 10 ml syringe and filter through a sterile filter.
16. Aliquot to 1 ml in Cryovials and store at -20°C.

4.2.1.4 Lentiviral transduction

Cells with inducible ADAMTS4 expression were generated using a lentiviral tetracycline-controlled expression system, consisting of ADAMTS4 expression vectors and the reverse tetracycline-controlled transactivator 3 (rtTA3) expression vector. Cells were infected sequentially with lentiviral particles expressing rtTA3 or ADAMTS4, with cells cultured to stability after each infection using the respective antibiotic for selection.

Materials:

Polybrene solution: 5 mg/ml in ddH_2O

Day 1:

1. Seed 5x10^5 cells per well on a poly-L-lysine coated 6-well plate.
2. Incubate for 24 h at 37°C.

Day 2:

3. Change the medium to 1 ml of cell culture medium and add 2 µl Polybrene per well for infection or change the medium to 2 ml for non-infected controls.
4. Thaw Cryovials containing lentiviral particles at 37°C for approximately 1 min.
5. Add 1 ml of lentiviral particles per well.
6. Incubate for 24 h at 37°C.

Day 3:

7. Change the medium to 2 ml of cell culture medium.
8. Incubate for 24 h at 37°C.

Day 4:

9. Remove the supernatant and discard.
10. Wash wells three times with PBS.
11. Add 0.5 ml trypsin-EDTA solution per well.
12. Incubate for 5 min at 37°C.
13. Resuspend the cells by adding 4.5 ml of cell culture medium per well.
14. Add 1 ml cell suspension to a 10 cm culture dish containing 9 ml of cell culture medium.
15. Add the respective antibiotic selection concentration and incubate at 37°C until non-infected cells are successfully eliminated.

4.2.1.5 Subcloning

All inducible ADAMTS4 cell lines were subcloned to obtain clones with a uniform culture derived from a single cell. Stably transfected mass cultures are highly heterogenous in their expression levels of the gene of interest. The cell suspension is diluted serially so that only 1 cell per well is plated on a 96-well plate. After approximately one week, single cell-derived colonies are trypsinized and transferred to 12-well plates. When the colonies are large

enough, they are transferred to 10 cm culture dishes and checked for ADAMTS4 expression to pick three clones with the best expression levels.

4.2.1.6 Induction with doxycycline (DOX)

Materials:

Doxycycline solution: 50 µg/ml Doxycycline in ddH_2O

→ Sterile filtration, store at 4°C

The cells generated for inducible ADAMTS4 expression employ a Tet-On system. The rtTA protein is only capable to bind to the ADAMTS4 promoter when it is bound by a tetracycline. Transcription of ADAMTS4 was initiated by adding 100 ng/ml of doxycycline (1:500), a tetracycline derivative, to cells of 90% confluency for 24 h. To generate conditioned supernatants, the medium was changed to half of the initial volume with the same final DOX concentration and incubated for an additional 24 h before sample collection.

	Volume of cell culture medium [ml]	
Plate size	**Normal culture**	**Conditioned supernatants**
6-well plate	2	1
10 cm culture dish	10	5

4.2.1.7 Immunocytochemistry

Immunocytochemistry is used to analyze the localization of a protein of interest in cells. A specific primary antibody is bound by a secondary antibody that has a conjugated fluorophore and thereby allows visualization of the protein under a fluorescence microscope.

Materials:

TBS, pH 7.4: 25 mM TRIS

137 mM NaCl

2.7 mM KCl

Fixation solution: 4% PFA (w/v) in ddH_2O

→ Store at -20°C

Permeabilization solution stock: 10% Saponin (w/v) in ddH_2O

→ Store at -20°C

→ Working solution: dilute 1:10 in TBS

Blocking solution: 5% BSA (w/v) in TBS

→ Sterile filtration

Antibody buffer: 4% BSA (w/v) in TBS

→ Sterile filtration

Primary antibody		**Secondary antibody**		
Name	**Dilution**	**Name**	**Conjugate**	**Dilution**
Anti-V5 tag	1:250	Anti-mouse IgG	Alexa Fluor 594	1:500
CT-15	1:500	Anti-rabbit IgG	Alexa Fluor 488	1:500

Day 1:

1. Seed 5x10^4 cells per well on poly-L-lysine coated coverslips in a 24-well plate.
2. Incubate for 24 h at 37°C.

Day 2:

3. Change the medium to cell culture medium containing 100 ng/ml DOX.
4. Incubate for 24 h at 37°C.

Day 3:

5. Remove the medium and wash wells with TBS.

6. Fix the cells with 1 ml of the fixation solution for 10 min at RT.
7. Wash wells twice with TBS.
8. Permeabilize the cells with 1 ml of the permeabilization solution for 20 min at RT.
9. Wash wells with TBS.
10. Block with 1 ml of the blocking solution for 1 h at RT.
11. Wash wells with TBS.
12. Incubate with primary antibodies diluted in 350 µl antibody buffer for 1 h at RT.
13. Wash wells three times with TBS.
14. Incubate with secondary antibodies diluted in 350 µl antibody buffer for 1 h at RT in the dark.
15. Wash wells three times with TBS.
16. Add 1 ml ddH_2O.
17. Mount the coverslips in mounting medium with DAPI onto microscope slides.
18. Let the mounting medium harden overnight at RT in the dark.
19. Analyze the slides using a confocal microscope.

4.2.1.8 BACE1 inhibitor treatment

Materials:

Inhibitor solution: 100 µM β-secretase inhibitor IV in cell culture medium

Day 1:

1. Seed $1x10^6$ cells per well on a poly-L-lysine coated 6-well plate.
2. Incubate for 24 h at 37°C.

Day 2:

3. Change the medium to 2 ml of cell culture medium containing 1 µM BACE-IV inhibitor (1:100) or DMSO control of the same concentration (0.01%) for non-treated cells.
4. Incubate for 24 h at 37°C.

Day 3:

5. Change the medium to 2 ml of cell culture medium containing BACE-IV or DMSO control and add 100 ng/ml DOX for induced cells.
6. Incubate for 24 h at 37°C.

Day 4:

7. Change the medium to 1 ml of cell culture medium containing the appropriate combination of BACE-IV, DMSO and DOX.
8. Incubate for 24 h at 37°C.

Day 5:

9. Collect the supernatant.

4.2.2 Primary oligodendrocyte culture

Oligodendrocyte progenitor cells (OPCs) were derived from C57Bl/6J wildtype or ADAMTS4$^{-/-}$ knockout mice. Sorted cells were cultured in supplemented DMEM/F12 and passaged onto new poly-L-lysine coated 10 cm culture dishes at 1.5x10^6 cells per dish approximately every four days. After removal of the medium, the dishes were incubated with 1.5 ml Accutase for 20 min at 37°C to dissociate cell monolayers. Addition of 5 ml PBS stopped the reaction and the solution was transferred to a 50 ml tube and centrifuged at 1000 rpm for 5 min. The supernatant was discarded and cells were resuspended in proliferation medium. Cell numbers were measured using the Vi-CELL XR cell counter and cells were plated on poly-L-lysine treated dishes or plates to prevent cell dissociation. Therefore, dishes or plates were incubated with the poly-L-lysine solution for 30 min at 37°C. After removal of the solution, dishes or plates were washed with PBS. OPCs spontaneously differentiate into mature oligodendrocytes when

plated at high density or after prolonged time in culture. Keep OPCs only up to approximately three weeks in culture and do not incubate to more than 50% confluency.

Materials:

Proliferation medium:	DMEM/F12, no glutamine
	1x GlutaMAX
	1x B-27 supplement, minus vitamin A
	1% Penicillin/Streptomycin (v/v)
	20 ng/ml FGF
	20 ng/ml PDGF
FGF and PDGF stock solution:	20 µg/ml FGF or PDGF in PBS + 0.1% BSA (v/v)
	→ Store at -80°C
	→ Add to medium directly before use (1:1000)

1. Decapitate the newborn mice (P1-P3) using scissors.
2. Dissect the whole brain and put it into a 10 cm culture dish containing cold PBS.
3. Place on ice while preparing additional brains.
4. Remove the meninges with forceps under a binocular microscope.
5. Transfer the brain into a 10 cm culture dish containing cold DMEM/F12.
6. Place on ice while preparing additional brains.
7. Disintegrate the brain with a scalpel.
8. Pipette the solution containing disintegrated brains into a 15 ml tube.
9. Centrifugation: 300 x g, 2 min, RT

10. Use the Neural Tissue Dissociation Kit (P) and follow manufacturer's instructions for manual dissociation but use PBS instead of HBSS.

11. Use Anti-A2B5 Microbeads for labeling and separate cells using MS columns according to manufacturer's instructions.

12. Determine the cell number and seed $1.5x10^6$ cells per poly-L-lysine coated 10 cm culture dish.

4.2.2.1 Adenoviral transduction

The APP695sw adenovirus was generated using the AdEasy system (Luo et al. 2007). Subsequently, adenoviral particles were sent to a service provider for amplification and purification (GeneCust, Luxembourg).

Day 1:

1. Seed $4x10^6$ cells on a poly-L-lysine coated 10 cm culture dish.

2. Incubate overnight at 37°C (less than 24 h to ensure that cells have not proliferated).

Day 2:

3. Change the medium to proliferation medium containing 1000 plaque-forming units (PFU)/cell adenoviral particles or proliferation medium for the non-infected control.

4. Incubate for 4 h at 37°C.

5. Wash plates with DMEM/F12 and add fresh proliferation medium.

6. Incubate for 24 h at 37°C.

Day 3:

7. Change the medium to 4 ml proliferation medium.

8. Incubate for 24 h at 37°C.

Day 4:

9. Collect the supernatant and prepare the cell lysate.

4.2.2.2 Oligodendrocyte differentiation

Differentiation of primary OPC cultures was carried out by our collaborative partner in the research group of Dr. Carsten Berndt (Department of Neurology, University of Duesseldorf).

Materials:

Differentiation medium:	DMEM/F12, no glutamine
	1x GlutaMAX
	1x B-27 supplement
	1% Penicillin/Streptomycin (v/v)
	40 ng/ml T3
	40 ng/ml T4
T3 and T4 stock solution:	40 µg/ml T3 or T4 in PBS
	→ Store at -20°C
	→ Add to medium directly before use (1:1000)

Day 1:

1. Seed $4x10^5$ cells per well on a poly-L-lysine coated 6-well plate in proliferation medium.
2. Incubate for 24 h at 37°C.

Day 2:

3. Collect the cells from the respective wells for d0 (non-differentiated control) as follows:
   a. Remove the supernatant and add 1 ml cold PBS.
   b. Scrape the cells off the plate and fill the solution into a 2 ml tube.
   c. Centrifugation: 13000 rpm, 3 min, 4°C
   d. Discard the supernatant and store the pellet at -20°C until RNA extraction.
4. For the remaining wells, change the medium to differentiation medium.

5. Incubate for 24 h or 72 h respectively at 37°C.

Day 3:

6. Collect the cells from the respective wells for d1 (day 1 of differentiation) as described above.

Day 5:

7. Change the medium to fresh differentiation medium.

8. Incubate for 48 h at 37°C.

Day 7:

9. Collect the cells for d5 as described above.

4.2.3 Supernatant and cell lysate preparation

Conditioned cell culture supernatant was collected for the analysis of secreted proteins and cells were lysed with NP-40 buffer to analyze intracellular proteins.

Materials:

25x Protease inhibitor (PI):	Dissolve one Protease inhibitor cocktail tablet per 2 ml ddH_2O. Store at -20°C.
NP-40 buffer:	50 mM TRIS-HCl, pH 7.8
	150 mM NaCl
	1% NP-40 (v/v)
	0.02% NaN_3 (w/v)
	→ Store at 4°C

1. Transfer the conditioned cell culture medium into a tube.
2. Add the appropriate amount of 1x PI (1:25).
3. Centrifugation: 13,000 rpm (volume < 2 ml) or 4000 rpm (> 2 ml), 3 min, 4°C
4. Transfer the supernatant into a fresh tube and store at -80°C.
5. Wash wells with cold PBS.
6. Add fresh, cold PBS and scrape the cells off the plate.
7. Transfer the scraped cells into a tube.
8. Centrifugation: 13,000 rpm (volume < 2 ml) or 4000 rpm (> 2 ml), 3 min, 4°C
9. Discard the supernatant and resuspend the cell pellet in NP-40 buffer + 1x PI.
10. Incubate the cell solution on ice for 20 min and vortex every 5 min.
11. Centrifugation: 13,000 rpm, 15 min, 4°C
12. Transfer the supernatant into a fresh tube and store at -20°C.

4.3 Transgenic mice

4.3.1 Housing and Breeding

Transgenic mice were housed and bred by our collaborative partner in the research group of Dr. Oliver Wirths (Department of Psychiatry, University of Goettingen). All experimental procedures in this thesis that involved animals were approved by the institutional animal care and use committee at University Medicine Goettingen. All animals were handled according to German guidelines for animal care and they were housed in groups of four in standard laboratory cages (33 cm×18 cm×14 cm) with food and water provided ad libitum.

The generation of 5xFAD mice (Tg6799) has been described previously (Oakley et al. 2006). 5xFAD mice were backcrossed for more than 10 generations to C57Bl/6J wildtype mice to obtain an incipient congenic line on a C57Bl/6J genetic background (Jawhar et al. 2012). Heterozygous ADAMTS4$^{+/-}$ knockout mice (strain: B6.129P2-*Adamts4*^{tm1Dgen}/J) were obtained from The Jackson Laboratory. To generate ADAMTS4 knockout mice in the 5xFAD background,

heterozygous ADAMTS4$^{+/-}$ mice were first crossed to generate homozygous ADAMTS4$^{-/-}$ knockout mice. These mice were crossed to heterozygous 5xFAD mice, which generated 5xFAD$^{+/-}$ / ADAMTS4$^{+/-}$ animals. These were crossed again to heterozygous ADAMTS4$^{+/-}$ knockout mice, which yielded the desired genotype 5xFAD$^{+/-}$ / ADAMTS4$^{-/-}$. To generate a sufficient number of mice with the desired genotype, these mice were repeatedly crossed with heterozygous ADAMTS4$^{+/-}$ knockout mice. In addition, the ADAMTS4 knockout mice have been backcrossed for more than 7 generations to C57Bl/6J wildtype mice.

4.3.2 Brain extraction

Brain preparation was carried out by our collaborative partner in the research group of Dr. Oliver Wirths (University of Goettingen). Mice were anesthetized using CO_2 asphyxiation, decapitated, and brain hemispheres were dissected and immediately deep frozen. Frozen hemispheres were sent either to our laboratory or to our collaborative partner in the research group of Dr. Patrick Fraering (Foundation Eclosion, Switzerland) for protein extraction and analysis.

4.3.2.1 TBS and SDS fractions

Materials:

25x Protease inhibitor (PI):	Dissolve one Protease inhibitor cocktail tablet per 2 ml ddH_2O. Store at -20°C.
TBS lysis buffer, pH 8.0:	120 mM NaCl 50 mM TRIS 1x PI
SDS lysis buffer:	2% SDS (w/v) in ddH_2O + 1x PI

1. Weigh the frozen hemisphere using a precision scale.
2. Homogenize the hemisphere in 7x volume of TBS lysis buffer using a pestle tissue grinder.
3. Transfer the solution into a 2 ml tube.
4. Centrifugation: 17,000 x g, 20 min, 4°C
5. Transfer the supernatant (TBS fraction) into a new 2 ml tube and store at -80°C.
6. Dissolve the pellet in 800 µl SDS lysis buffer by sonication.
7. Centrifugation: 17,000 x g, 20 min, RT
8. Transfer the supernatant (SDS fraction) into a new 2 ml tube and add 1 µl Benzonase.
9. Incubate for 5 min on a rotary shaker at RT and afterwards store at -80°C.

4.3.2.2 FA fraction

Formic acid extraction of Aβ peptides from brain hemispheres was carried out by our collaborative partner in the research group of Dr. Patrick Fraering (Foundation Eclosion, Plan-Les-Ouates, Switzerland).

Materials:

25x Protease inhibitor (PI):	see 4.3.2.1
PBS, pH 7.4:	137 mM NaCl
	2.7 mM KCl
	8 mM Na_2HPO_4
	1.5 mM KH_2PO_4

1. Homogenize the frozen hemisphere in liquid nitrogen.
2. Resuspend the brain powder in 300 µl PBS + 1x PI by sonication.
3. Add 660 µl formic acid and dissolve by sonication.
4. Centrifugation: 17,000 x g, 20 min, 4°C
5. Transfer the supernatant (FA fraction) into a new tube and store at -80°C until IP/MS analysis.

4.3.3 Immunohistochemistry

Brain preparation and immunohistochemical analysis was carried out by our collaborative partner in the research group of Dr. Oliver Wirths (University of Goettingen). Mice were anesthetized using CO_2 asphyxiation, decapitated, and brain hemispheres were dissected and post-fixed in 4% phosphate-buffered formalin at 4°C. Immunohistochemistry was performed on 4 µm sagittal paraffin sections as described previously (Wirths *et al.* 2002, Huttenrauch *et al.* 2016).

Primary antibody		**Secondary antibody**		
Name	**Dilution**	**Name**	**Conjugate**	**Dilution**
Anti-GFAP	1:1000	Anti-guinea pig IgG	DyLight 488	1:500
Anti-Iba1	1:1000	Anti-guinea pig IgG	DyLight 488	1:500
Anti-CNPase	1:1000	Anti-mouse IgG	DyLight 594	1:500
Anti-β-Galactosidase	1:500	Anti-rabbit IgG	DyLight 594 or DyLight 488	1:500
PSL-029-2	1:500	Anti-guinea pig IgG	Biotin	1:200

Secondary antibodies were either conjugated to fluorescent dyes for analysis of co-localization or biotin to stain Aβ peptides. The Aβ staining was visualized with the ABC method using a Vectastain kit and diaminobenzidine (DAB) as chromogen.

4.4 Protein analysis

4.4.1 Bicinchoninic acid (BCA) protein assay

Protein concentrations from cell lysates or extracted brain fractions were measured against a BSA standard using the BCA Protein Assay Kit.

1. Prepare a 1 mg/ml BSA stock solution in the respective sample buffer:

   a. Cell lysates: NP-40 buffer (see 4.2.3)

   b. Brain fractions: Respective homogenization buffer (see 4.3.2.1)

2. For the standard, dilute the BSA stock solution as follows:

Final BSA concentration [µg/ml]	Volume of BSA stock solution [µl]	Volume of sample buffer [µl]
0	0	100
100	10	90
200	20	80
300	30	70
400	40	60
500	50	50
600	60	40

3. Load 25 µl per well of the BSA standard in duplicates onto a 96-well plate.
4. Load 22.5 µl per well of sample buffer and add 2.5 µl of the respective sample.
5. Mix BCA Reagent A and B in a 50:1 ratio.
6. Add 200 µl of the mixed BCA reagent solution to the BSA standard and the protein samples.
7. Incubate the plate for 30 min at 60°C.
8. Measure the absorbance at 540 nm wavelength using a microplate reader and calculate the sample concentration.

4.4.2 SDS-Polyacrylamide gel electrophoresis (SDS-PAGE)

SDS-PAGE is a method to separate proteins based on their molecular weight. The anionic detergent SDS binds to the amino acids of the proteins, denatures all structural elements and provides these now linear polypeptide chains with a negative charge. The proteins can then be separated by their charge to mass ratio within an applied electric field. Therefore, they are loaded onto gels that consist of acrylamide which has been cross-linked with bisacrylamide to form networks of polyacrylamide. This polymerization is initiated by adding a source (APS) and a stabilizer (TEMED) of free radicals.

Materials:

Bis-Tris buffer:	1.6 M Bis-Tris, pH 6.4
	→ Sterile filtration
APS solution:	10% APS (w/v) in ddH_2O
	→ Store at 4°C
MES buffer:	50 mM MES
	50 mM TRIS
	3.5 mM SDS
	1 mM EDTA
4x SDS sample buffer:	1.44 M Bis-Tris
	0.64 M Bicine
	100 mM DTT
	4% SDS (w/v)
	25% Glycerol (w/v)

0.05% Bromophenol blue (w/v)

1. Prepare the resolving solution for a Bis-Tris gel with the respective polyacrylamide concentration as follows:

	Resolving solution		**Stacking solution**
	12%	**7%**	
30% Acrylamide/Bisacrylamide (37.5:1)	2.64 ml	1.54 ml	350 µl
Bis-Tris buffer	1.65 ml	1.65 ml	500 µl
ddH_2O	2.26 ml	3.36 ml	1.14 ml
APS solution	33 µl	33 µl	20 µl
TEMED	11 µl	11 µl	5 µl

2. Fill the resolving gel solution into a Novex gel cassette and overlay with 0.5 ml ddH_2O.
3. Let the gel polymerize for 15 min at RT.
4. Prepare the stacking solution.
5. Remove ddH_2O, fill the stacking gel solution on top of the resolving gel and add a 12-tooth comb.
6. Let the gel polymerize for 10 min at RT.
7. Remove the comb and wash the 12 slots with ddH_2O.
8. Place the gel cassette into the electrophoresis chamber and fill the electrophoresis chamber with MES buffer.
9. Dilute the protein samples in 4x SDS sample buffer to a total volume of 20 µl.
10. Heat the samples for 5 min at 95°C and spin them down.
11. Load the 20 µl protein samples and 3 µl of the Protein ladder onto the gel.
12. Run the SDS-PAGE at 150 V for approximately 1 h.

4.4.3 Western Blot

Separated proteins are transferred from the gel onto a PVDF membrane by wet Western blotting. Subsequently, proteins are immunostained by application of specific antibodies.

Materials:

Transfer buffer:	25 mM TRIS
	192 mM Glycine
	20% Ethanol (v/v)
	→ Store at 4°C

1. Prepare one transfer cassette with 2 sponges and 2 Whatman filter papers per Western blot.
2. Place the transfer cassette in the tank blotter and fill it with transfer buffer.
3. Activate the PVDF membrane with ethanol for 1 min then rinse in transfer buffer.
4. Take out the transfer cassette and build the blotting sandwich as follows:

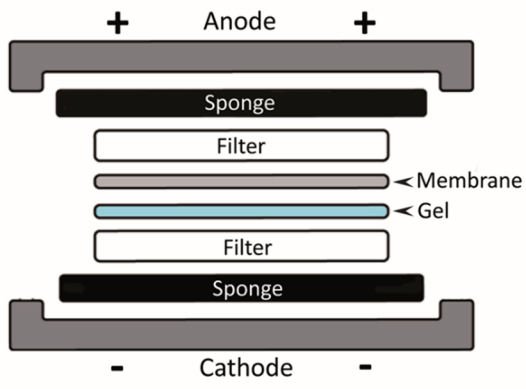

5. Place the transfer cassette in the tank blotter.
6. Blot at 200 mA for 90 min at 4°C.

4.4.3.1 Immunostaining of membranes

Materials:

TBS, pH 7.4: 25 mM TRIS

137 mM NaCl

2.7 mM KCl

TBST: TBS + 0.1% Tween-20 (v/v)

Blocking solution: 3% Gelatin from cold water fish skin (w/v) in PBS

Primary antibody		**Secondary antibody**		
Name	**Dilution**	**Name**	**Conjugate**	**Dilution**
Anti-Actin	1:2000	Rabbit IgG	IRDye 800CW	1:10,000
CT-15	1:3500			
Anti-FLAG M2	1:1000	Mouse IgG	IRDye 800CW	1:10,000
Anti-V5 Tag	1:500			
IG7/5A3	1:1000			
22C11	1:1000			
6A1	1:50			

Day 1:

1. After Western blotting, put the membrane into a blot container on a shaker.
2. Block the membrane with the blocking solution for 1 h at RT.
3. Wash the membrane with TBST for 5 min.
4. Incubate the membrane with the primary antibody diluted in TBST overnight at 4°C.

Day 2:

5. Wash the membrane twice for 30 min with TBST.
6. Incubate the membrane with the secondary antibody diluted in TBST for 1 h at RT in the dark.
7. Wash the membrane twice for 30 min with TBST.

8. Wash the membrane with TBS for 5 min.

9. Analyze the fluorescent signal using the LI-COR ODYSSEY CLx.

The LI-COR system employs near-infrared fluorescent signals to detect antibody-labelled proteins. For quantitative analysis, the fluorescence signal was calculated using the Image Studio Software 2.1.

4.4.4 Immunoprecipitation (IP)

IP is a method to detect and purify antigens. The antibody against the target protein is bound to a solid matrix by covalent binding to an attached IgG antibody. The matrix-bound antibody is incubated with the sample solution and forms an immune complex with the specific target protein. After washing of the immobilized complex to eliminate any proteins that are not precipitated, the bound protein can be used for analysis.

4.4.4.1 Antibody coupling

Materials:

IP buffer: 0.1% BSA (w/v) in PBS

→ Sterile filtration

1. Pipet 1 ml of Dynabeads M-280 with the respectively attached IgG into a 1.5 ml tube.

2. Immobilize the beads with a magnet for 2 min.

3. Remove the supernatant and add 1 ml IP buffer.

4. Incubate for 3 min on a rotary shaker at RT.

5. Spin down and immobilize the beads with a magnet for 2 min.

6. Remove the supernatant and repeat washing step.

7. Add 1 ml IP buffer containing 40 µg of antibody as follows:

Antibody		Dynabeads coupled to
Name	**Volume [µl]**	
Anti-V5 Tag	80	Mouse IgG
Anti-FLAG M2	40	
CT-15	40	Rabbit IgG

8. Incubate for 2 h on a rotary shaker at RT.
9. Spin down and immobilize the beads with a magnet for 2 min.
10. Wash the beads four times for 30 min with IP buffer on a rotary shaker at 4°C.
11. Spin down and immobilize the beads with a magnet for 2 min.
12. Remove the washing buffer and store the beads in 1 ml of IP buffer containing 0.02% NaN_3 at 4°C.

4.4.4.2 ADAMTS4 *in vitro* assay

The catalytic activity of secreted ADAMTS4 was analyzed using an *in vitro* assay. The immunoprecipitated, antibody-bound ADAMTS4 was incubated with the possible substrate of Aβ1-40 recombinant peptides. The cleavage product Aβ4-40 was subsequently detected in the supernatant by ELISA analysis.

Materials:

IP buffer: see 4.4.4.1

Cell culture medium: see 4.2.1

4x SDS sample buffer: see 4.4.2

→ Working solution (1x): dilute 1:4 in ddH_2O

Day 1:

1. Add 25 µl of anti-V5 tag antibody-coupled beads to 1 ml of conditioned cell culture supernatant.
2. Incubate for 2 h on a rotary shaker at RT.
3. Spin down and immobilize the beads with a magnet for 2 min.
4. Remove the supernatant and wash the beads twice with IP buffer.
5. Add 350 µl of fresh cell culture medium containing 15 ng Aβ1-40.
6. Incubate overnight at 37°C on a shaker.

Day 2:

7. Spin down and immobilize the beads with a magnet for 2 min.
8. Transfer the supernatant into a fresh tube and store at -80°C until ELISA analysis.
9. Add 25 µl of 1x SDS sample buffer to the beads.
10. Heat the samples for 5 min at 95°C.
11. Spin down and immobilize the beads with a magnet for 2 min.
12. Transfer the supernatant into a fresh tube and store at -20°C until analysis with SDS-PAGE and Western Blot.

4.4.4.3 Co-Immunoprecipitation (Co-IP)

Co-IP is based on the fact that the IP reaction can also capture other proteins that are bound to the primary target. The antigen and possible interaction partners are eluted from the matrix and analyzed by SDS-PAGE and Western Blot.

Materials:

IP buffer:	see 4.4.1
TRIS buffer:	10 mM TRIS, pH 7.5

4x SDS sample buffer: see 4.4.2

→ Working solution (1x): dilute 1:4 in ddH_2O

Day 1:

1. Add 25 µl of antibody-coupled beads to the cell lysate solution with 100 µg of total protein and fill up to 500 µl total volume with NP-40 buffer.
2. Incubate overnight on a rotary shaker at 4°C.

Day 2:

3. Spin down and immobilize the beads with a magnet for 2 min.
4. Remove the supernatant and wash the beads three times for 5 min with IP buffer on a rotary shaker at RT.
5. Spin down and immobilize the beads with a magnet for 2 min.
6. Remove the washing buffer and wash the beads with TRIS buffer for 3 min on a rotary shaker at RT.
7. Spin down and immobilize the beads with a magnet for 2 min.
8. Remove the TRIS buffer and add 25 µl of 1x SDS sample buffer.
9. Heat the samples for 5 min at 95°C.
10. Spin down and immobilize the beads with a magnet for 2 min.
11. Transfer the supernatant into a fresh tube and store at -20°C until analysis with SDS-PAGE and Western Blot.

4.4.5 Enzyme-linked immunosorbent assay (ELISA)

Aβ peptide levels in cell culture supernatants and brain fractions were analyzed using a sandwich ELISA system. Capture antibodies specifically detecting the N- or C-terminal ends of the Aβ peptide are bound to a microtiter plate. Antigens from the sample are then immobilized to the plate by antibody binding. Addition of a specific secondary antibody directed at the other end of the Aβ peptide leads to a complex formation with the antigen.

This detection antibody is covalently linked to the enzyme horseradish peroxidase (HRP) which produces a detectable color change relative to the quantity of antigen in the sample when the suitable substrate is added.

4.4.5.1 HRP coupling of detection antibodies

Materials:

Carbonate buffer: 0.06 M $NaHCO_3$

0.14 M Na_2CO_3

→ Autoclave and store at RT

PBS, pH 7.4: 137 mM NaCl

2.7 mM KCl

8 mM Na_2HPO_4

1.5 mM KH_2PO_4

→ Autoclave and store at RT

Day 1:

1. Immerse a Slide-A-Lyzer Dialysis Cassette in carbonate buffer for 30 s.
2. Dilute the antibody in carbonate buffer to a total volume of 1 ml.

   a. BAP-24, BAP-15, and BAP-29: 1 mg/ml

   b. PSL-029-2: 0.5 mg/ml
3. Fill the antibody solution into a syringe and inject the sample through one of the syringe ports.
4. Remove excess air from the cassette with the syringe and then eject the syringe.
5. Place the cassette into the float buoy and put it into 1 l of carbonate buffer.

6. Dialyze overnight at 4°C with gentle stirring.

Day 2:

7. Fill a new syringe with a volume of air equal to the sample size.
8. Insert the needle into a different syringe port and introduce the air into the cassette.
9. Withdraw the sample into the syringe.
10. Inject the sample into the HRP vial of the EZ-Link Plus Activated Peroxidase kit.
11. Incubate for 1 h on a rotary shaker at RT.
12. Add 10 µl reductant solution.
13. Incubate for 15 min at RT under the fume hood.
14. Add 20 µl Quench buffer.
15. Incubate for 15 min at RT.
16. Fill the sample into a new dialysis cassette as described above.
17. Dialyze against 1 l of PBS overnight at 4°C with gentle stirring.

Day 3:

18. Withdraw the sample with a new syringe as described above and fill into a tube.
19. Add 1 ml of glycerol to the HRP-coupled antibody solution.
20. Aliquot and store at -20°C.

4.4.5.2 IC16 and PSL-029-2 ELISA

Materials:

PBS, pH 7.4:	see 4.4.5.1
PBST:	PBS + 0.05% Tween-20 (v/v)

Assay buffer: PBS

1% BSA (w/v)

0.05% Tween-20 (v/v)

→ Sterile filtration, store at 4°C

Stop solution: 2 M H_2SO_4

Day 1:

1. Dilute the capture antibody in PBS to the respective final concentration as follows:

Antibody			
Name	**Epitope**	**Final concentration**	**Aβ peptides to be detected**
BAP-24	Aβx-40 C-terminus	3 µg/ml	4-40
BAP-15	Aβx-42 C-terminus		4-42
IC16	Aβ1-x N-terminus	4 µg/ml	1-40, 1-42, and 1-38

2. Add 100 µl per well of the capture antibody solution to a 96-well high-binding plate.

3. Incubate overnight at 4°C.

Day 2:

4. Prepare the respective Aβ standards diluted in assay buffer as follows:

Aβ standard peptides [ng/ml]				
1-40	**1-42**	**1-38**	**4-40**	**4-42**
6	3	4	0.75	1.5
4	2	3	0.5	1
3	1.5	2	0.375	0.75
2	1	1.5	0.25	0.5
1.5	0.5	1	0.125	0.25
1	0.25	0.5	0.0625	0.125
0.5	0.125	0.25	0.03125	0.0625
0	0	0	0	0

5. Remove the capture antibody solution and add 50 µl assay buffer per well.

6. Add 50 µl of standard + 50 µl of respective buffer per well in duplicates.

   a. Conditioned cell culture supernatants: Cell culture medium (see 4.2.1)

   or proliferation medium (see 4.2.2)

   b. Brain fractions: Assay buffer

7. Add 100 µl of sample diluted in medium or assay buffer per well in duplicates.

8. Dilute the detection antibody in assay buffer as follows:

HRP-coupled antibody			
Name	**Epitope**	**Dilution**	**Aβ peptides to be detected**
BAP-24	Aβx-40 C-terminus	1:1000	1-40
BAP-15	Aβx-42 C-terminus		1-42
BAP-29	Aβx-38 C-terminus		1-38
PSL-029-2	Aβ4-x N-terminus	1:200	4-40 and 4-42

9. Add 50 µl of the detection antibody solution per well to standards and samples.

10. Incubate overnight at 4°C.

Day 3:

11. Remove the supernatant, wash wells three times with 100 µl/well PBST and once with 100 µl/well PBS.

12. Add 50 µl of TMB-ELISA substrate solution per well.

13. Incubate at RT until solution shows blue color (approximately 5 min).

14. Add 50 µl of stop solution per well.

15. Measure the absorbance at 450 nm wavelength using a microplate reader and calculate the sample concentration.

4.4.5.3 4G8 ELISA

Materials:

Well-coating buffer, pH 8.5:	200 mM Na_2HPO_4
	2 mM NaH_2PO_4
	0.1% NaN_3 (w/v)
	→ Sterile filtration, store at 4°C
Well fixing buffer, pH 7.4:	90 mM Na_2HPO_4
	7 mM NaH_2PO_4
	73 mM Sucrose
	0.25% BSA (w/v)
	0.1% NaN_3 (w/v)
	→ Sterile filtration, store at 4°C
Specimen diluent, pH 7.4:	1,7 mM Na_2HPO_4
	15 mM NaH_2PO_4
	145 mM NaCl
	0.05% Triton X-100 (v/v)
	0.6% BSA (w/v)
	0.1% NaN_3 (w/v)
	→ Sterile filtration, store at 4°C
PBS, pH 7.4:	see 4.4.5.1

Day 1:

1. Dilute the capture antibody (4G8) in well-coating buffer to a final concentration of 3 µg/ml.
2. Add 100 µl per well of the capture antibody solution to a 96-well high-binding plate.
3. Incubate overnight at RT.

Day 2:

4. Remove the capture antibody solution.
5. Add 300 µl of well fixing buffer per well.
6. Incubate for 1 h at RT.
7. Remove the well fixing buffer and wash wells three times with 100 µl/well PBS.
8. Prepare the Aβ standards diluted in specimen diluent as follows:

Aβ standard peptides [ng/ml]	
1-40	**1-42**
6	3
4	2
3	1.5
2	1
1.5	0.5
1	0.25
0.5	0.125
0	0

9. Add 100 µl of standard per well in duplicates.
10. Add 100 µl of sample diluted in specimen diluent per well in duplicates.
11. Incubate for 2 h at RT.
12. Remove the sample solution and wash wells three times with 100 µl/well PBS.
13. Dilute the respective HRP-coupled detection antibody 1:1000 in specimen diluent.

    a. BAP-24: detects Aβx-40 peptides

b. BAP-15: detects Aβx-42 peptides

14. Add 50 µl of the detection antibody solution per well to standards and samples.
15. Incubate for 2 h at RT.
16. Remove the detection antibody solution and wash wells three times with 100 µl/well PBS.
17. Prepare the substrate solution using the QuantaBlu Fluorogenic Peroxidase Substrate Kit.
18. Add 100 µl of substrate solution per well.
19. Incubate for 20 min at RT.
20. Add 100 µl of stop solution from the kit.
21. Measure the fluorescence at 325/420 nm wavelength using a microplate reader and calculate the sample concentration.

4.4.6 Matrix Assisted Laser Desorption Ionization - Time of Flight - Mass Spectrometry (MALDI-TOF-MS) analysis

Conditioned cell culture supernatants and brain hemispheres for FA extraction were sent to our collaborative partner in the research group of Dr. Patrick Fraering (Foundation Eclosion, Plan-Les-Ouates, Switzerland; formerly EPFL Lausanne). IP/MS analysis of Aβ peptides was carried out as described previously using either a mixture of 4G8 and 6E10 antibodies or only the 4G8 antibody (Alattia *et al.* 2011, Dimitrov *et al.* 2013, Gerber *et al.* 2017).

4.5 Expression analysis with quantitative real-time PCR (qPCR)

4.5.1 Primary oligodendrocyte cultures

RNA extraction and cDNA synthesis from oligodendrocytes at different timepoints of differentiation was carried out by our collaborative partner in the research group of Dr. Carsten Berndt (University of Duesseldorf) as described previously (Lepka *et al.* 2017). The

cDNA was subsequently used as a template in qPCR analysis to quantitate the respective gene expression. This method combines PCR amplification and quantitative detection of gene expression products. A fluorescent dye (SYBR Green), which emits fluorescence only when bound to double-stranded DNA, is used to label PCR products during thermal cycling. The accumulation of fluorescent signal is measured during the exponential phase of the reaction and is directly proportional to the amount of target in the input sample.

1. Prepare the 13x Master Mix for one target gene primer pair as follows:

Reagent	**Volume [µl]**
SYBR Green	130
Forward Primer (10 µM)	13
Reverse Primer (10 µM)	13
Sterile H_2O	65

2. Add 17 µl of master mix per well on a Fast Optical 96-well reaction plate in the following pattern:

	Target gene primer pair			
Sample	**ADAMTS4**	**CNPase**	**MBP**	**GAPDH**
cDNA d0	3x	3x	3x	3x
cDNA d1	3x	3x	3x	3x
cDNA d5	3x	3x	3x	3x
Sterile H_2O	3x	3x	3x	3x

3. Dilute the cDNA 1:5 in sterile H_2O (1 µg RNA was used for cDNA synthesis).

4. Add 3 µl of cDNA per well or add 3 µl sterile H_2O per well as control.

5. Seal the plate with Optical adhesive film and spin down.

6. Analyze in a Real-Time PCR Cycler and calculate the relative expression levels.

For quantitative analysis, the fluorescence signal was calculated with the StepOnePlus Software 2.0 using the $2^{-\Delta\Delta C_T}$ method. Expression levels were normalized twice; first to the housekeeping gene GAPDH and then to the expression levels of non-differentiated controls at d0.

4.5.2 Human brain samples

Human brain tissue was obtained from The Netherlands Brain Bank (www.brainbank.nl). RNA extraction, cDNA synthesis, and qPCR analysis of human brain samples was carried out as described previously (Bien et al. 2012).

5. Results

5.1 Effects of ADAMTS4 on APP processing and Aβ generation in a tissue culture model with inducible ADAMTS4 expression

Based on the ADAMTS4 consensus cleavage motif as described by Hills et al., the Aβ sequence contains two putative ADAMTS4 cleavage sites after the glutamic acid residues in position 3 and 11 (Hills et al. 2007) [Figure 8].

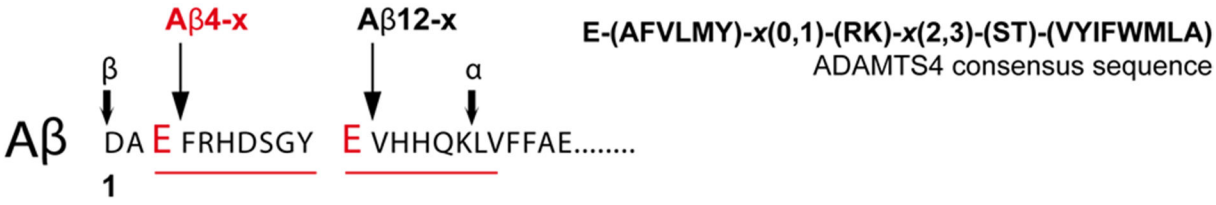

Figure 8: Putative ADAMTS4 cleavage sites in the Aβ sequence based on the ADAMTS4 consensus sequence described by Hills et al. (Hills et al. 2007). Cleavage at those positions would produce N-terminally truncated Aβ peptides Aβ4-x and Aβ12-x.

In preliminary experiments with transient overexpression of ADAMTS4 in HEK293-APP695sw cells, we had seen an increase in total Aβ levels by Western blotting of tissue culture supernatants (data not shown). Since high, transient overexpression of proteases is often associated with non-physiological cleavage of proteins that are not natural substrates, a stable and inducible cellular system that allowed for careful adjustment of ADAMTS4 expression was generated. To examine the effects of ADAMTS4 on APP processing and Aβ generation, the HEK293-APP695sw cell line with stable overexpression of human APP695 containing the Swedish mutation was stably transduced with a lentiviral vector system that conferred doxycycline (DOX)-inducible overexpression of V5-tagged human ADAMTS4 (HEK293-APP695sw/TetOn-ADAMTS4-V5 cells). HEK293-APP695sw cells were chosen as a parental cell line since they secrete high Aβ levels that can easily be detected by standard methods. After the selection of stable mass cultures, the cells were subcloned and several single cell clones were analyzed for ADAMTS4 expression by Western blotting. DOX-induced cell clones displayed near equal expression levels of the immature and the furin-processed, catalytically-

active form of ADAMTS4 in cell lysates [Figure 9 A] and in tissue culture supernatants [Figure 9 B] as shown by anti-V5 Western blotting. In both cell lysates and supernatants, the mature form of ADAMTS4 migrated below the 100 kDa molecular weight (MW) marker, which is consistent with previous results in the literature (the predicted MW of mature ADAMTS4 is 68 kDa) (Flannery *et al.* 2002, Wang et al. 2004, Gendron *et al.* 2007). In cell lysates, slight background expression of mostly immature ADAMTS4 was detected in non-induced cells, likely due to leaky expression of the DOX-controlled expression system.

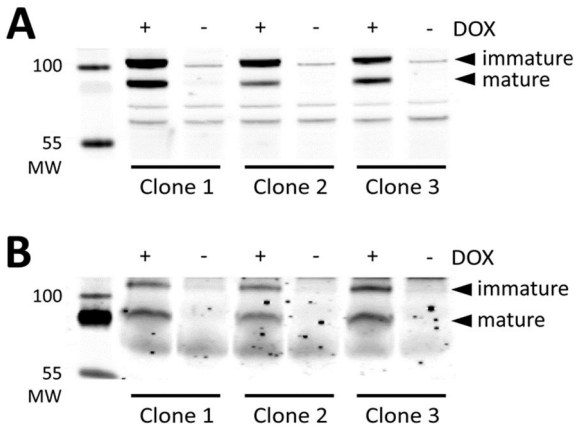

Figure 9: ADAMTS4 protein levels in HEK293-APP695sw cells with stable, DOX-inducible expression of V5-tagged ADAMTS4. The cells were induced with 100 ng/ml of doxycycline for 48 hours, and cell lysates and tissue culture supernatants were analyzed by Western blotting with the anti-V5 antibody. (**A**) ADAMTS4 protein expression in cell lysates of three independent cell clones. (**B**) ADAMTS4 protein expression in cell culture supernatants of the same three cell clones.

The evaluation of putative ADAMTS4 cleavage sites within APP revealed two sequence motifs that might be recognized by the protease [Figure 8]. Cleavage at these sites with glutamic acid in the P1 position would generate N-terminally truncated Aβ peptides such as Aβ4-x and Aβ12-x. To determine whether ADAMTS4 might cleave at additional sites in the Aβ sequence and might influence total Aβ levels, three of the most abundant full-length Aβ isoforms, Aβ1-40, Aβ1-42, and Aβ1-38 were examined in tissue culture supernatants by ELISA. In this sandwich ELISA assay, the antibody IC16, which preferentially detects Aβ peptides starting with the aspartate in position 1 of the Aβ sequence, was used as a coating antibody and was combined with different anti-Aβ C-terminus specific detection antibodies. Measurements did not show

any differences between DOX-induced ADAMTS4 expressing cells and non-induced control cells for three independent clones of HEK293-APP695sw/TetOn-ADAMTS4-V5 cells [Figure 10 A]. In addition, antibody 4G8 was used as a coating antibody and combined with the anti-Aβ C-terminus specific detection antibodies. 4G8 has an epitope in the mid-region of the Aβ sequence (AA 17-24) and can thereby detect not only full-length but also most N-terminally truncated Aβ peptides. Again, ELISA measurements did not reveal any differences in Aβx-40 and Aβx-42 levels after induction of ADAMTS4 expression as compared to non-induced control cells [Figure 10 B]. These results were expected as the putative ADAMTS4 cleavage sites after the glutamic acid residues 3 and 11 would not have predicted an increase in the total levels of Aβ peptides.

Next, the Aβ peptides secreted by HEK293-APP695sw/TetOn-ADAMTS4-V5 cells were analyzed by mass spectrometry. In contrast to ELISA, this method allowed to detect all Aβ species including N- and C-terminally truncated species for which no specific antibodies are available. Tissue culture supernatants from three independent cell clones were immunoprecipitated with a mixture of the monoclonal anti-Aβ antibodies 4G8 and 6E10, and analyzed by MALDI-TOF mass spectrometry. Tissue culture supernatants of DOX-induced cells revealed Aβ4-40 as well as Aβ12-40 peaks [Figure 11 B] while the non-induced control cells did not [Figure 11 A]. This showed that ADAMTS4 can generate Aβ4-x peptides and that the second, less-conserved recognition site after the glutamic acid in position 11 is also cleaved by ADAMTS4 to generate Aβ12-x peptides. This mass spectrometry data provided strong qualitative support that ADAMTS4 is indeed able to cleave APP at the predicted recognition sites, and that this results in the secretion of Aβ4-40 and Aβ12-40 peptides into tissue culture supernatants.

To generate quantitative data and to confirm the generation of Aβ4-x peptides by ADAMTS4 with an independent method, the polyclonal guinea pig antibody PSL-029-2 was used as a detection antibody and combined with an Aβ40 specific coating antibody in a sandwich ELISA. The PSL-029-2 antibody was developed by Dr. Oliver Wirths (Department of Psychiatry, University of Goettingen) and exclusively detects Aβ4-x peptides with the phenylalanine in position 4 (Wirths et al. in press). ELISA measurements revealed around 2 ng/ml of Aβ4-40 peptides in tissue culture supernatants after induction of ADAMTS4 expression [Figure 10 C]. In non-induced control cells, no background of Aβ4-40 peptides was detectable, which indicated that ADAMTS4 alone was responsible for the generation of these peptides.

Quantitatively, Aβ4-40 levels were approximately 20-fold lower compared to Aβx-40 levels as measured with the 4G8 ELISA, which is consistent with the fact that induction of ADAMTS4 expression did not change Aβx-40 levels as shown in Figure 10 B.

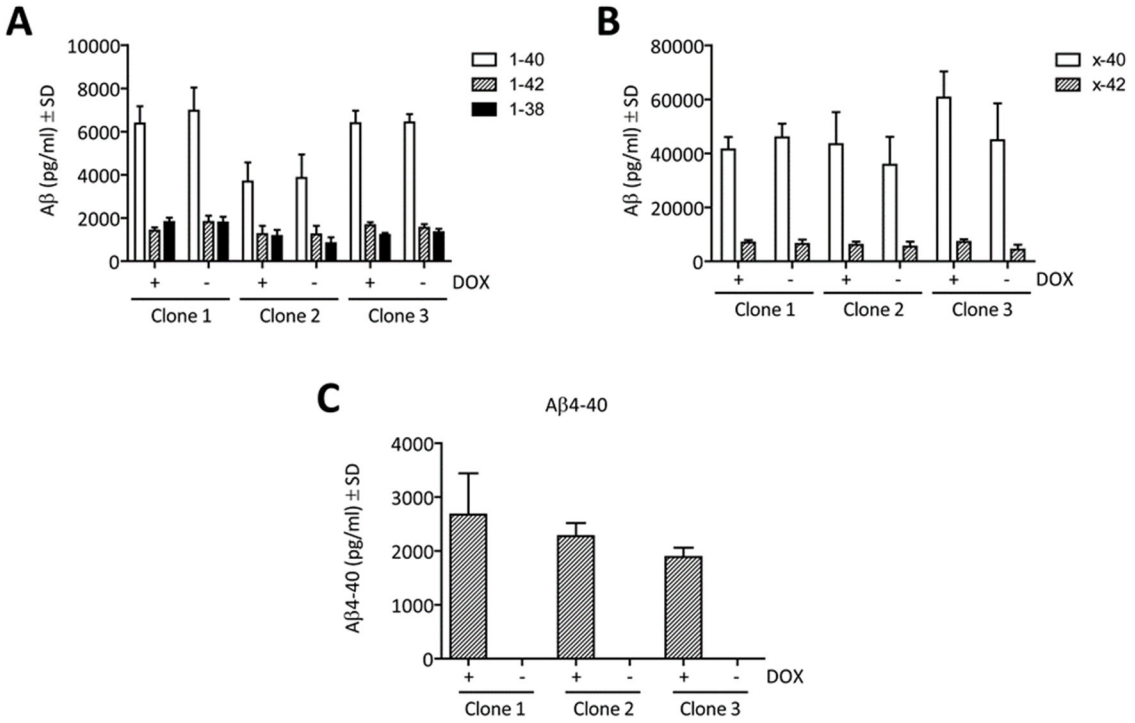

Figure 10: Measurement of Aβ peptide levels in tissue culture supernatants of HEK293-APP695sw/TetOn-ADAMTS4-V5 cells with different sandwich ELISA assays. Three independent biological experiments with two technical replicates for each of the three cell clones were performed and the concentrations for each Aβ species were averaged from all three experiments. Error bars represent standard deviation (SD). (**A**) To measure full-length Aβ1-x peptides, antibody IC16 was used for coating and combined with C-terminus specific Aβ detection antibodies. Aβ1-40, Aβ1-42, and Aβ1-38 levels were unchanged after induction of ADAMTS4 expression as compared to non-induced control cells. (**B**) To measure full-length and N-terminally truncated Aβ peptides, antibody 4G8 with an epitope in the middle of the Aβ sequence was used for coating and combined with C-terminus specific Aβ detection antibodies. Measurements of Aβx-40 and Aβx-42 peptide levels revealed no differences in ADAMTS4 expressing cells versus non-induced control cells. (**C**) To specifically measure N-terminally truncated Aβ4-40 peptides, a C-terminus specific Aβ40 antibody was used for coating and combined with the Aβ4-x specific antibody PSL-029-2 for detection. Robust levels of Aβ4-40 peptides were detected in tissue culture supernatants after induction of ADAMTS4 expression with no background in non-induced control cells.

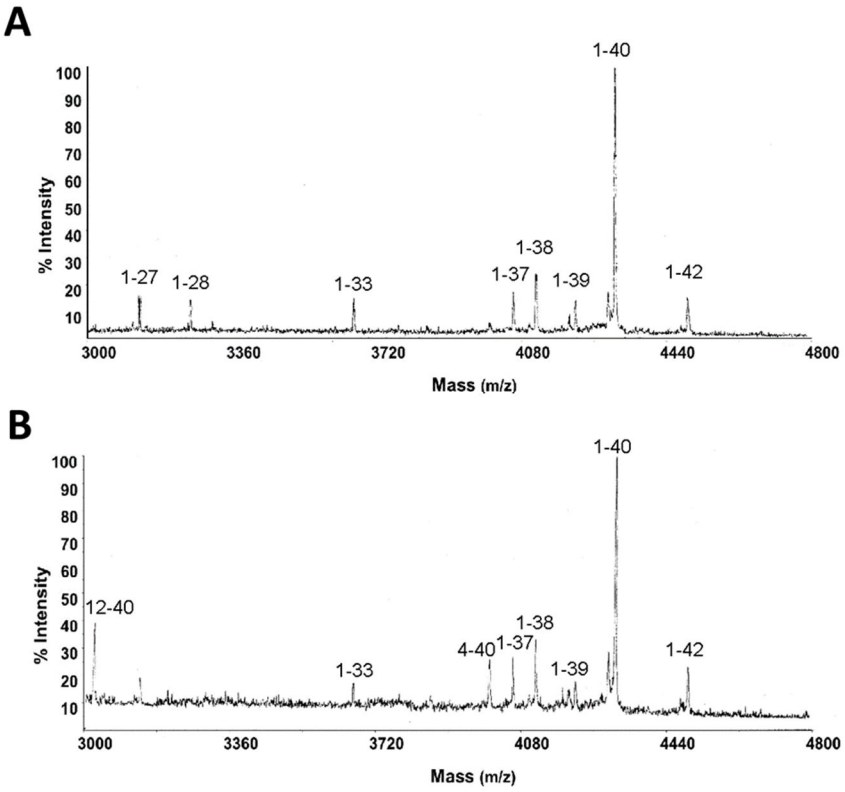

Figure 11: Mass spectrometry analysis of Aβ peptides in conditioned cell culture supernatants of HEK293-APP695sw/TetOn-ADAMTS4-V5 cells. Nearly identical spectra were acquired from three independent cell clones. (**A**) The spectrum of non-induced control cells showed peaks for the common Aβ species like Aβ1-40, Aβ1-42, and Aβ1-38 but no peaks for Aβ4-40 or Aβ12-40 (**B**) Mass spectrum of Aβ species in culture supernatants after induction of ADAMTS4 expression. Aβ4-40 and Aβ12-40 peptides were clearly detected while the other Aβ species remained unchanged. The mass spectrometry analysis shown in this figure was performed by Mitko Dimitrov, a graduate student in the research group of Dr. Patrick Fraering (EPFL Lausanne).

To further assess whether ADAMTS4 might cleave APP outside of the Aβ sequence and whether ADAMTS4 might have any influence on the metabolism of APP, steady-state levels of full-length APP and of APP C-terminal fragments resulting from ectodomain shedding of APP by α- or β-secretase were quantified in cell lysates of HEK293-APP695sw/TetOn-ADAMTS4-V5 cells. ADAMTS4 expression was induced in the cell clones by treatment with DOX and cell lysates were analyzed by Western blotting with the CT-15 antibody against the C-terminus of APP. This revealed a significant, greater than 50% reduction of the mature, glycosylated form of APP after induction of ADAMTS4 expression in all three independent cell clones. In contrast, the immature, non-glycosylated form of APP remained unchanged [Figure 12 A and B]. Furthermore, an additional APP fragment (marked with *) with a molecular weight between

25 and 35 kDa was observed after ADAMTS4 induction in cell lysates of all three clones [Figure 12 C]. No apparent effect on the levels of APP CTFs, neither CTF-α nor CTF-β, was seen after DOX-induction of ADAMTS4 expression [Figure 12 C]. These findings indicated that overexpression of ADAMTS4 reduced the levels of mature, glycosylated forms of APP, which are localized to late compartments of the secretory pathway and the cell surface (Kaether *et al.* 2002). The appearance of additional APP C-terminal fragments substantially larger than a CTF-α or CTF-β in cell lysates further indicated that ADAMTS4 cleaves APP in its ectodomain further N-terminal to the β-secretase cleavage site.

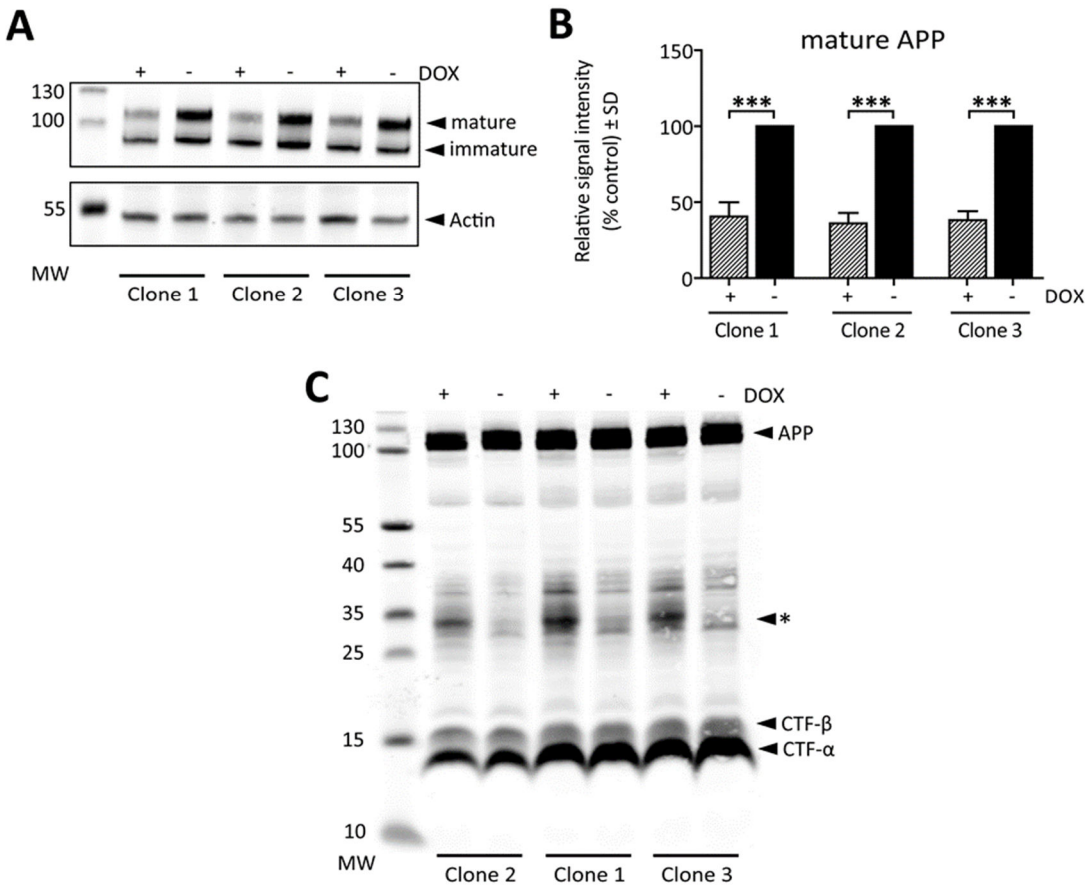

Figure 12: Effects of ADAMTS4 expression on APP levels in cell lysates of three independent clones of HEK293-APP695sw/TetOn-ADAMTS4-V5 cells. (**A**) APP full-length protein levels were detected by Western blotting with the antibody CT-15 against the C-terminus of APP. The mature, glycosylated forms of APP migrated substantially slower and were reduced after induction of ADAMTS4 expression. As a loading control, the same blot was incubated with an antibody against actin. (**B**) Quantification of mature APP levels in HEK293-APP695sw/TetOn-ADAMTS4-V5 cells. Induction of ADAMTS4 expression reduced mature APP levels by more than 50% in all three cell clones. Three independent experiments (biological replicates) were performed for each cell clone and were separately analyzed by Western blotting. The signal intensities of the mature APP forms were normalized to actin

levels. Subsequently, the mature APP levels of non-induced control cells were set to 100% and the levels of DOX-induced cells were calculated as % control for each clone. Unpaired t-test was used to compare the mean relative signal intensities from DOX-induced cells to non-induced controls. Error bars represent standard deviation (SD). ***, $p < 0.001$. (**C**) Additional APP C-terminal fragments (marked with *) between 25-35 kDa in size were detected after induction of ADAMTS4 expression in cell lysates analyzed by Western blotting with antibody CT-15. In contrast, levels of APP CTF-α and APP CTF-β appeared unchanged.

To further determine the effects of ADAMTS4 overexpression on secreted metabolites of APP, total levels of the soluble ectodomain APPs and of the β-secretase generated isoform APPs-β were measured in conditioned cell culture media of the three independent HEK293-APP695sw/TetOn-ADAMTS4-V5 cell clones by Western blotting with different antibodies against the APP ectodomain [Figure 13]. Overall, a substantial reduction in APPs levels was observed in ADAMTS4 expressing cells versus non-induced control cells. The monoclonal antibody 22C11 detects the N-terminus of APP (AA 66-81) and revealed an additional, smaller APPs fragment of approximately 70 kDa in DOX-induced cells (marked with *), while the full-length APPs levels were reduced [Figure 13 A]. There was some background of this smaller APPs fragment in non-induced cells, which might result from leaky expression of ADAMTS4 as observed in cell lysates [Figure 9 A]. This provided further evidence that APP is cleaved in its ectodomain by ADAMTS4, and the smaller N-terminal fragment generated by ADAMTS4 might correspond to the larger C-terminal APP fragment of approximately 30 kDa that was observed in cell lysates after induction of ADAMTS4 expression [Figure 12 C]. The epitope of the monoclonal antibodies IG7/5A3 lies in the mid-region of the APP ectodomain (AA 380-665). Western blotting with these antibodies revealed a substantial decrease of total APPs levels after induction of ADAMTS4 expression, but no additional smaller fragment [Figure 13 B]. The smaller ectodomain fragment detected by 22C11 is approximately 30 kDa shorter at the C-terminus compared to the ectodomains generated by α- and β-secretase cleavage of APP. However, the epitope recognized by the IG7/5A3 antibodies comprises almost all of the C-terminal half of the full-length APPs ectodomain. It is therefore possible that part of this epitope is missing in the shorter ectodomain fragment, which could explain its lack of detection by IG7/5A3. The monoclonal antibody 6A1 recognizes the neoepitope at the C-terminus of the APPs-β ectodomain generated by β-secretase cleavage of APP. Western blotting of tissue culture supernatants with this antibody showed a strong reduction of APPs-

β when ADAMTS4 expression was induced [Figure 13 C]. Again, no additional smaller APPs fragment was detected likely because C-terminal truncation of full-length APPs by ADAMTS4 removed the epitope of the 6A1 antibody. Taken together, induction of ADAMTS4 expression caused a reduction in the levels of full-length APPs and the appearance of a novel, shorter ectodomain fragment that was only detectable with N-terminal APP antibody 22C11. This could be explained either by intracellular competition between α- / β-secretase and ADAMTS4 for the substrate APP, or by subsequent C-terminal truncation of secreted APPs-α / APPs-β ectodomains by ADAMTS4 in the extracellular space.

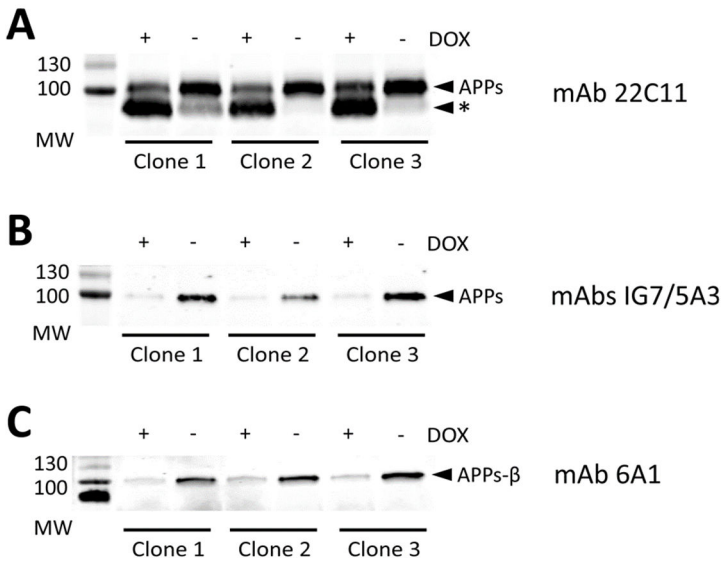

Figure 13: Effects of ADAMTS4 expression on APPs levels in tissue culture supernatants of three independent clones of HEK293-APP695sw/TetOn-ADAMTS4-V5 cells. (**A**) Western blotting of culture supernatants with the antibody 22C11 against the N-terminus of APP (AA 66-81) revealed a decrease in total full-length APPs levels and an additional fragment of approximately 70 kDa (marked with *) after DOX-induction of ADAMTS4 expression. (**B**) Western blotting with the antibodies IG7/5A3 against the mid-region of APP (AA 380-665) showed a substantial reduction in total full-length APPs levels in culture supernatants of induced versus control cells. (**C**) Levels of the APPs-β ectodomain as detected by antibody 6A1, which recognizes the neoepitope generated by β-secretase cleavage of APP, were also strongly decreased after induction of ADAMTS4 expression.

Several other cell lines with DOX-inducible ADAMTS4 expression analogous to the HEK293-APP695sw/TetOn-ADAMTS4-V5 cells were generated to confirm the effects of ADAMTS4 in cells with wild type and endogenous APP expression [Figure 14]. HEK293 cells with stable overexpression of wild type (wt) APP695 did not reveal any qualitative or obvious quantitative

differences in the processing of APPwt by ADAMTS4 as compared to APP containing the Swedish mutation. The mature form of APP was substantially reduced in cell lysates and total APPs and APPs-β levels were decreased in conditioned tissue culture media of ADAMTS4 expressing cells compared to non-induced control cells [Figure 14 A - C, right panels]. HEK293 cells with inducible ADAMTS4 expression revealed the same effects for endogenous APP. The mature, glycosylated form of APP was substantially reduced in cell lysates after induction of ADAMTS4 expression, while the immature form remained unchanged compared to control cells. Furthermore, full-length APPs forms as detected with the N-terminal 22C11 antibody were almost completely abolished in tissue culture supernatants and the additional, smaller 70 kDa APPs fragment was prominent (marked with *) after induction of ADAMTS4 expression [Figure 14 A and B, left panels]. The murine glioma cell line SMA-560 with endogenous expression of mouse APP showed weaker effects in both cell lysates and tissue culture supernatants. However, an additional, smaller APPs fragment was clearly detectable when ADAMTS4 expression was induced as compared to control cells [Figure 14 A and B, middle panels]. Taken together, these results showed that APP processing by ADAMTS4 was not affected by the Swedish mutation, and that human ADAMTS4 was also able to cleave mouse APP.

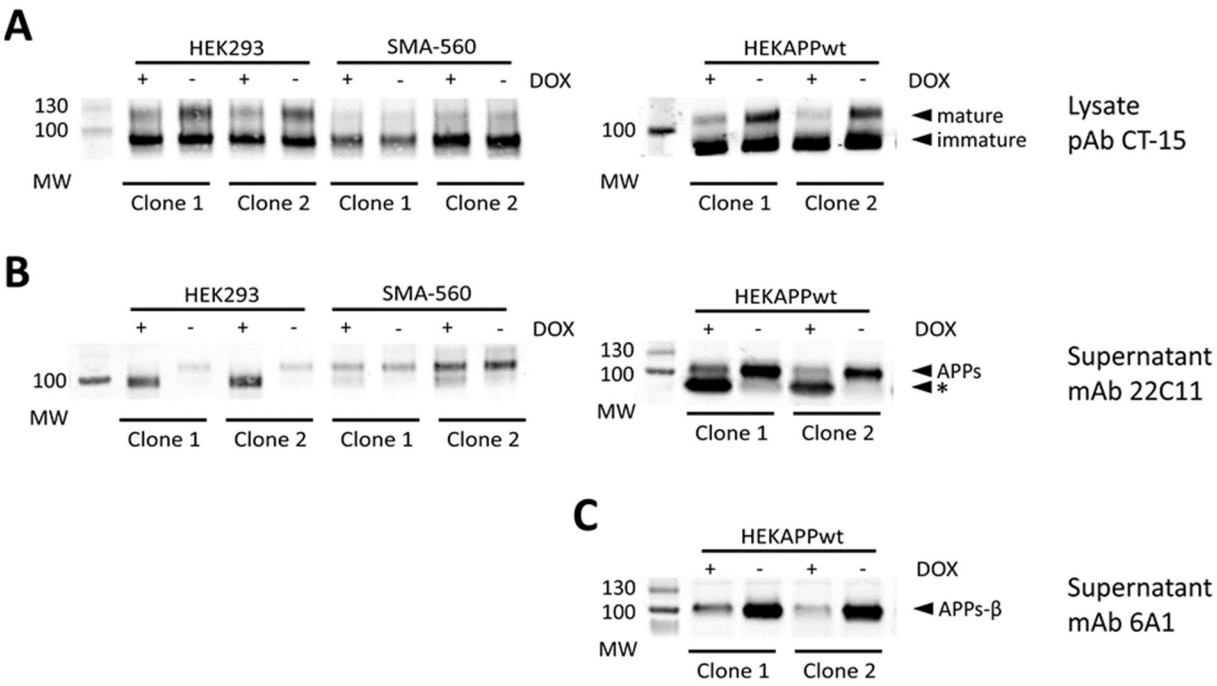

Figure 14: APP processing in additional cell lines with DOX-inducible ADAMTS4 expression. HEK293 cells with endogenous human APP expression, SMA-560 cells with endogenous mouse APP expression, and HEK293-APP695wt cells with stable overexpression of human wild type APP695 were stably transduced with a lentiviral vector system that conferred DOX-inducible overexpression of V5-tagged human ADAMTS4. Two independent cell clones of each cell line were analyzed. (**A**) Western blotting of cell lysates with CT-15 revealed a reduction of mature APP levels in HEK293 and HEK-APP695wt cell lines after induction of ADAMTS4 expression. SMA-560 cells did not show this effect, but mature APP levels were low in this cell line. (**B**) Total APPs levels in tissue culture supernatants as detected with the N-terminal APP antibody 22C11 were reduced and the appearance of a shorter APP ectodomain fragment (marked with *) was observed after induction of ADAMTS4 expression in each line. (**C**) By Western blotting with antibody 6A1, a decrease of the APPs-β ectodomain was seen in tissue culture supernatants of HEK293-APP695wt cells after induction of ADAMTS4 expression.

To assess whether ADAMTS4 and APP might interact within the cell, co-immunoprecipitation experiments were performed. Due to the slightly leaky expression of ADAMTS4 observed in cell lysates of the inducible HEK293-APP695sw/TetOn-ADAMTS4-V5 cell lines [Figure 9 A], the non-induced cells could not serve as an adequate control. Therefore, HEK293 cells were transiently co-transfected with human APP695 containing the Swedish mutation (APP695sw) and FLAG-tagged human ADAMTS4 or FLAG-tagged rat FE65 as a positive control. FE65 is a cytosolic adaptor protein and has been shown to interact with the C-terminus of APP to modulate its processing (Ando *et al.* 2001). Cell lysates were subsequently incubated with magnetic beads coupled to the anti-FLAG antibody M2 or coupled to the APP C-terminal antibody CT-15. The immunoprecipitated material was then resolved on an SDS-PAGE gel and analyzed by Western blotting with either anti-FLAG or CT-15 antibodies. Two types of control experiments were performed. First, cells were transfected with only one of the expression plasmids as a negative control. Second, immunoprecipitations were performed without primary antibodies coupled to the beads to exclude non-specific binding of proteins to the bead material. Western blotting with the CT-15 antibody revealed that immunoprecipitation of the FLAG-tagged FE65 with the anti-FLAG antibody co-immunoprecipitated APP with a molecular weight of approximately 100 kDa as expected [Figure 15 A, left panel]. In addition, immunoprecipitation of the FLAG-tagged ADAMTS4 co-immunoprecipitated APP [Figure 15 A, left panel]. When FLAG-tagged FE65 or ADAMTS4 were transfected alone, no APP was detected by Western blotting with the CT-15 antibody [Figure 15 A, left panel]. Furthermore, when cell lysates of co-transfected cells were incubated with beads that had not been coupled

to the anti-FLAG antibody, non-specific bands were not detected [Figure 15 A, middle panel]. To verify that the immunoprecipitation of ADAMTS4 and FE65 was successful, the same samples were also blotted with the anti-FLAG antibody. This showed a band for FE65 running slightly below the 100 kDa MW marker consistent with previous results in the literature (predicted MW of FE65 is 77 kDa) (Borg *et al.* 1996). Furthermore, protein bands for both mature and immature ADAMTS4 were observed when lysates of cell transfected with ADAMTS4 were immunoprecipitated and blotted with the anti-FLAG antibody [Figure 15 B, right panel]. In the reverse experiment, immunoprecipitation of APP with CT-15 and Western blotting with anti-FLAG antibody showed co-immunoprecipitation of the positive control FE65 and of immature ADAMTS4 [Figure 15 B, left panel]. A slight unidentified background signal was detected when APP was transfected alone or when APP and FE65 co-transfected lysates were incubated with beads only [Figure 15 B, left and middle panels]. Successful immunoprecipitation of APP was confirmed by Western blotting of the same samples with the CT-15 antibody [Figure 15 A, right panel]. Taken together, these results indicated that APP and ADAMTS4 interacted in an intracellular compartment. Most likely this occurred in the early secretory pathway since most of ADAMTS4 that was pulled down together with APP was still in the immature pro-form prior to furin cleavage in the trans-Golgi network. In addition, most of the APP that co-immunoprecipitated with ADAMTS4 appeared to be immature APP, while FE65 co-immunoprecipitated both immature and mature APP forms [compare Figure 15 A, right panel, lanes 2 and 3]. This further indicated that the APP/ADAMTS4 interaction occurred in the early secretory pathway.

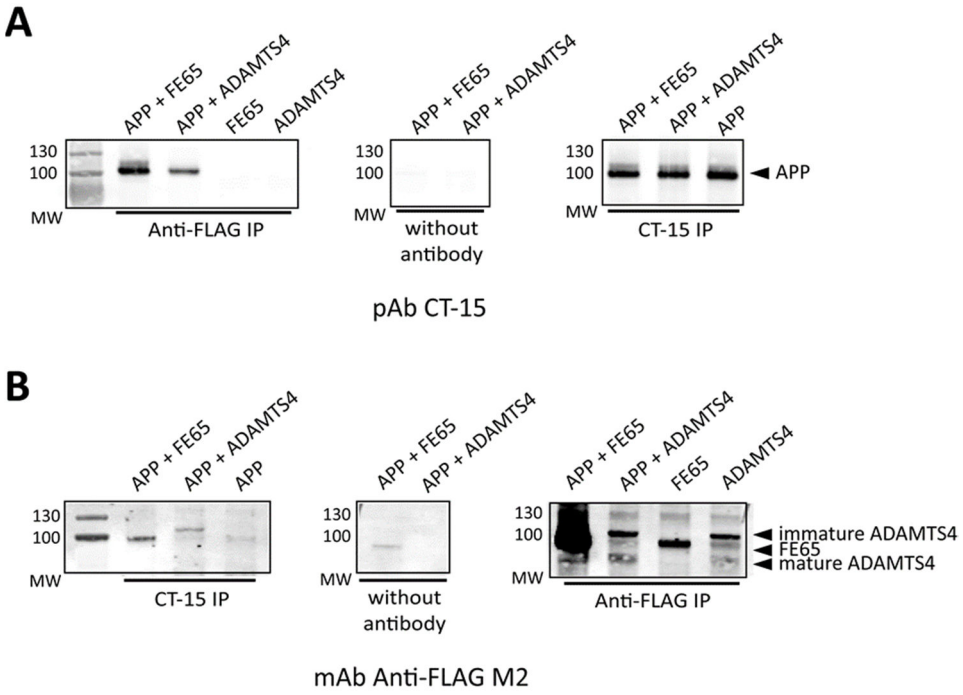

Figure 15: Co-immunoprecipitation of APP and ADAMTS4 in transiently transfected HEK293 cells. Cells were co-transfected with human APP695sw and FLAG-tagged human ADAMTS4 or rat FE65. Cell lysates were incubated with magnetic beads coupled either to anti-FLAG or CT-15 antibodies. As controls, the expression plasmids were transfected separately, or cell lysates were incubated with beads only. Three independent experiments were performed and one representative experiment is shown. (**A**) Immunoprecipitation with the anti-FLAG antibody and Western blotting with the CT-15 antibody showed co-immunoprecipitation of APP with both FLAG-tagged ADAMTS4 and FLAG-tagged FE65 (left panel). No background signal was detected in the single plasmid or no antibody controls (left and middle panels). CT-15 Western blotting of the samples immunoprecipitated with CT-15 antibody showed that the immunoprecipitation of APP was successful (right panel). (**B**) Immunoprecipitation with CT-15 and Western blotting with the anti-FLAG antibody revealed that both FE65 and immature ADAMTS4 were pulled down together with APP (left panel). Slight non-specific background signals were observed in the single plasmid control (left panel, lane 4) or when cell lysates of cells co-transfected with APP and FE65 were incubated with beads only (middle panel, first lane). Anti-FLAG Western blotting of the samples immunoprecipitated with the anti-FLAG antibody confirmed the successful immunoprecipitation of FE65 and both immature and mature ADAMTS4 (right panel).

To further investigate where in the cell APP and ADAMTS4 might interact, the HEK293-APP695sw/TetOn-ADAMTS4-V5 cells were examined by immunocytochemistry. One cell clone was plated on glass cover slips and induced for 24 hours with DOX. Immunocytochemistry was performed using the anti-V5 antibody to detect ADAMTS4 and the CT-15 antibody to stain APP. Secondary Alexa-fluorophore coupled antibodies were used to enable fluorescence

microscopy, with ADAMTS4 stained red and APP stained green [Figure 16]. ADAMTS4 staining was mostly found associated with the cell nucleus and in extending cell protrusions. APP was also localized to a high extent close to the nucleus as well as in cell extensions, potentially at the cell surface. Co-localization of ADAMTS4 and APP was detected in an intracellular compartment close to the cell nucleus as indicated by the yellow overlay [Figure 16]. This indicated that APP and ADAMTS4 co-localized in the secretory pathway, presumably in the ER and early Golgi compartments that are located close to the nucleus. These results are consistent with the co-immunoprecipitation studies described above, which showed that the immature pro-form of ADAMTS4 bound to immature APP species with limited or no apparent glycosylation [Figure 15 A and B, left panels].

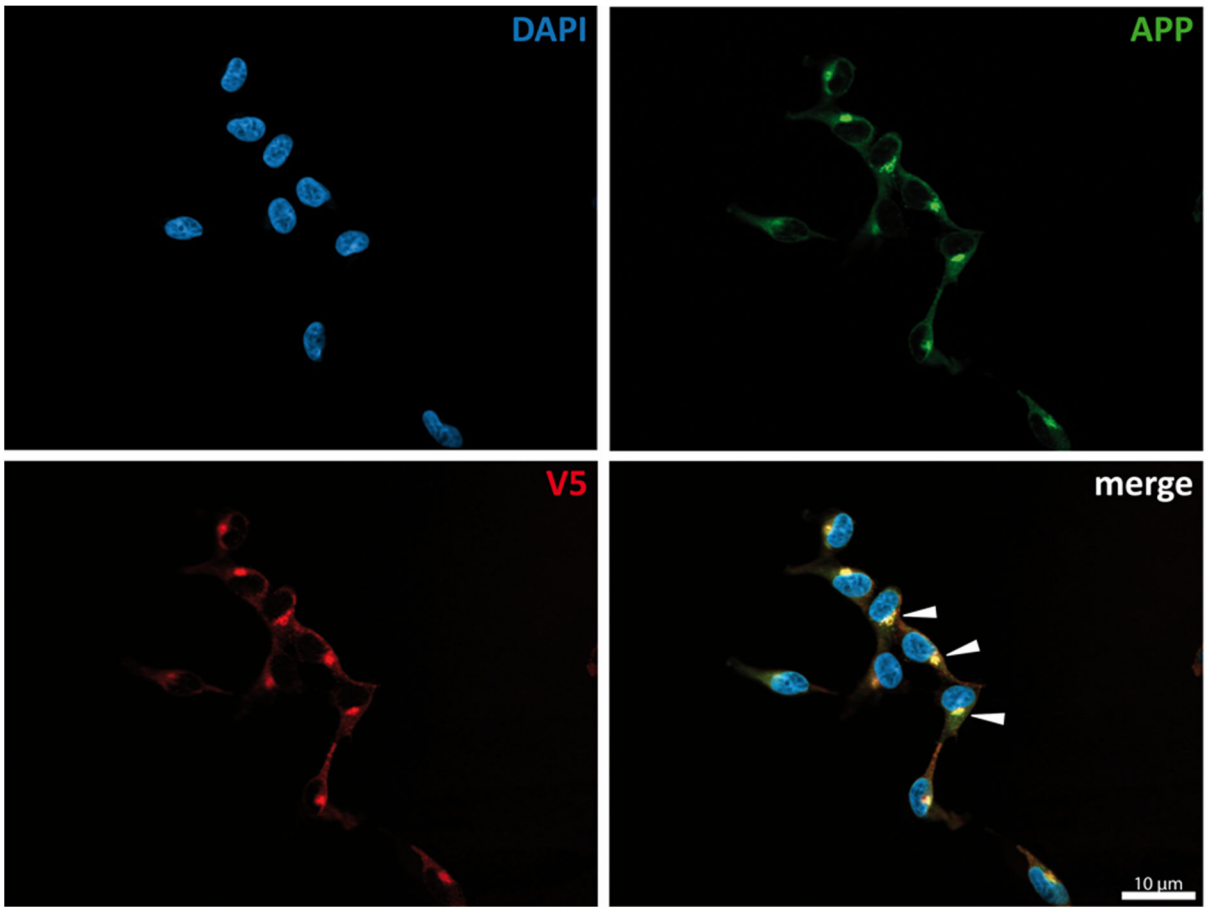

Figure 16: Co-immunostaining of DOX-induced HEK293-APP695sw/TetOn-ADAMTS4-V5 cells with antibodies against the V5-tag of ADAMTS4 (red) and against APP (CT-15, green). Co-localization indicated by arrows and the yellow color was found close to the DAPI-stained cell nucleus (blue), presumably in the ER/Golgi compartments. Scale bar 10 µm.

To investigate whether ADAMTS4 is itself capable of cleaving APP and generating Aβ4-x peptides within the cell, or whether ADAMTS4 would act only as an exopeptidase by removing the first three amino acids from Aβ peptides with an intact N-terminus, putatively in the extracellular space, HEK293-APP695sw/TetOn-ADAMTS4-V5 cells were treated with a potent β-secretase inhibitor to suppress the cellular production of Aβ1-x peptides. Treatment with the BACE1 inhibitor essentially abolished Aβ1-40 production in three independent cell clones either with or without ADAMTS4 expression [Figure 17 A]. Subsequently, the same conditioned culture media were analyzed with the Aβ4-40 specific ELISA. After induction of ADAMTS4 expression, Aβ4-40 levels were not decreased in the BACE1 inhibitor-treated cells compared to the non-treated control cells [Figure 17 B]. This demonstrated that ADAMTS4 is capable of cleaving APP and generating N-terminally truncated Aβ4-x peptides within the cell or at the cell surface without prior cleavage of APP by β-secretase.

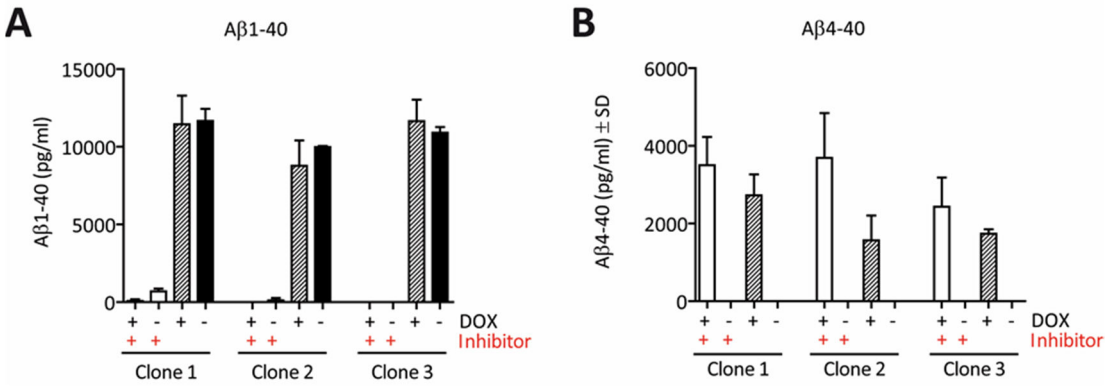

Figure 17: Aβ4-40 generation by ADAMTS4 is not dependent on prior cleavage of APP by β-secretase. HEK293-APP695sw/TetOn-ADAMTS4-V5 cells were pre-treated with 1 µM of the BACE1 inhibitor BACE-IV for 24 h. Then ADAMTS4 expression was induced for 24 h with DOX in the presence of the BACE1 inhibitor. Finally, culture media were changed and conditioned for another 24 h, again in the presence of DOX and the BACE1 inhibitor. These conditioned media were analyzed with sandwich ELISA assays specific for Aβ1-40 and Aβ4-40. In control experiments, cells were not treated with the BACE1 inhibitor and/or induction of ADAMTS4 expression was omitted. (**A**) Aβ1-40 levels were not affected by induction of ADAMTS4 expression consistent with the experiments shown in Figure 10 A, but were completely abolished after treatment with the BACE1 inhibitor. (**B**) Induction of ADAMTS4 expression resulted in the detection of Aβ4-40 peptides. However, concomitant inhibition of BACE1 did not reduce Aβ4-40 levels indicating that ADAMTS4 cleavage of APP and generation of Aβ4-40 peptides did not require prior cleavage of APP by β-secretase. Three independent biological experiments with two technical replicates for each of the three clones were performed and the Aβ4-40 concentrations were averaged from all three experiments. Error bars represent standard deviation (SD).

Finally, we wanted to explore whether ADAMTS4 could also convert Aβ1-40 peptides to Aβ4-40 peptides, in addition to *de novo* generation of Aβ4-40 by APP cleavage. To investigate this question, HEK293/TetOn-ADAMTS4-V5 cells were used, which express endogenous APP and secrete only minor amounts of Aβ undetectable with our ELISA systems. Tissue culture supernatants from HEK293/TetOn-ADAMTS4-V5 cells after induction of ADAMTS4 expression and from non-induced control cells were incubated with the anti-V5 antibody coupled to magnetic beads to immunoprecipitate ADAMTS4. ADAMTS4 bound to the beads was then incubated with fresh culture medium containing recombinant Aβ1-40 peptides for 24 hours. Finally, the levels of N-truncated Aβ4-40 peptides were measured by ELISA. This showed a significant, approximately 4-fold increase in Aβ4-40 levels when ADAMTS4 was immunoprecipitated from DOX-induced HEK293/TetOn-ADAMTS4-V5 cells as compared to non-induced control cells [Figure 18 A]. Western blotting of the immunoprecipitated material with the anti-V5 antibody confirmed that the mature, catalytically-active form of ADAMTS4 was successfully immunoprecipitated from cell culture supernatants after induction of ADAMTS4 expression with DOX [Figure 18 B]. Some background ADAMTS4 signal was observed in the control samples, probably due to the slightly leaky expression of ADAMTS4 in HEK293/TetOn-ADAMTS4-V5 cells without DOX-induction and further enrichment by the immunoprecipitation [Figure 18 B]. These experiments confirmed that ADAMTS4 can mediate the conversion of Aβ1-40 to Aβ4-40 peptides, indicating that ADAMTS4 might truncate secreted full-length Aβ peptides at the N-terminus in the extracellular space.

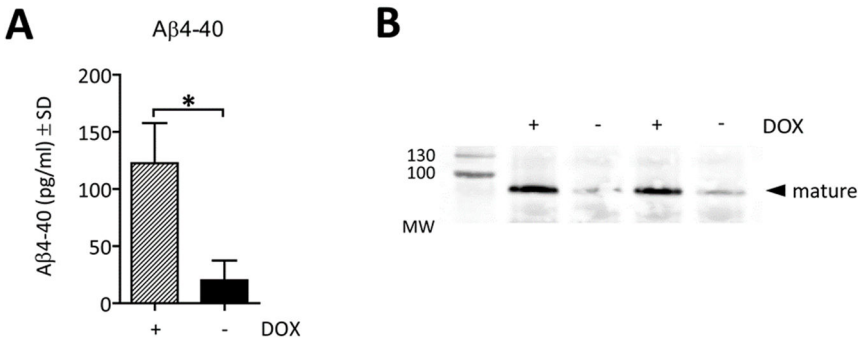

Figure 18: ADAMTS4 converted recombinant Aβ1-40 to Aβ4-40. Tissue culture supernatants of HEK293/TetOn-ADAMTS4-V5 cells treated with DOX or from non-induced control cells were immunoprecipitated with the anti-V5 antibody coupled to magnetic beads. Bound ADAMTS4 was then incubated with recombinant Aβ1-40 in fresh culture medium. The medium was removed and analyzed with the Aβ4-40 specific ELISA. Finally, the beads were boiled in sample buffer and analyzed by Western blotting with the anti-V5 antibody. (**A**) Aβ4-40 levels were

significantly increased approximately 4-fold when recombinant Aβ1-40 was incubated with immunoprecipitated ADAMTS4. Three independent experiments with two technical replicates each were performed and the Aβ4-40 concentrations were averaged from all three experiments. Unpaired t-test was used to compare the means from DOX-induced cells to non-induced controls. Error bars represent standard deviation (SD). *, $p < 0.05$. (**B**) Western blotting with the anti-V5 antibody confirmed the successful immunoprecipitation of the mature, catalytically-active form of ADAMTS4 from tissue culture media of HEK293/TetOn-ADAMTS4-V5 cells treated with DOX. Some background expression in the non-induced control cells was observed.

5.2 Expression and effects of ADAMTS4 in the mouse brain

5.2.1 APP processing and Aβ generation in brain tissue of 5xFAD / ADAMTS4$^{-/-}$ mice

To confirm the relevance of ADAMTS4 for APP processing in the brain and for Aβ levels *in vivo*, ADAMTS4 knockout mice (The Jackson Laboratory strain B6.129P2-*Adamts4*^{tm1Dgen}/J) were crossed to the 5xFAD mouse model of AD to introduce human APP and to facilitate Aβ detection in the brain. All animal breedings were performed in the animal facility of the University of Goettingen under the supervision of Dr. Oliver Wirths (Department of Psychiatry). Mice with the desired genotypes 5xFAD / ADAMTS4$^{-/-}$ and 5xFAD / ADAMTS4$^{+/+}$ controls were aged in two cohorts to 12 or 15 months. Animals were sacrificed, brains were sequentially extracted, and APP metabolites and Aβ levels were analyzed by Western blotting, mass spectrometry, and ELISA. Soluble APP metabolites were detected in the TBS (soluble) brain fraction and membrane-bound APP metabolites in the SDS (insoluble) brain fraction of 12-month-old knockout and control animals by Western blotting with different anti-APP antibodies. C57Bl/6J wild type mice served as no-transgene controls (Ntg) [Figure 19]. In the SDS fraction, the levels of full-length APP were unchanged between the genotypes as detected with the CT-15 antibody [Figure 19 A]. However, there was a significant, approximately 30% increase in total APPs levels as detected with the 22C11 antibody [Figure 19 B] and in APPs-β levels as detected with the 6A1 antibody [Figure 19 C] in the TBS fraction of 5xFAD / ADAMTS4$^{-/-}$ animals when compared to 5xFAD / ADAMTS4$^{+/+}$ controls. This partially confirmed the effects of ADAMTS4 on APP processing as observed in the cell culture models, namely that ADAMTS4 activity affects APP ectodomain shedding and APPs levels. Presumably, in the absence of ADAMTS4, more APP is cleaved in the α- and β-secretase pathways, which could explain the increased APPs levels in the brain. Alternatively, ADAMTS4 might be involved in the degradation of APPs and might thereby contribute to the regulation of APPs levels in the

extracellular space. These results are also internally consistent with the tissue culture experiments, which showed decreased full-length APPs levels with overexpression of ADAMTS4. Overall, the effects on APPs levels were less prominent in the brains of 5xFAD / ADAMTS4$^{-/-}$ mice as compared to the tissue culture models, and no effects on steady-state levels of full-length APP were observed. However, this is not unexpected as mice express only endogenous levels of ADAMTS4 in the brain, whereas overexpression of ADAMTS4 in tissue culture cells likely results in protein levels substantially above normal endogenous levels. Furthermore, it is not clear whether ADAMTS4 is ubiquitously expressed in the brain or whether its expression is restricted to certain cell types, which could further reduce the availability of the enzyme in the brain.

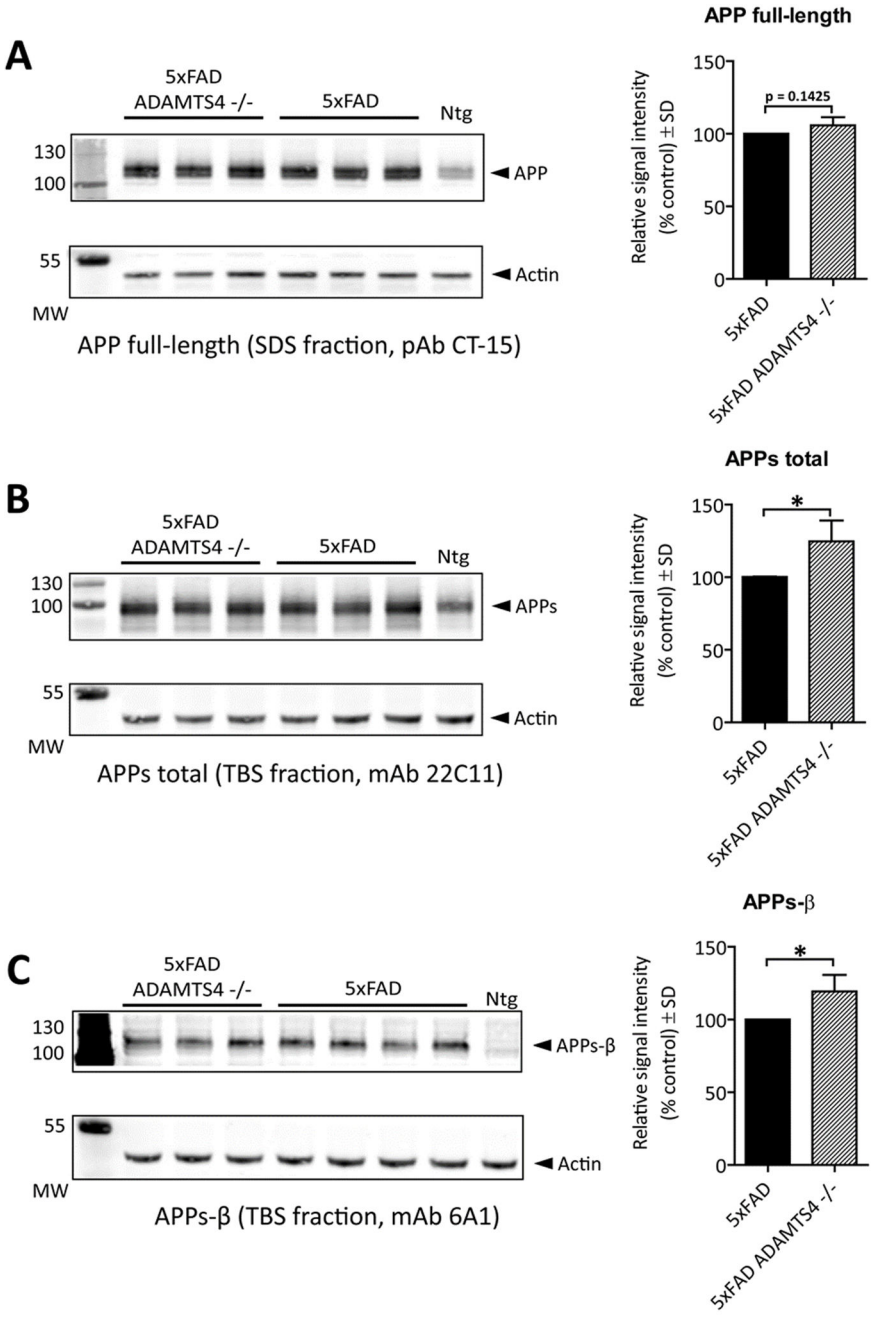

Figure 19: Effects of ADAMTS4 knockout on APP processing *in vivo*. 5xFAD mice were crossed to ADAMTS4 knockout mice and animals with the genotypes 5xFAD / ADAMTS4$^{-/-}$ (n = 3) and 5xFAD / ADAMTS4$^{+/+}$ (n = 3-4) were aged to 12 months. Brains were sequentially extracted, and APP and APPs levels were analyzed in the TBS- and SDS-soluble fractions by Western blotting. Each Western blot was repeated three times and the signal intensities were quantified. APP and APPs levels were normalized to actin levels and the values from three technical replicates were averaged for each individual animal. Mean values were calculated for each genotype and the values of the 5xFAD / ADAMTS4$^{+/+}$ genotype were set to 100%. Unpaired t-test was used to compare the means from both genotypes. Error bars represent standard deviation (SD). *, $p < 0.05$. (**A**) Steady-state full-length APP levels were not different in the SDS fraction of 5xFAD / ADAMTS4$^{-/-}$ and 5xFAD / ADAMTS4$^{+/+}$ control animals as detected with the CT-15 antibody. (**B**) A significant increase in total APPs levels was measured with antibody

22C11 in the TBS fraction of 5xFAD / ADAMTS4$^{-/-}$ animals as compared to 5xFAD / ADAMTS4$^{+/+}$ controls. (**C**) APPs-β levels were also increased in the TBS fraction of 5xFAD / ADAMTS4$^{-/-}$ animals as measured with antibody 6A1.

To determine whether Aβ4-x peptides were detectable in the 5xFAD mouse model of AD and whether their levels in the brain might be influenced by the genetic deletion of ADAMTS4, mass spectrometry analysis of formic acid (FA) extracted brains from 12-month-old animals with the genotypes 5xFAD / ADAMTS4$^{-/-}$ and 5xFAD / ADAMTS4$^{+/+}$ was performed. Aβ peptides were immunoprecipitated with the monoclonal anti-Aβ antibody 4G8, which recognizes both full-length and N-terminally truncated peptides. MALDI-TOF-MS analysis of 5xFAD / ADAMTS4$^{+/+}$ control animals revealed spectra, in which the largest peaks represented Aβ1-42 and Aβ1-40 [Figure 20 A]. In enlargements of the spectra, peaks for both Aβ4-40 and Aβ4-42 were clearly detectable alongside C-terminally truncated species such as Aβ1-38 and Aβ1-37 and N-terminally truncated pGlu-Aβ3-42 and Aβ5-42 peptides. These mass spectra were largely consistent with previously published mass spectrometry data for the 5xFAD model (Wittnam et al. 2012, Reinert *et al.* 2016). However, the spectra of 5xFAD / ADAMTS4$^{-/-}$ mice were not substantially different. The same Aβ peptides species, including Aβ4-40 and Aβ4-42, were detected in the FA fraction as seen in 5xFAD / ADAMTS4$^{+/+}$ control animals [Figure 20 B].

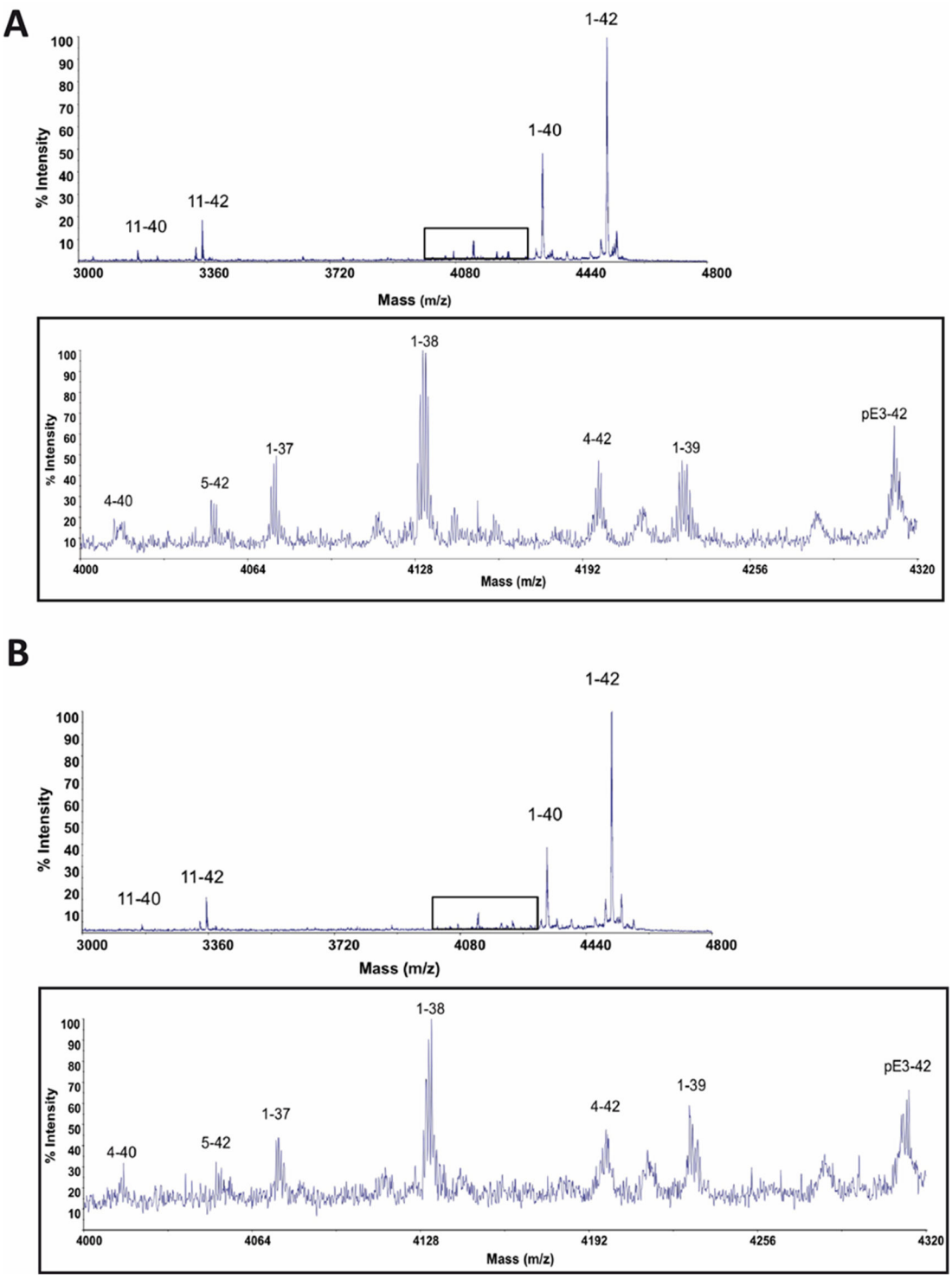

Figure 20: Mass spectrometry analysis of Aβ peptides in formic acid brain extracts of 12-month-old 5xFAD / ADAMTS4$^{+/+}$ and 5xFAD / ADAMTS4$^{-/-}$ mice. 3 animals of each genotype were analyzed and representative spectra are shown. (**A**) Full spectrum and enlarged view (black box) of Aβ peaks of a 5xFAD / ADAMTS4$^{+/+}$ control animal. Among the common Aβ species, Aβ4-40 and Aβ4-42 peptides were clearly detected. (**B**) The full mass spectrum and the enlarged view of Aβ peptides in the FA brain fraction of a 5xFAD / ADAMTS4$^{-/-}$ mouse showed no obvious differences compared to the 5xFAD / ADAMTS4$^{+/+}$ control. Aβ4-x peptides were still detected in the absence of ADAMTS4. FA brain extraction and the mass spectrometry analysis shown in this figure were performed by

Hermeto Gerber, a graduate student in the research group of Dr. Patrick Fraering (Foundation Eclosion, Plan-Les-Ouates, Switzerland).

Mass spectrometry analysis is not quantitative and the peak heights in the spectra shown in Figure 20 do not correlate to the abundance of individual Aβ peptides. In addition, the peaks generated by Aβ4-40 and Aβ4-42 peptides were very small compared to the Aβ1-42 and Aβ1-40 peaks. This implied that differences in the spectra of the 5xFAD / ADAMTS4$^{-/-}$ and 5xFAD / ADAMTS4$^{+/+}$ genotypes could have only been expected if genetic deletion of ADAMTS4 would have completely abolished the generation of Aβ4-x peptides. Therefore, ELISA measurements were performed to assess possible changes in the absolute levels of Aβ4-x peptides. SDS brain fractions of 12-month-old animals were analyzed with the Aβ4-40 specific sandwich ELISA. This showed that Aβ4-40 levels were indeed significantly reduced by approximately 50% in 5xFAD / ADAMTS4$^{-/-}$ knockout animals when compared to 5xFAD / ADAMTS4$^{+/+}$ controls [Figure 21 A]. To detect possible changes in full-length Aβ peptides, the TBS and SDS brain fractions of the same animals were analyzed with ELISA assays specific for Aβ1-42 and Aβ1-40. There were no significant differences in the SDS fractions for Aβ1-40 [Figure 21 B] or Aβ1-42 [Figure 21 C] between the genotypes. In the TBS fraction, only Aβ1-42 was detectable and was also unchanged [Figure 21 D]. Additionally, ELISA measurements of Aβx-40 peptides in SDS fractions and Aβx-42 peptides in TBS and SDS fractions showed no significant differences between the two genotypes [Figure 21 E – G]. Consistent with these ELISA measurements of Aβ1-40/42 and Aβx-40/42 peptides, a quantification of the amyloid plaque load at the age of 12 months by anti-Aβ immunohistochemistry and image analysis also did not show differences between 5xFAD / ADAMTS4$^{-/-}$ and 5xFAD / ADAMTS4$^{+/+}$ animals (data not shown; plaque load analysis was performed in the laboratory of Dr. Oliver Wirths).

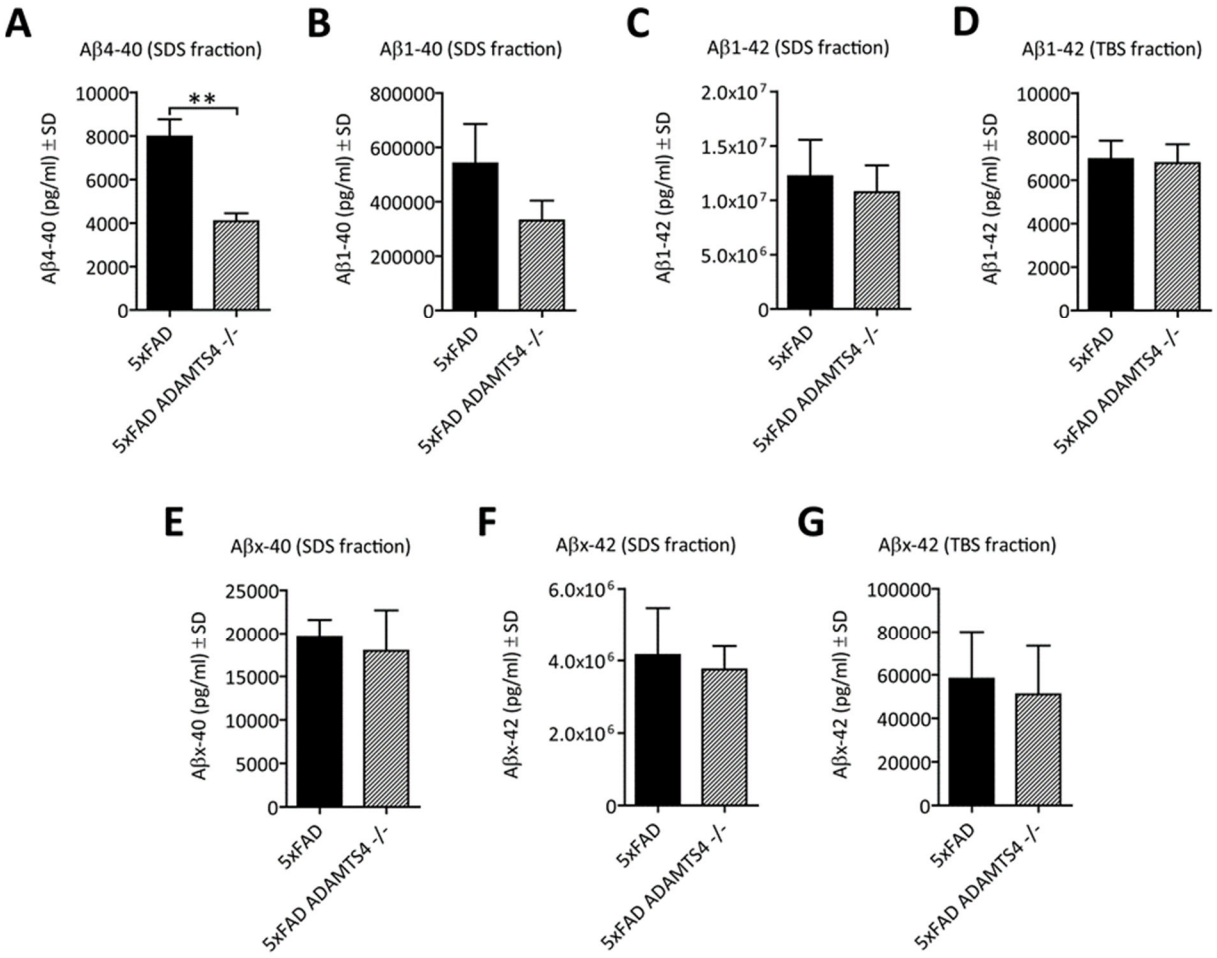

Figure 21: ELISA measurements of different Aβ peptide species in the TBS and SDS brain fractions of 12-month-old 5xFAD / ADAMTS4$^{-/-}$ (n = 3) and 5xFAD / ADAMTS4$^{+/+}$ (n = 3) control animals. Three technical replicate values from each animal were averaged, and unpaired t-test was used to compare the means from both genotypes. Error bars represent standard deviation (SD). **, $p < 0.01$. (**A**) Aβ4-40 levels in the SDS fraction of 5xFAD / ADAMTS4$^{-/-}$ animals were significantly reduced by approximately 50% compared to the 5xFAD / ADAMTS4$^{+/+}$ controls. In the SDS fractions, there were no significant differences in Aβ1-40 (**B**), Aβ1-42 (**C**), Aβx-40 (**E**), and Aβx-42 (**F**) levels between the two genotypes. There were also no differences in Aβ1-42 (**D**) and Aβx-42 (**G**) levels in the TBS fractions between the genotypes.

In addition, to confirm these results in a second, independent cohort of animals, 15-month-old mice were analyzed. Again, TBS and SDS brain fractions were measured with Aβ4-x and Aβ1-40/42 specific ELISAs as described above. Analysis of Aβ1-40 and Aβ1-42 levels revealed no significant differences between 5xFAD / ADAMTS4$^{-/-}$ and 5xFAD / ADAMTS4$^{+/+}$ control animals [Figure 22 C – E]. However, ELISA measurements of Aβ4-40 peptides confirmed a significant decrease of about 30% in Aβ4-40 levels in 5xFAD / ADAMTS4$^{-/-}$ mice as compared

to control animals [Figure 22 A]. In contrast, Aβ4-42 levels were not significantly different between the two genotypes [Figure 22 B].

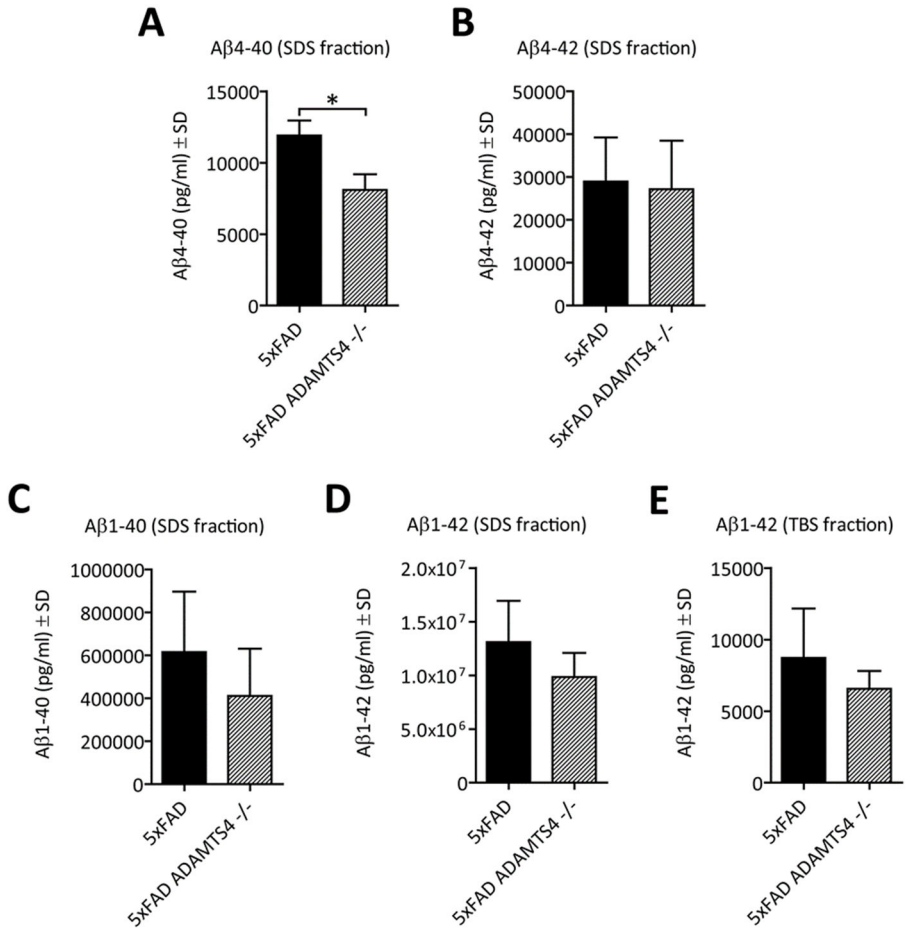

Figure 22: Aβ levels in TBS and SDS brain fractions of 15-month-old 5xFAD / ADAMTS4$^{-/-}$ (n = 3) and 5xFAD / ADAMTS4$^{+/+}$ (n = 3) control animals. Three technical replicate values from each animal were averaged, and unpaired t-test was used to compare the means from both genotypes. Error bars represent standard deviation (SD). *, $p < 0.05$. (**A**) Aβ4-40 levels were significantly decreased in SDS fractions of 5xFAD / ADAMTS4$^{-/-}$ mice compared to 5xFAD / ADAMTS4$^{+/+}$ controls. (**B**) Aβ4-42 levels in the SDS fractions were not different between the two genotypes. There was also no difference in Aβ1-40 (**C**) and Aβ1-42 (**D**) levels in the SDS fractions and Aβ1-42 levels in the TBS fractions (**E**) between the genotypes.

While these data confirmed that ADAMTS4 is crucial for the generation of Aβ4-x peptides *in vivo*, the lack of ADAMTS4 did not appear to affect overall Aβ accumulation and the development of the amyloid pathology in the 5xFAD mouse model in a major way. This could be related to the fact that Aβ4-x peptides are much less abundant in the brains of AD mouse

models as compared to AD patients, and might be less critical for the amyloid pathology in mice (Kawarabayashi et al. 2001, Kalback et al. 2002, Schieb et al. 2011). The reasons for the low abundance of Aβ4-x peptides in AD mouse models are unclear. However, in the 5xFAD and in other AD mouse models the APP transgene is expressed under the control of the neuron-specific Thy-1 promoter, which directs APP expression in the brain predominantly to neurons. ADAMTS4 expression in the mouse brain has been reported in neurons and in all types of glial cells, but studies have shown contradictory results (Hamel et al. 2005, Tauchi et al. 2012, Levy et al. 2015). Therefore, it is possible that in the brains of AD mouse models the expression of the human APP transgene and of ADAMTS4 might not or only partially overlap.

5.2.2 ADAMTS4 expression in the mouse brain

Reports about the expression of ADAMTS4 in the mouse brain have been conflicting. To clarify this issue, we again employed the ADAMTS4 knockout mice, which are also ADAMTS4 reporter mice. To generate the ADAMTS4$^{-/-}$ knockout mice, the bacterial β-galactosidase (lacZ) gene was inserted into the ADAMTS4 locus such that the endogenous ADAMTS4 promoter regulates the expression of the lacZ gene. This enabled the investigation of the cellular expression pattern of ADAMTS4 in the mouse brain by β-galactosidase immunohistochemistry. Therefore, cortical sections of a 6.5-month-old 5xFAD / ADAMTS4$^{-/-}$ mouse were stained with specific markers for different types of glial cells [Figure 23]. Expression of the β-galactosidase reporter (red) did not co-localize with the astrocytic marker GFAP [Figure 23 A] or the microglia marker Iba1 [Figure 23 B] (both green). Likewise, no β-galactosidase positive cells with a neuronal morphology were found. In contrast, a high number of β-galactosidase positive cells were observed in the corpus callosum and other fiber tracts indicating that the labeled cells might be oligodendrocytes. To confirm this, an antibody against the oligodendrocyte marker Cyclic nucleotide phosphodiesterase (CNPase) was used, which is expressed throughout the oligodendrocyte lineage from precursor cells to mature oligodendrocytes and continues to be expressed at high levels in the adult CNS (Sprinkle 1989, Baumann & Pham-Dinh 2001). Indeed, cells in the cortex with β-galactosidase positive nuclei (green) also displayed cellular CNPase expression (red) [Figure 23 C] and the β-galactosidase staining also co-localized with CNPase in the corpus callosum [Figure 23 D]. These findings indicated that ADAMTS4 is solely expressed in oligodendrocytes in the adult murine brain.

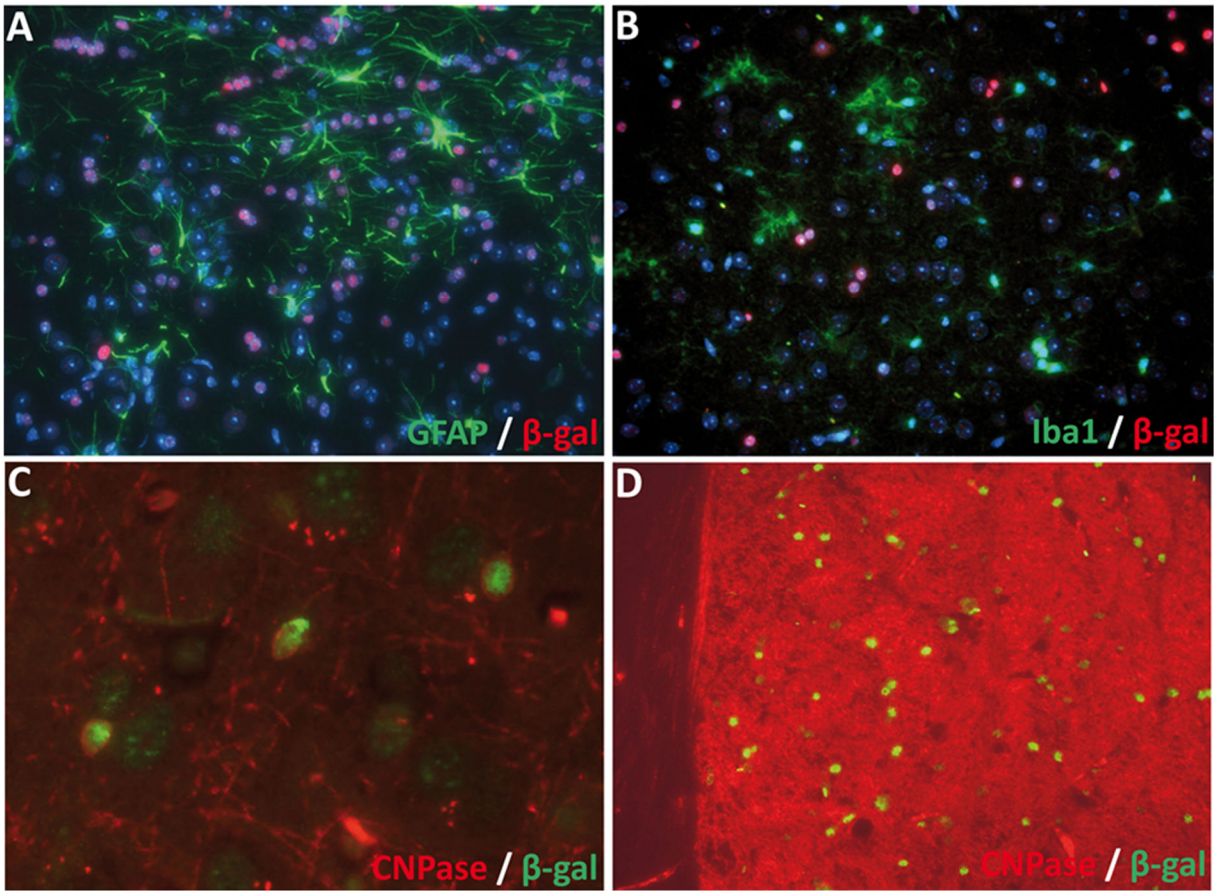

Figure 23: Immunohistochemical analysis of ADAMTS4 expression in the cortex of a 6.5-month-old 5xFAD / ADAMTS4$^{-/-}$ knockout mouse. To generate the ADAMTS4 knockout mice, the lacZ gene was inserted into the ADAMTS4 locus so that staining of β-galactosidase would represent ADAMTS4 expression. β-Galactosidase staining (red) did not co-localize with the astrocytic marker GFAP (**A**) or the microglia marker Iba1 (**B**) in the cortex (both in green, DAPI in blue). In contrast, β-galactosidase expression (green) in the cortex (**C**) and corpus callosum (**D**) was associated with the oligodendrocyte marker CNPase (red). The immunohistochemical stainings shown in this figure were performed by Dr. Oliver Wirths (University of Goettingen).

5.3 APP processing and Aβ generation in primary oligodendrocyte cultures

To study the role of ADAMTS4 in APP processing and Aβ generation specifically in oligodendrocytes, primary mouse oligodendrocyte cultures from ADAMTS4$^{-/-}$ knockout and wild type control mice were used. Initially, to confirm ADAMTS4 expression in oligodendrocytes, oligodendrocyte progenitor cells (OPCs) were extracted from newborn C57Bl/6J wild type mice (P1-P3) by whole brain homogenization and magnetic sorting with the oligodendrocyte progenitor specific marker A2B5. OPC cultures can be induced to differentiate into mature oligodendrocytes by addition of the thyroid hormones T3 and T4.

This process takes approximately 5 days to form mature oligodendrocytes with a characteristic marker expression profile. mRNA from cultures at three different time points was extracted; before hormone addition (d0), one day after induction of differentiation (d1), and at day five when differentiation was completed (d5), and analyzed by quantitative real-time PCR [Figure 24]. ADAMTS4 expression was confirmed in both OPCs and differentiated oligodendrocytes, and a trend for increased expression throughout the differentiation process was observed [Figure 24 A]. The expression levels of the oligodendrocyte markers CNPase [Figure 24 B] and MBP [Figure 24 C] increased as expected in the course of the differentiation, with MBP as a structural component of myelin preferentially expressed in mature, myelinating oligodendrocytes.

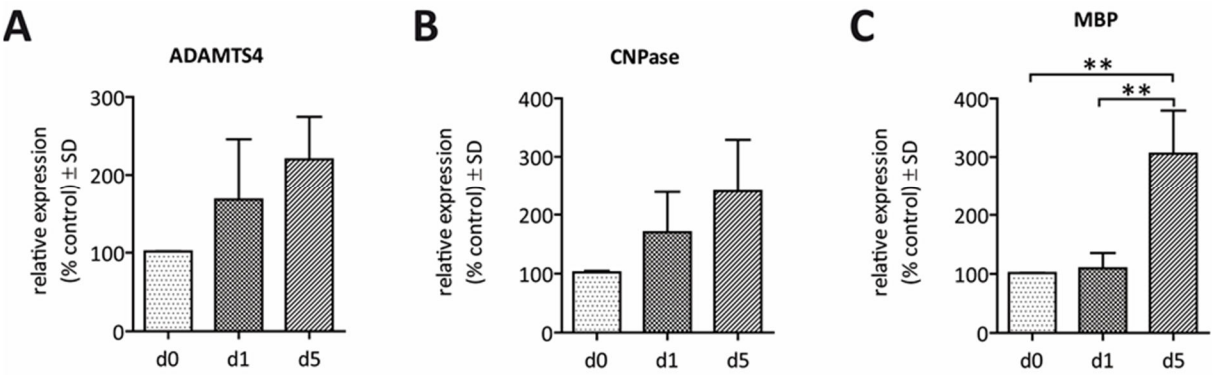

Figure 24: Relative mRNA expression levels of ADAMTS4, CNPase, and MBP in proliferating OPCs and differentiated oligodendrocyte cultures from days 0 to 5 measured by quantitative real-time PCR. One preparation of OPCs was cultured and differentiated. OPC preparation, differentiation, mRNA extraction, and cDNA synthesis were performed by Klaudia Lepka, a graduate student in the research group of Dr. Carsten Berndt (Department of Neurology, University of Duesseldorf). Each qPCR analysis was repeated three times. The expression levels of all three genes were normalized to GAPDH expression, and the expression levels at d0 were set to 100%. The mean relative expression levels of all three qPCR measurements were compared by one-way ANOVA with Tukey's post tests. Error bars represent standard deviation (SD). **, $p < 0.01$. (**A**) ADAMTS4 expression was detected in OPCs and its levels appeared to increase around 2-fold during the differentiation to mature oligodendrocytes. (**B**) The OPC and mature oligodendrocyte marker CNPase showed a trend for increased expression from d0 to d5. (**C**) MBP gene expression was significantly increased in differentiated, mature oligodendrocytes at d5 compared to OPCs at d0 and d1.

Next, OPCs were prepared from newborn ADAMTS4$^{-/-}$ knockout and ADAMTS4$^{+/+}$ wild type control animals. OPC cultures were transduced with an adenoviral vector expressing human

APP containing the Swedish mutation (APP695sw) to facilitate Aβ detection, while non-transduced cells served as negative controls. Cells were infected for 4 hours and subsequently cultured for 48 hours until conditioned supernatants and cell lysates were prepared. Through dense seeding of the cells and the stress of virus infection, OPCs spontaneously started to differentiate into mature oligodendrocytes as observed by visual inspection. Cell lysates and conditioned supernatants from three independent infection experiments were analyzed for changes in APP processing [Figure 25]. In cell lysates of virus-infected cultures, full-length APP levels showed some variability between the three independent experiments as detected by CT-15 Western blotting, likely due to differences in the viral infection efficiencies between the experiments [Figure 25 A]. Western blotting of tissue culture supernatants with the APP N-terminal antibody 22C11 revealed an increase of total APPs levels in ADAMTS4$^{-/-}$ knockout cells when compared to wild type control cells [Figure 25 B]. Quantitative analysis was performed by normalizing APPs levels to the corresponding APP full-length levels in cell lysates, which in turn were normalized to actin levels. The results confirmed a significant, more than 2-fold increase in total APPs levels in culture supernatants of ADAMTS4$^{-/-}$ knockout cells when compared to ADAMTS4$^{+/+}$ control cells [Figure 25 C].

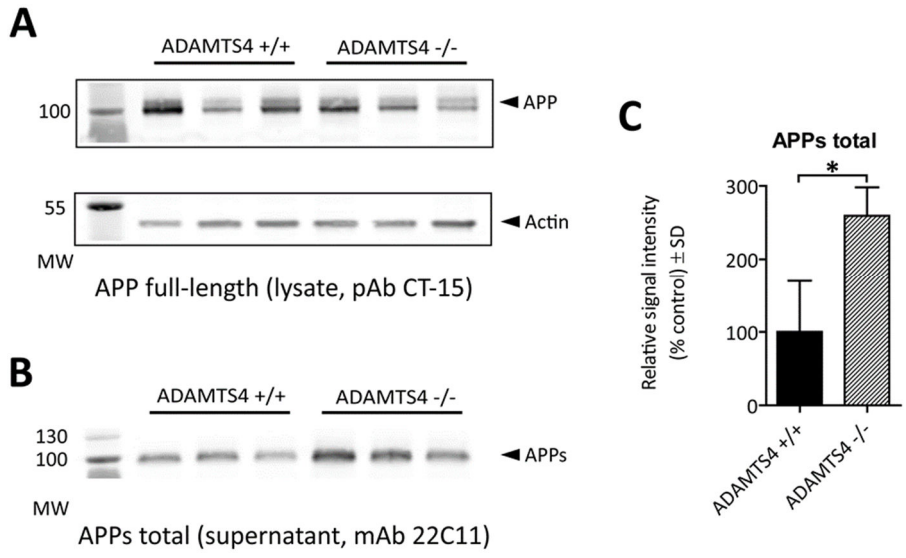

Figure 25: APP processing is changed in murine oligodendrocyte cultures lacking ADAMTS4. OPCs were cultured from ADAMTS4$^{-/-}$ knockout and ADAMTS4$^{+/+}$ control animals and transduced with an adenoviral vector expressing human APP with the Swedish mutation. Three independent infection experiments were performed. (**A**) Full-length APP levels in cell lysates detected by Western blotting with CT-15 did not appear to be substantially different between ADAMTS4$^{-/-}$ knockout and control cells, but showed some variability between the three

independent infection experiments. (**B**) Detection of total APPs with antibody 22C11 revealed increased levels in culture supernatants of ADAMTS4$^{-/-}$ knockout versus wild type control cells. (**C**) Quantitative analysis of the three independent infection experiments confirmed a significant, more than 2-fold increase in total APPs levels in ADAMTS4$^{-/-}$ knockout cells versus ADAMTS4$^{+/+}$ control cells. Each Western blot was repeated two times and the signal intensities of full-length APP in cell lysates were normalized to actin levels. Subsequently, APPs levels in culture supernatants were normalized to full-length APP levels. Unpaired t-test was used to compare the mean APPs values from all three independent experiments. Error bars represent standard deviation (SD). *, $p < 0.05$.

Importantly, the control cultures that were not transduced with the APP adenovirus showed the same effect on endogenous mouse APPs levels [Figure 26]. In the OPC cultures, the lack of ADAMTS4 had no apparent effect on endogenous APP full-length levels in cell lysates as detected by Western blotting with CT-15 [Figure 26 A] and by quantitative analysis normalized to actin levels [Figure 26 B]. In contrast, total APPs levels in conditioned cell culture supernatants were increased in ADAMTS4$^{-/-}$ knockout cells when compared to wild type control cells as detected by the 22C11 antibody [Figure 26 C]. This increase was confirmed by quantitative analysis of three independent experiments, which showed a significant, approximately 3-fold increase in total APPs levels in ADAMTS4$^{-/-}$ knockout cells versus ADAMTS4$^{+/+}$ control cells [Figure 26 D]. These results corroborated the effects of ADAMTS4 on APPs levels that we had observed in the cell culture overexpression experiments and in the ADAMTS4$^{-/-}$ knockout mice *in vivo*. When ADAMTS4 is absent, an increase in total APPs levels is observed, presumably because more APP is cleaved by α- and β-secretase or because of reduced degradation of APPs by ADAMTS4 in the extracellular space. However, in contrast to ADAMTS4 overexpression in HEK293 cells [Figures 12 and 14], endogenous expression levels of ADAMTS4 in OPCs and in the mouse brain did not appear to affect the mature form of full-length APP.

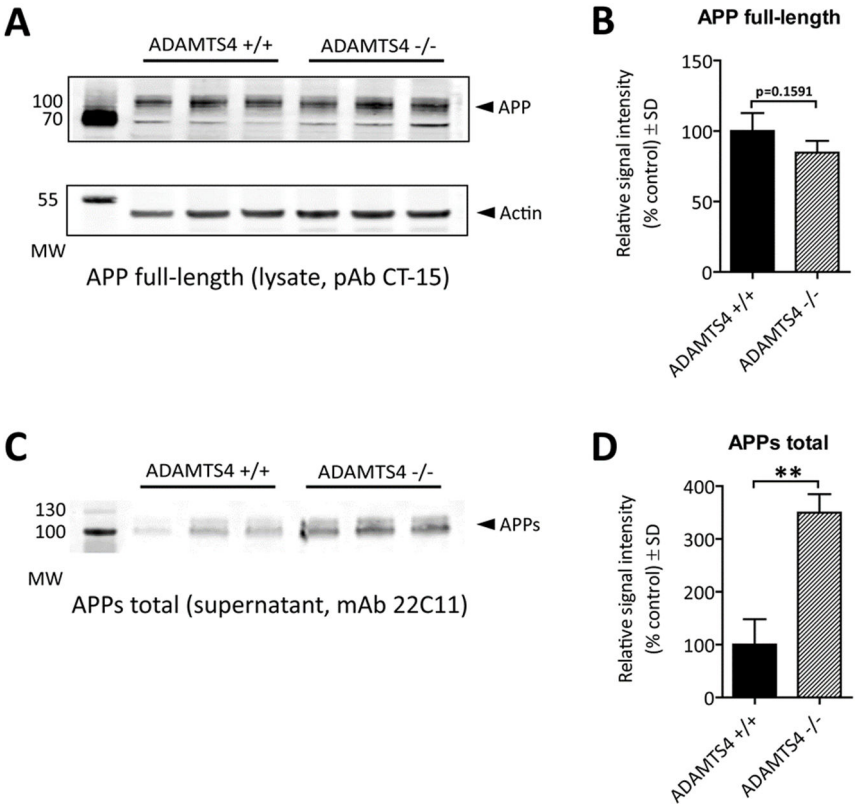

Figure 26: Endogenous APP processing is changed in murine oligodendrocyte cultures lacking ADAMTS4. OPCs were cultured from ADAMTS4$^{-/-}$ knockout and ADAMTS4$^{+/+}$ control animals. Three independent experiments were performed. (**A**) Western blotting with CT-15 to detect full-length APP in cell lysates showed no apparent differences between ADAMTS4$^{-/-}$ knockout and control cells. (**B**) Quantitative analysis of mean APP full-length values from three independent experiments revealed no significant difference in APP full-length levels between the two genotypes. The Western blot was repeated two times and the signal intensities of full-length APP in cell lysates were normalized to actin levels. Unpaired t-test was used to compare the mean APP full-length values from all three independent experiments. Error bars represent standard deviation (SD). (**C**) In contrast, total APPs levels were increased in tissue culture supernatants of ADAMTS4$^{-/-}$ knockout versus ADAMTS4$^{+/+}$ control cells as detected by Western blotting with antibody 22C11. (**D**) Quantitative analysis of three independent experiments revealed a significant, more than 3-fold increase in total APPs levels in ADAMTS4$^{-/-}$ knockout cells versus ADAMTS4$^{+/+}$ control cells. Each Western blot was repeated two times and the signal intensities of full-length APP in cell lysates were normalized to actin levels. Subsequently, APPs levels in culture supernatants were normalized to full-length APP levels. Unpaired t-test was used to compare the mean APPs values from all three independent experiments. Error bars represent standard deviation (SD). **, $p < 0.01$.

The effect of ADAMTS4 on Aβ generation in oligodendrocyte cultures was analyzed by mass spectrometry. Conditioned cell culture media of ADAMTS4$^{-/-}$ knockout cells and ADAMTS4$^{+/+}$ control cells infected with the APP adenovirus were immunoprecipitated with the anti-Aβ

antibody 4G8 to detect both full-length and N-terminally truncated species. The resulting mass spectra confirmed the generation of Aβ peptides by oligodendrocytes with Aβ1-40, Aβ1-38, and Aβ1-42 representing the main Aβ species [Figure 27]. Additionally, C-terminally truncated isoforms such as Aβ1-37 and N-terminally truncated forms like pGlu-Aβ3-42 and Aβ11-40 were detected. A definite peak for Aβ4-40 peptides was visible in the mass spectra of ADAMTS4 expressing control oligodendrocytes [Figure 27 A], while the spectra generated from ADAMTS4$^{-/-}$ knockout cells showed no such peak [Figure 27 B]. This confirmed the results by Skaper et al. that oligodendrocytes are indeed able to generate Aβ peptides, and that the profile of Aβ species produced by oligodendrocytes was rather similar to other cell types (Skaper et al. 2009). More importantly, these experiments showed that oligodendrocytes are able to generate N-terminally truncated Aβ4-x peptides and that this activity is dependent on the presence of ADAMTS4.

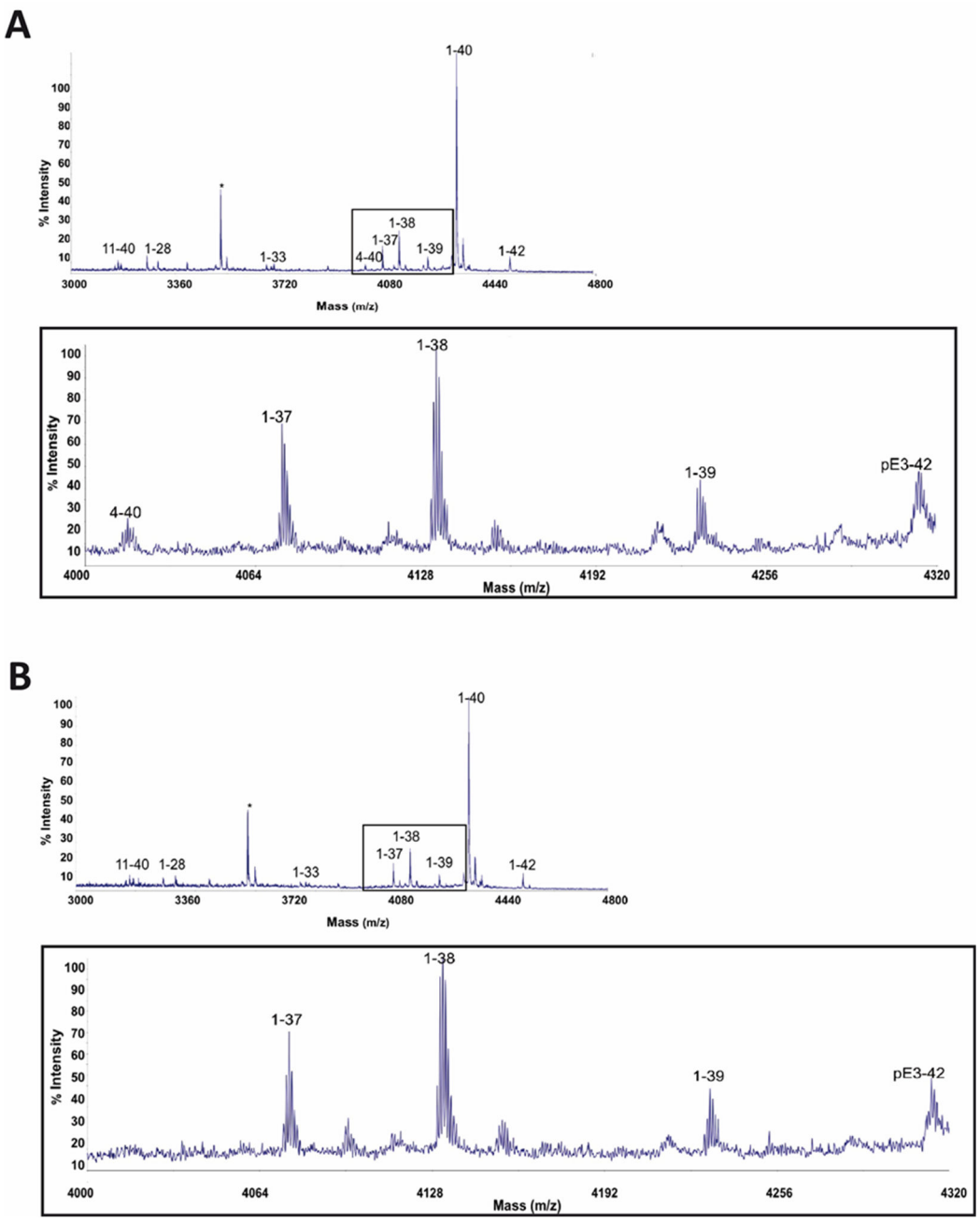

Figure 27: Mass spectrometry analysis of Aβ peptides in conditioned cell culture supernatants of ADAMTS4$^{+/+}$ wild type and ADAMTS4$^{-/-}$ knockout murine OPCs. The cultures were transduced with an adenovirus expressing human APPsw, and culture supernatants were immunoprecipitated with the anti-Aβ antibody 4G8 and analyzed by MALDI-TOF mass spectrometry. Three independent experiments were performed and representative mass spectra are shown. Unidentified background signals are marked with *. (**A**) Full spectrum and enlarged view (black box) of Aβ peaks from ADAMTS4$^{+/+}$ expressing cells. Aβ4-40 peptides were clearly detected alongside the more common species like Aβ1-40, Aβ1-42, and Aβ1-38. (**B**) The mass spectra acquired from ADAMTS4$^{-/-}$ knockout cells showed no peak for Aβ4-40 while the other Aβ species remained unchanged. The mass spectrometry analysis shown in this figure was performed by Hermeto Gerber in the research group of Dr. Patrick Fraering (Foundation Eclosion, Plan-Les-Ouates, Switzerland).

To quantitatively assess differences in Aβ peptide levels produced by ADAMTS4$^{-/-}$ knockout oligodendrocytes and wild type control cells, ELISA measurements of conditioned cell culture supernatants were performed. Analysis of Aβ1-40 and Aβ4-40 levels by ELISA was only possible after infection of OPC cultures with the APPsw adenovirus, while non-infected cells with endogenous, murine Aβ levels showed no background signals. Aβ1-40 peptides were detected in supernatants of both ADAMTS4 expressing and knockout cells and levels showed no substantial differences between the two genotypes in three independent infection experiments [Figure 28 A]. In marked contrast, Aβ4-40 peptides could only be measured in culture supernatants of wild type oligodendrocytes while cells prepared from ADAMTS4$^{-/-}$ knockout mice displayed no signal for Aβ4-40. Near identical results were obtained from the three independent infection experiments [Figure 28 B]. These results confirmed that ADAMTS4 did not affect the production of full-length Aβ1-40 peptides, but that the enzyme was essential for Aβ4-40 generation in oligodendrocytes.

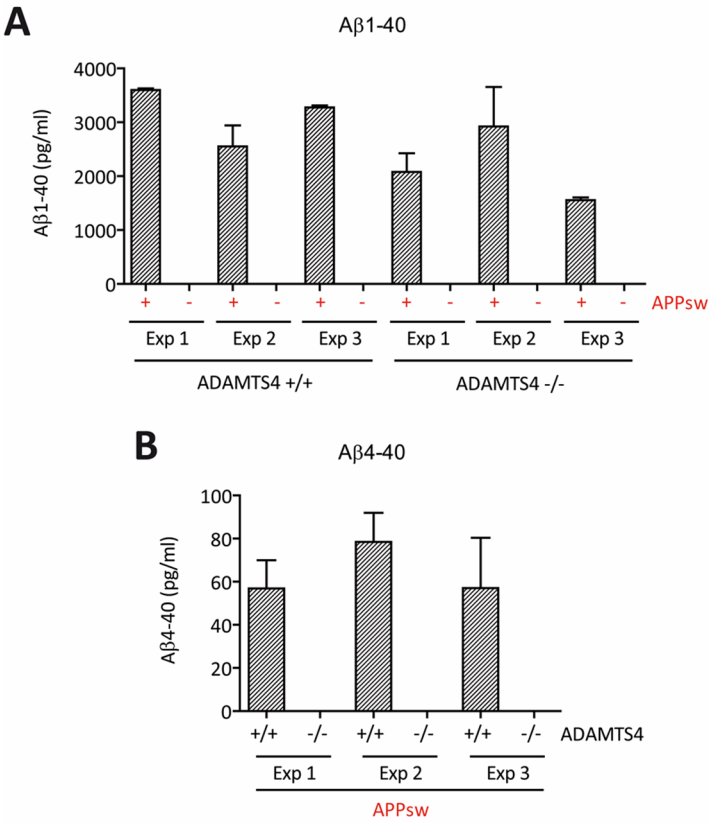

Figure 28: ELISA measurements of Aβ1-40 and Aβ4-40 peptides in conditioned supernatants from ADAMTS4$^{+/+}$ wild type and ADAMTS4$^{-/-}$ knockout murine OPC cultures. (**A**) Aβ1-40 was only detected in cultures transduced with the APP adenovirus (APPsw) and levels showed no substantial differences between ADAMTS4 expressing

and knockout cells in three independent experiments. (**B**) Measurements with the Aβ4-40 specific ELISA showed that Aβ4-40 was only detectable in culture supernatants of ADAMTS4$^{+/+}$ expressing cells while ADAMTS4$^{-/-}$ knockout cells displayed no background signal, indicating that ADAMTS4 is essential for the generation of Aβ4-x peptides in oligodendrocytes.

5.4 Aβ4-x staining pattern in 5xFAD and 5xFAD / ADAMTS4$^{-/-}$ mouse brains

The Aβ4-x specific PSL-029-2 antibody was used to determine whether the genetic deletion of ADAMTS4 would change the abundance or distribution of Aβ4-x peptides in the mouse brain. Therefore, paraffin-embedded, cortical sections of a 12-month-old 5xFAD / ADAMTS4$^{-/-}$ knockout and a 5xFAD / ADAMTS4$^{+/+}$ control animal were stained with PSL-029-2 using the ABC method. In the 5xFAD / ADAMTS4$^{+/+}$ control animal, extracellular amyloid plaques were abundantly detected. The antibody appeared to stain mostly the amyloid plaque cores [Figure 29 A], which is consistent with the PSL-029-2 staining pattern that has been previously observed in two AD animal models including 5xFAD mice and in AD brains (Wirths et al. in press). In white matter fiber tracts, fewer amyloid plaques were stained. However, in addition, a vesicular staining pattern was observed potentially showing intracellular, insoluble Aβ4-x peptides [Figure 29 A, marked by arrows]. Interestingly, this vesicular staining pattern was almost completely absent in the 5xFAD / ADAMTS4$^{-/-}$ knockout animal [Figure 29 B]. Furthermore, extracellular amyloid plaques appeared to be fewer in number and less intensely stained [Figure 29 B]. Overall, these stainings indicated that the abundance of Aβ4-x peptides in the 5xFAD / ADAMTS4$^{-/-}$ knockout brain is reduced but that the production of these Aβ species is not completely abolished, consistent with the ELISA analysis of SDS brain fractions shown in Figures 21 A and 22 A and B. The vesicular staining in the white matter could result from oligodendrocytes generating Aβ4-x peptides, and its absence in the 5xFAD / ADAMTS4$^{-/-}$ knockout brain is consistent with the finding that primary oligodendrocytes from ADAMTS4$^{-/-}$ knockout animals are unable to produce Aβ4-x peptides [Figures 27 and 28]. However, it is important to note that more definitive conclusions would require to repeat the stainings in a larger number of animals and to perform careful image analysis and quantification of amyloid plaque numbers, plaque sizes, and of the vesicular staining pattern.

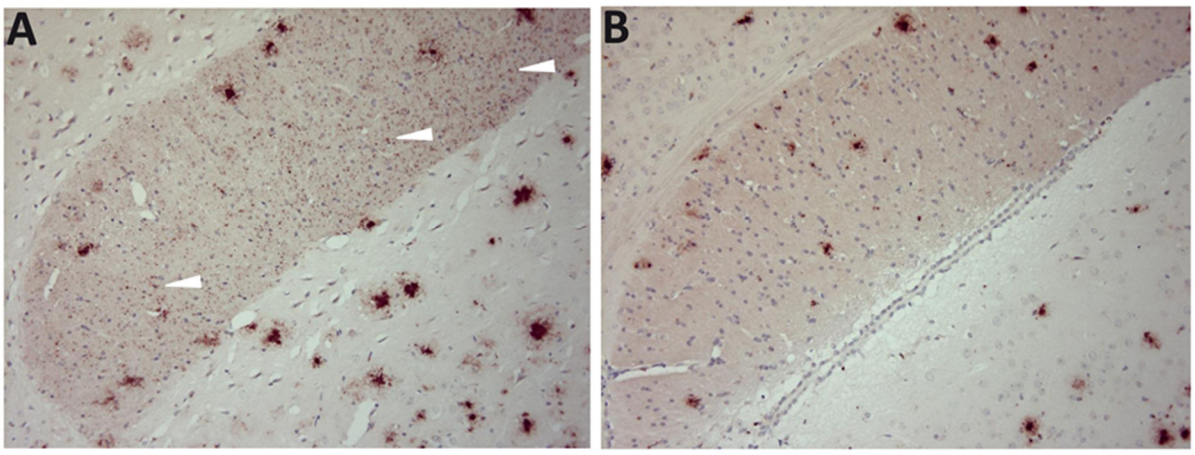

Figure 29: Immunohistochemical analysis of Aβ4-x peptides in the cortex of 5xFAD / ADAMTS4$^{+/+}$ control and 5xFAD / ADAMTS4$^{-/-}$ knockout animals. (**A**) Aβ4-x peptides were detected in the cores of abundantly stained extracellular amyloid plaques in a 5xFAD / ADAMTS4$^{+/+}$ control animal. Fiber tracts of the white matter showed a prominent vesicular staining (indicated by arrows). (**B**) In the cortex of a 5xFAD / ADAMTS4$^{-/-}$ knockout animal, the vesicular staining within the fiber tracts was largely absent, and the number and size of Aβ4-x positive amyloid plaques appeared to be reduced. The immunohistochemical stainings shown in this figure were performed by Dr. Oliver Wirths (University of Goettingen).

5.5 ADAMTS4 expression in human brain samples

Previous results in the literature obtained by immunohistochemical analysis had indicated that ADAMTS4 might be slightly under-expressed in AD brains compared to controls (Pehlivan et al. 2016). To investigate whether the expression of ADAMTS4 might be altered in AD brains on the mRNA level, human tissue samples were obtained from The Netherlands Brain Bank (www.brainbank.nl). RNA was extracted from brain tissue of 20 AD patients and 20 age-matched, non-demented control individuals, and qPCR analysis was performed. No difference in ADAMTS4 mRNA expression between AD samples and non-demented control samples was observed [Figure 30].

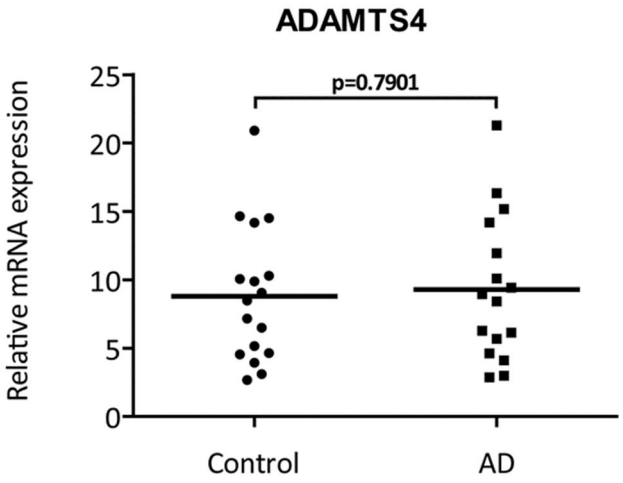

Figure 30: ADAMTS4 mRNA levels in brains of AD patients compared with age-matched control individuals. Quantitative real-time PCR analysis of total RNA extracted from brain tissue of 20 AD patients and 20 age-matched healthy individuals revealed no differences in the levels of ADAMTS4 mRNA. ADAMTS4 expression levels were normalized to the expression of the ARF-1 housekeeping gene, and statistical analysis was performed using unpaired t-test.

6. Discussion

The metalloprotease ADAMTS4 is expressed in various CNS structures including the cortex and hippocampus. Expression was detected in all cell types of the brain, i.e. neurons, astrocytes, microglia, and oligodendrocytes (Hamel et al. 2005, Tauchi et al. 2012, Levy et al. 2015). It might have a function in neuronal plasticity by enabling neurite and axonal outgrowth through ECM remodeling (Lemarchant et al. 2017). In the developing and adult mouse brain, ADAMTS4 is the highest expressed proteoglycanase of the ADAMTS family, and its upregulation coincides with several important aspects of neural development including myelination (Levy et al. 2015). ADAMTS4 might also play a role in the pathogenesis of CNS diseases and injuries (Zha et al. 2010, Wagstaff et al. 2011). Besides its prominent role in cartilage destruction in arthritic diseases, remodeling of the ECM and the altered release of pro-inflammatory mediators caused by ADAMTS4 affected several CNS pathologies, including ischemic stroke, spinal cord injury, amyotrophic lateral sclerosis, multiple sclerosis, and seizures (Arner et al. 1999, Haddock et al. 2006, Tauchi et al. 2012, Demircan et al. 2014, Lemarchant et al. 2014, Lemarchant et al. 2016a, Lemarchant et al. 2016b). Overall, these studies suggested that ADAMTS4 expression might be upregulated in response to inflammatory conditions, which are also present in AD. Only a few studies have addressed the potential involvement of ADAMTS4 in AD. An immunohistochemical study did not provide evidence for elevated expression of ADAMTS4 in brain tissue of AD patients (Pehlivan et al. 2016). However, ADAMTS4 was upregulated in astrocytes treated with Aβ peptides, and enhanced cleavage of proteoglycans was found in the vicinity of amyloid plaques in a transgenic mouse model of AD (Satoh et al. 2000, Ajmo et al. 2010). Based on the consensus sequence of the ADAMTS4 cleavage motif as reported by Hills et al., we have identified two putative ADAMTS4 cleavage sites within the Aβ region of APP (Hills et al. 2007). These cleavage events would lead to the production of N-terminally truncated Aβ species starting at the phenylalanine in position 4 and the valine in position 12 (Aβ4-x and Aβ12-x), indicating that ADAMTS4 might also be directly involved in the production of Aβ peptides.

Recently, several additional proteases have been identified that generate alternative APP fragments and may produce N-terminally truncated Aβ peptides (Willem et al. 2015, Zhang et al. 2015, Andrew et al. 2016, Baranger et al. 2016). A great diversity of Aβ peptide species varying in length at the N- and the C-terminus has been found in brain tissues of AD patients

and AD mouse models (Portelius et al. 2010, Antonios et al. 2013, Portelius et al. 2015). The most common isoforms starting at position 1 (Aβ1-x) are generated by BACE1 cleavage of APP (Hussain et al. 1999, Vassar et al. 1999). Peptides with varying C-terminal length are produced by γ-secretase cleavage, which is affected by FAD mutations in APP and PSEN resulting in increased generation of longer isoforms such as Aβx-42. These longer peptides have higher aggregation propensities and deposit preferentially into insoluble amyloid plaques (Gravina et al. 1995, Mann et al. 1996, Citron et al. 1997, Lichtenthaler et al. 2011). Several N-terminally truncated forms of Aβ have been found that cannot be attributed to BACE1 activity, and the origin of most of these peptides is undetermined (Masters et al. 1985, Sergeant et al. 2003, Bayer & Wirths 2014). So far, only the zinc metalloprotease meprin β was shown to generate N-truncated peptides starting at position 2 (Aβ2-x) by direct cleavage of APP independent of BACE1 (Wiltfang et al. 2001, Jefferson et al. 2011, Bien et al. 2012, Schonherr et al. 2016, Becker-Pauly & Pietrzik 2017). Aβ2-x levels were elevated in brain extracts from AD patients but this Aβ species is not a highly abundant peptide in amyloid plaques (Wiltfang et al. 2001, Jefferson et al. 2011, Bien et al. 2012, Schonherr et al. 2016, Becker-Pauly & Pietrzik 2017). The most common N-truncated peptides found in AD brain tissue are Aβ4-x peptides, which also deposit early during amyloid plaque formation and whose origin is not known until now (Sergeant et al. 2003, Portelius et al. 2010, Portelius et al. 2015). In general, N-terminal truncations of Aβ enhance peptide aggregation, which is correlated with higher neurotoxicity (Pike et al. 1995). The observations that Aβ4-x peptides are abundant in AD brains and that BACE1 is not responsible for their production suggested that other proteases might be involved in the generation of these N-terminally truncated Aβ peptides.

As part of this thesis, it was shown that ADAMTS4 is able to generate both Aβ4-40 and Aβ12-40 peptides in a stable and inducible cell culture system based on human HEK293 cells. In this culture system, ADAMTS4 expression can be induced by application of doxycycline. This allowed careful adjustment of expression levels and non-induced cells served as direct controls [Figure 9]. After induction of ADAMTS4 expression, conditioned cell culture media of three independent cell clones revealed no differences in the levels of Aβ peptides starting at position 1 as measured by ELISA [Figure 10 A]. However, using a specific antibody that detected only Aβ peptides starting at the phenylalanine in position 4, ELISA analysis

demonstrated that ADAMTS4 was able to generate Aβ4-40 peptides [Figure 10 C]. There was no background signal in non-induced cells, which indicated that ADAMTS4 was solely responsible for the generation of these truncated Aβ peptides. Quantitatively, the concentration of Aβ4-40 peptides in tissue culture supernatants was approximately 3-fold lower compared to Aβ1-40 peptides and 20-fold lower compared to Aβx-40 peptides, which included both full-length and N-truncated peptides ending with the valine in position 40 of the Aβ sequence [Figure 10 B]. This explained why the induction of ADAMTS4 expression and the generation of Aβ4-40 did not change the overall amount of Aβ peptides detectable in tissue culture supernatants, and showed that Aβ4-40 peptides were produced in smaller amounts as compared to other Aβ species such as Aβ1-40. In addition, mass spectrometry analysis of tissue culture supernatants revealed the presence of Aβ4-40 as well as Aβ12-40 peptides only when ADAMTS4 was expressed [Figure 11]. This confirmed that ADAMTS4 cleaved APP at the two putative cleavage sites resulting in the secretion of both N-terminally truncated species [Figure 31].

Further studies showed that overexpression of ADAMTS4 not only led to the secretion of N-terminally truncated Aβ4-40 and Aβ12-40 peptides but also changed the metabolism of APP and generated alternative APP fragments that appeared in both cell lysates and in cell culture supernatants [Figure 12 C and 13 A]. Additional APP C-terminal fragments detected in cell lysates were substantially larger than CTF-α or CTF-β (between 25-35 kDa), indicating that ADAMTS4 cleaves APP at another recognition site in its ectodomain further N-terminal to the β-secretase cleavage site [Figure 31]. Moreover, total APPs levels in tissue culture supernatants were substantially reduced when ADAMTS4 was expressed [Figure 13 A and B], and a smaller N-terminal fragment (ca. 70 kDa) was detected in the cell culture medium. This N-terminal fragment was approximately 30 kDa shorter at the C-terminus compared to the ectodomains generated by α- and β-secretase cleavage of APP (around 100 kDa), which indicated that it might correspond to the ADAMTS4 generated C-terminal fragment of around 30 kDa in cell lysates. However, this needs to be further investigated by mapping the exact ADAMTS4 cleavage site in the APP ectodomain and by determining the N- and C-termini of the additional APP cleavage fragments. Importantly, ADAMTS4 cleaved endogenously expressed human, wild type APP in HEK293 cells and endogenous mouse APP in a murine glioma cell line in a similar manner [Figure 14 A and B], indicating that these effects were neither cell line specific nor dependent on APP overexpression or on the Swedish mutation in

the APP substrate. However, we noticed that the processing of endogenous murine APP in a mouse astrocytoma cell line was possibly less efficient compared to the processing of endogenous human APP in HEK293 cells [Figure 14 A and B]. This could be related to the fact that the ADAMTS4 consensus recognition motif is completely present in the human Aβ sequence starting with the glutamic acid in the P1 position with the exception of a glycine in the P6' position (P1-EF**R**HDSG-P6'). However, the murine sequence contains a non-conservative exchange of arginine for glycine in the P2' position (P1-EF**G**HDSG-P6'), which might reduce the cleavage efficiency. Potentially, the additional APP fragments generated by ADAMTS4 could have physiological functions. Both δ- and η-secretase cleavage of APP by AEP and MT5-MMP have been shown to generate alternative APP fragments, which were neurotoxic and increased Aβ production and aggregation (Willem et al. 2015, Zhang et al. 2015, Baranger et al. 2016). The processing of APP by ADAMTS4 also showed interesting similarities to the previously described processing of APP by the metalloprotease meprin β. Meprin β also cleaved APP at multiple sites, which in addition to the secretion of N-terminally truncated Aβ2-x peptides resulted in the release of small N-terminal fragments (approximately 11 and 20 kDa), which were detected in mouse brain extracts but had no influence on neuronal cell viability *in vitro* (Jefferson et al. 2011). However, in contrast to ADAMTS4, the processing of APP by meprin β was blocked by the Swedish mutation, which is likely due to the fact that the recognition site for meprin β in APP is changed by the Swedish mutation, while the recognition site for ADAMTS4 in APP is located three amino acids further C-terminal to the Swedish mutation site (Schonherr et al. 2016). In any case, prior to additional functional studies of the alternative APP fragments generated by overexpression of ADAMTS4 *in vitro*, it was important to verify that these fragments were indeed detectable *in vivo*, which was further investigated in the ADAMTS4 knockout mice (see below).

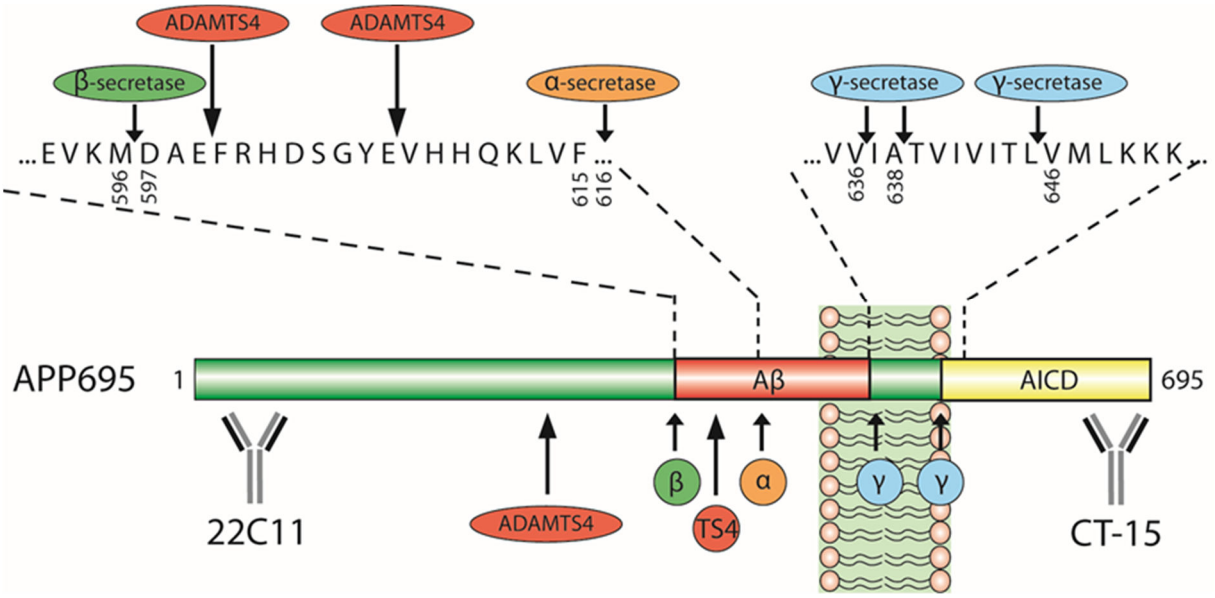

Figure 31: ADAMTS4 cleavage sites in APP. As demonstrated in cultured HEK293 cells with inducible overexpression of ADAMTS4, the protease can cleave APP at two sites in the Aβ sequence to generate N-terminally truncated Aβ4-x and Aβ12-x peptides. Since these ADAMTS4 cleavage sites are very close to the α- and β-secretase cleavage sites, the resulting APP fragments (APPs ectodomain and membrane-bound APP-CTF) would be similar in size to the fragments generated by α- and β-secretase. Additionally, ADAMTS4 appears to cleave APP in the ectodomain N-terminal to the β-secretase cleavage site. This leads to the production of additional APP fragments: a membrane-bound C-terminal fragment with a size between 25-35 kDa, which was detected in cell lysates with the C-terminal APP antibody CT-15, and a shorter APPs ectodomain with a size of approximately 70 kDa, which was detected in cell culture supernatants with the N-terminal APP antibody 22C11.

APP is a type-1 transmembrane protein located in the secretory pathway and at the cell surface, whereas ADAMTS4 is a secreted soluble metalloprotease with its main ECM substrates in the extracellular space. Therefore, interesting and important questions were in which cellular compartments APP and ADAMTS4 interact and whether ADAMTS4 cleaves APP intracellularly or only in the extracellular space. While not fully conclusive, the data in this thesis indicated that APP cleavage by ADAMTS4 might occur both within the cell and in the extracellular space, but also strongly supported that at least the generation of Aβ4-40 peptides could occur intracellularly. By transient co-transfection into HEK293 cells and subsequent co-immunoprecipitation experiments, ADAMTS4 was shown to interact with APP in the early secretory pathway [Figure 15]. The fact that the ADAMTS4 that was pulled down bound to APP was the catalytically-inactive pro-form and that the bound APP was the non-glycosylated immature form suggested that the interaction occurred in the early secretory

pathway before activation of ADAMTS4 by furin cleavage in the trans-Golgi network could take place. This was further confirmed by immunocytochemical analysis of HEK293 cells with stable co-expression of APP695sw and ADAMTS4. Co-localization between APP and ADAMTS4 was mainly found in a cellular compartment close to the cell nucleus, which indicated that the interaction of ADAMTS4 and APP likely occurred in the ER or the early Golgi system [Figure 16]. Why APP could not be co-immunoprecipitated with the proteolytically-active, mature form of ADAMTS4 is unclear. However, this might be due to the often transient and very short-lived interaction between active proteases and their substrates. In addition, after transient transfection, the amount of active mature ADAMTS4 was substantially lower compared to the immature pro-form, which could have resulted in levels of mature ADAMTS4 below the detection limit in the co-immunoprecipitation experiments. Nevertheless, several observations strongly indicated that APP must have interacted with the catalytically-active form of ADAMTS4 in the trans-Golgi or later compartments of the secretory pathway, and that APP cleavage by ADAMTS4 at least in part happened within the cell. First, ADAMTS4 overexpression caused an approximately 50% reduction of the mature, glycosylated forms of APP [Figure 12 A and B], which are localized to late compartments of the secretory pathway and the cell surface (Kaether et al. 2002). In contrast, the levels of the immature non-glycosylated forms of APP, which are localized to early compartments of the secretory pathway, were unaffected by ADAMTS4 overexpression. Second, Aβ4-40 levels in tissue culture supernatants after induction of ADAMTS4 expression were not negatively affected by concomitant treatment of the cells with a BACE1 inhibitor, which reduced Aβ1-x peptides in culture supernatants to undetectable levels [Figure 17]. Under these conditions, it is not possible that the detected Aβ4-40 peptides were generated through truncation of Aβ1-x peptides by ADAMTS4 in the extracellular space. Instead, these Aβ4-40 peptides must have been generated intracellularly, first by ADAMTS4 cleavage of APP within the Aβ domain and then by γ-secretase cleavage, which in its catalytically active form is also enriched in late compartments of the secretory pathway and on the cell surface (Kaether et al. 2002). These experiments further indicated that ADAMTS4 did not compete with BACE1 for cleavage of APP since Aβ1-x levels were unchanged after induction of ADAMTS4 expression, and in turn BACE1 inhibition did not lead to substantially increased Aβ4-40 production. Lastly, additional experiments demonstrated that ADAMTS4 was also able to generate Aβ4-40 peptides by truncating pre-existing, recombinant Aβ1-40 peptides in a cell-free assay, and might therefore

also use Aβ1-x full-length peptides generated by BACE1 as a substrate in the extracellular space [Figure 18]. It is much less obvious where in the cell ADAMTS4 might cleave APP in its ectodomain to release the smaller, approximately 70 kDa APPs fragment that was observed after induction of ADAMTS4 expression. On the one hand, this might have occurred intracellularly or at the cell surface, which is supported by the detection of a novel approximately 30 kDa C-terminal APP fragment in cell lysates. However, the release of the 70 kDa APPs fragment was accompanied by strongly reduced levels of full-length APPs and APPs-β. While the reduced APPs-β levels in particular could be explained by competition between ADAMTS4 and BACE1, the experiments with the BACE1 inhibitor appeared to rule out this possibility. An alternative explanation is that ADAMTS4 might truncate soluble APPs molecules in the extracellular space at the C-terminus to generate the 70 kDa APPs fragment. In this respect, ADAMTS4 might have a role in degrading APPs and controlling its extracellular levels (see below). Whether ADAMTS4 is, in principle, able to recognize and cleave APPs could be tested by incubating purified ADAMTS4 with a recombinant APPs substrate in a cell-free assay, similar to the experiments with purified ADAMTS4 and recombinant Aβ1-40 peptides.

Neurons are thought to be the main source of Aβ peptides in the brain, but glial cells also produce Aβ (Haass et al. 1991, LeBlanc et al. 1996). In one *in vitro* study, primary astrocytes and microglia predominantly secreted N-terminally truncated forms while neurons almost exclusively generated full-length peptides (Oberstein et al. 2015). Additionally, oligodendrocytes have been suggested to produce Aβ peptides in similar amounts as compared to neurons (Skaper et al. 2009). Since glial cells outnumber neurons in the brain, their contribution to the brain Aβ pool, in particular with N-truncated Aβ forms, might influence amyloidogenesis and amyloid plaque formation in a major way (Herculano-Houzel 2014). Previous studies had detected ADAMTS4 protein expression by immunohistochemistry in the human, mouse, and rat brain and spinal cord in neurons, astrocytes, and oligodendrocytes (Haddock et al. 2006, Krstic et al. 2012, Lemarchant et al. 2016b, Dubey et al. 2017). In addition, ADAMTS4 mRNA was measured by qPCR in primary cultures of murine astrocytes and microglia cells (Tauchi et al. 2012, Lemarchant et al. 2016a). Surprisingly, our studies using β-galactosidase reporter mice demonstrated that ADAMTS4 was exclusively expressed by oligodendrocytes in the adult murine brain, providing no evidence for expression

in neurons, astrocytes, or microglia cells. Co-localization of β-galactosidase expression in the brains of ADAMTS4$^{-/-}$ knockout mice was restricted to cells expressing CNPase, a marker enzyme expressed throughout the oligodendrocyte lineage from precursor cells to mature oligodendrocytes (Baumann & Pham-Dinh 2001) [Figure 23]. While our data appears to contradict some studies in the literature, several arguments support that ADAMTS4 is indeed specifically expressed in oligodendrocytes. First, none of the immunohistochemistry studies had included genetic controls (meaning tissue samples from ADAMTS4$^{-/-}$ knockout mice) to proof the specificity of the applied commercial antibodies. Second, the detection of mRNA in cultured cells does not necessarily correlate with protein expression, and many genes are aberrantly expressed when acutely isolated cells are adopted to *in vitro* culture conditions. Third, several previous studies had also suggested that ADAMTS4 could be an oligodendrocyte specific gene. An *in situ* hybridization study by Levy et al. had detected ADAMTS4 mRNA specifically in oligodendrocytes of the mouse hippocampus and cortex at P21, and in co-localization studies the riboprobe bound to cells positive for the oligodendrocyte marker Olig2 but not to cells stained with neuronal, astrocytic, or microglia markers (Levy et al. 2015). In addition, both transcriptomic and proteomic studies of cultured murine brain cells had indicated that ADAMTS4 is specifically and highly expressed in oligodendrocytes (Zhang *et al.* 2014, Sharma *et al.* 2015). Most importantly, during the preparation of this thesis, we learned that another research group had employed the same ADAMTS4$^{-/-}$ knockout reporter mouse strain to study the expression of ADAMTS4 in the brain, and had reached the same conclusions (Pruvost *et al.* 2017). In the adult mouse brain, expression of β-galactosidase was exclusively localized to Olig2-positive oligodendrocytes, and co-localization with markers for neurons, astrocytes, microglia, and endothelial cells was excluded. Further studies demonstrated that ADAMTS4 expression was restricted to cells co-expressing adenomatous-polyposis-coli protein (APC), a marker for mature oligodendrocytes, whereas there was no co-localization with platelet-derived growth factor receptor α (PDFGRα), a marker for OPCs (Pruvost et al. 2017).

Subsequently, primary oligodendrocyte cultures were prepared from ADAMTS4$^{-/-}$ knockout and wild type control animals to assess the expression of ADAMTS4 and its effects on APP processing and Aβ generation. Similarities but also clear differences were observed in this primary culture model with endogenous ADAMTS4 expression in comparison to the HEK293 cells with stable overexpression of ADAMTS4. By mRNA analysis, it was shown that

oligodendrocyte progenitor cells (OPCs) as well as differentiated oligodendrocytes expressed ADAMTS4 with a trend for higher expression levels in the mature cells [Figure 24 A]. To facilitate Aβ detection in the OPC cultures, the cells were transduced with an adenovirus expressing human APP695 containing the Swedish mutation, which also initiated spontaneous differentiation into mature oligodendrocytes. Importantly, mass spectrometry analysis of conditioned OPC culture medium confirmed the generation of Aβ4-40 peptides in ADAMTS4 expressing cells while spectra generated from ADAMTS4$^{-/-}$ knockout oligodendrocytes did not show a peak for Aβ4-40. This confirmed that murine oligodendrocytes express the enzymes required to produce Aβ4-40 peptides and that ADAMTS4 is essential for Aβ4-40 production in this cell type [Figure 27]. In contrast to HEK293 cells with ADAMTS4 overexpression, the mass spectra from wild type oligodendrocytes did not show a peak corresponding to Aβ12-40. Similarly, mass spectra of the formic acid brain fraction of 5xFAD mice with endogenous ADAMTS4 expression did display peaks for Aβ4-40 and Aβ4-42 but not for Aβ12-40 peptides [Figure 20]. This indicated that endogenously expressed ADAMTS4 might not recognize the second ADAMTS4 cleavage site starting with the glutamic acid in position 11 of the Aβ sequence to any measurable degree. The reason for this could be that this second cleavage site is much less conserved when compared to the ADAMTS4 consensus recognition sequence as proposed by Hills et al. (Hills et al. 2007). Quantitative analysis by ELISA revealed that full-length Aβ1-40 was produced in both ADAMTS4 expressing and knockout oligodendrocytes to similar amounts [Figure 28 A]. This confirmed the data from HEK293 cells, in which overexpression of ADAMTS4 expression did not affect the levels of Aβ1-x peptides and further supported that ADAMTS4 and BACE did not compete for the substrate APP [Figure 10]. In contrast, using the Aβ4-40 specific ELISA, a signal was only detected in ADAMTS4 expressing oligodendrocytes validating the mass spectrometry results [Figure 28 B]. Overall, Aβ4-40 levels in primary wild type oligodendrocytes infected with the APP695sw adenovirus were around 40-fold lower than those produced by HEK293 cells with stable overexpression of ADAMTS4 and APP695sw while Aβ1-40 levels were comparable between the two cell systems [Figures 10 and 28]. This resulted in around 60-fold lower levels of Aβ4-40 as compared to Aβ1-40 in oligodendrocytes indicating that Aβ4-x peptides are a minor Aβ species and that Aβ4-40 levels in HEK293 cells are likely artificially elevated by ADAMTS4 overexpression. The differentiation of OPCs is not entirely restricted to oligodendrocytes, some minor amounts of astrocytes and even smaller numbers of neurons can also be generated (Crawford et al. 2014,

Ettle et al. 2015). Therefore, it is possible that some cells in our OPC cultures differentiated into astrocytes that contributed to the Aβ peptides measured by mass spectrometry and ELISA. However, since our immunohistochemistry had shown that ADAMTS4 is exclusively expressed in oligodendrocytes in the murine brain, this effect should be neglectable when investigating Aβ4-x peptide levels and the contribution of ADAMTS4. While the Aβ results were rather similar between primary oligodendrocytes with endogenous ADAMTS4 expression and HEK293 cells with overexpression of ADAMTS4, more substantial differences were observed with respect to APP processing in these tissue culture models. First, endogenous APP levels including the mature forms were similar in cell lysates of ADAMTS4$^{-/-}$ knockout oligodendrocytes and wild type cells, while HEK293 cells had shown a more than 50% decrease in mature APP levels after induction of ADAMTS4 expression [Figures 12 and 26]. Second, ADAMTS4 overexpression in HEK293 cells had resulted in the appearance of novel APP C-terminal fragments in cell lysates and a smaller APPs fragment in culture supernatants [Figures 12 and 13]. In contrast, by comparing cell lysates and supernatants of ADAMTS4$^{-/-}$ knockout oligodendrocytes and wild type cells in the same molecular weight range, no obviously different protein bands were observed. It is possible that in cells with endogenous ADAMTS4 expression the additional APP fragments seen in the experiments with HEK293 cells are generated only in very low amounts below the detection limit of the Western blotting method. However, a more plausible explanation seems to be that these additional APP fragments and the strong decrease in mature APP level were artefacts caused by the overexpression of ADAMTS4 in HEK293 cells and are not relevant in cells with endogenous levels of ADAMTS4 expression. Despite that, levels of the secreted ectodomain APPs were dramatically changed in ADAMTS4$^{-/-}$ knockout oligodendrocytes. Endogenous full-length APPs levels were 3-fold higher in tissue culture supernatants of ADAMTS4$^{-/-}$ knockout compared to wild type cells, an effect that is in agreement with the dramatically reduced full-length APPs levels in culture supernatants of HEK293 cells overexpressing ADAMTS4 [Figures 13 and 26]. This clearly demonstrated that the effects of ADAMTS4 are not limited to the generation of Aβ4-x peptides, and that ADAMTS4 has a very substantial influence on APPs levels. The exact molecular mechanism through which ADAMTS4 regulates APPs levels in oligodendrocytes remains unclear and will have to be investigated in future studies.

The well-characterized 5xFAD mouse model was used to determine the effects of ADAMTS4 on APP processing and Aβ generation *in vivo*. The ADAMTS4$^{-/-}$ knockout mouse line was crossed with the 5xFAD line to introduce human APP and to facilitate Aβ detection in brain extracts. Mass spectrometry analysis of Aβ peptides in FA brain extracts at 12 months of age revealed no differences between 5xFAD / ADAMTS4$^{-/-}$ and 5xFAD / ADAMTS4$^{+/+}$ control animals [Figure 20]. Aβ4-40 and Aβ4-42 peptides were detected in both genotypes and the mass spectra showed no qualitative differences in any Aβ species. However, quantitative analysis with the Aβ4-x specific ELISA system revealed a decrease in Aβ4-40 levels of approximately 50% in the 5xFAD / ADAMTS4$^{-/-}$ knockout compared to 5xFAD / ADAMTS4$^{+/+}$ control animals, while Aβ4-42 peptides were undetectable at this age [Figure 21 A]. In a separate cohort of animals at 15 months of age, Aβ4-40 levels were significantly reduced by about 30% in 5xFAD / ADAMTS4$^{-/-}$ versus 5xFAD / ADAMTS4$^{+/+}$ control animals, while Aβ4-42 levels were not different between the genotypes [Figure 22 A and B]. At first sight, the mass spectrometry and the ELISA results appeared to contradict each other. However, this discrepancy can easily be explained by the fact that our mass spectrometry method did not provide quantitative data, meaning that peak heights in the spectra did not correlate with the abundance of individual peptides. Since the peaks for Aβ4-40 and Aβ4-42 were rather small, a clear difference in the spectra would have only been expected if the generation of Aβ4-x peptides had been completely abolished in the 5xFAD / ADAMTS4$^{-/-}$ knockout animals. Hence, the ELISA analysis verified that ADAMTS4 is responsible for a substantial fraction but not all of the Aβ4-40 generation in the adult murine brain.

Total Aβ levels in TBS and SDS brain fractions as measured with Aβ1-40/42 or Aβx-40/42 specific ELISA assays were unchanged between the genotypes in 12-month as well as in 15-month-old animals [Figure 21 B – G, 22 C – E]. In addition, a quantification of the amyloid plaque load by image analysis at 12 months of age performed in the laboratory of Prof. Dr. Oliver Wirths did not show differences between 5xFAD / ADAMTS4$^{-/-}$ and 5xFAD / ADAMTS4$^{+/+}$ animals. In the SDS brain fractions of 5xFAD / ADAMTS4$^{+/+}$ animals, the levels of Aβ4-x peptides were much lower compared to Aβ1-x peptides. At 12 months of age, Aβ4-40 levels were approximately 60-fold lower than Aβ1-40 levels and more than 1000-fold lower than Aβ1-42 levels. Aβ4-42 levels could only be measured in 15-month-old animals and were approximately 20-fold and 450-fold lower than Aβ1-40 and Aβ1-42 levels. These data largely concurred with our previous ELISA measurements in 5-month-old 5xFAD mice, in which Aβ1-

40 and Aβ1-42 peptides were approximately 75 and 200-fold more abundant than Aβ4-40 peptides (Wirths et al. in press). This demonstrated that, in the 5xFAD mouse model, the contribution of Aβ4-x peptides to the total Aβ peptide pool in the brain is small, and likely explained why the development of the amyloid pathology was unchanged in 5xFAD / ADAMTS4$^{-/-}$ as compared to 5xFAD / ADAMTS4$^{+/+}$ control animals. With respect to APP processing, the findings in the mouse brains were similar to the results in primary oligodendrocyte cultures. Total and mature APP levels were unchanged between 5xFAD / ADAMTS4$^{-/-}$ and 5xFAD / ADAMTS4$^{+/+}$ animals, and the APP protein band pattern in TBS and SDS brain fractions obtained with antibodies against C-and N-terminal epitopes did not show any obvious differences, providing no evidence for additional APP cleavage fragments as seen in HEK293 cells overexpressing ADAMTS4. However, the same effect of ADAMTS4 on APPs and APPs-β levels as observed in the oligodendrocyte cultures was detected in the TBS brain fractions of 12-month-old mice [Figure 19 B and C]. When ADAMTS4 was knocked out, an approximately 30% increase in APPs and APPs-β levels was observed when compared to 5xFAD / ADAMTS4$^{+/+}$ control animals. A similar but more prominent effect on APPs levels has been reported in meprin β knockout as compared to wild type control mice (Schonherr et al. 2016). Overall, the *in vivo* data obtained in 5xFAD / ADAMTS4$^{-/-}$ mice raised three important issues, none of which can be conclusively answered now. First, since Aβ4-40 levels in 12-month-old 5xFAD / ADAMTS4$^{-/-}$ mice were only reduced by 50%, which mechanism is responsible for the generation of the remaining Aβ4-x peptides? One possibility is that Aβ4-x could be generated by spontaneous non-enzymatic truncation of full-length Aβ peptides, although not much evidence is available to support such a mechanism (Lyons *et al.* 2016, Dubey et al. 2017). A further possibility is that another homologous protease from the ADAMTS family, some of which are expressed in the brain, might be able to generate Aβ4-x peptides (Hamel et al. 2005, Tauchi et al. 2012, Levy et al. 2015). Second, since biochemical studies of human tissue samples have supported that Aβ4-x peptides are among the most abundant Aβ peptides in the brains of AD patients (Masters et al. 1985, Miller et al. 1993, Lewis *et al.* 2006, Portelius et al. 2010, Moore et al. 2012), the question is why the abundance of Aβ4-x peptides is comparatively low in the 5xFAD mouse model of AD? The most likely explanation is that the expression patterns of the substrate APP and the enzyme ADAMTS4 only partially overlap in the 5xFAD mouse model. In 5xFAD and other AD mouse models, the APP transgene is expressed under the control of the neuron-specific Thy-1 promoter, which

directs APP expression in the brain predominantly or exclusively to neurons. This means that the human APP transgene is likely not at all or only very lowly expressed in cells of the oligodendrocyte lineage. In contrast, in the human brain, oligodendrocytes themselves might produce substantial amounts of Aβ4-x peptides. In addition, ADAMTS4 expression could be much more widespread in the human than in the murine brain with more cell types contributing to the Aβ4-x peptide pool, but there is no data to support this idea at this point. Finally, an open question is where in the mouse brain enzyme and substrate meet to produce Aβ4-x peptides. Our experiments in primary cultures suggest that co-expression of APP and ADAMTS4 in oligodendrocytes is sufficient to generate Aβ4-x peptides and these cells might produce a fraction of the Aβ4-x peptides. However, given that the APP transgene is likely not expressed in oligodendrocytes and because the endogenous mouse APP might be less efficiently processed by ADAMTS4, this possibility seems doubtful. Alternatively, ADAMTS4 might be secreted by oligodendrocytes and could process transgene-derived APP present on the surface of myelinated axons. APP is targeted to both axons and dendrites in neurons and has been localized to the surface of axonal membranes (DeBoer *et al.* 2014). Yet another possibility is that ADAMTS4 is secreted by oligodendrocytes and taken up by neurons through endocytosis, leading to processing of transgene-derived APP by ADAMTS4 in intracellular vesicular compartments. In cartilage, it has been demonstrated that extracellular ADAMTS4 can be internalized via low density lipoprotein receptor-related protein (LRP1), which is also abundantly expressed in neurons (Yamamoto *et al.* 2014, Pohlkamp *et al.* 2017). Interestingly APP is also internalized via LRP1, and LRP1 has been shown to affect APP processing and to promote Aβ generation (Knauer *et al.* 1996, Ulery *et al.* 2000, Pietrzik *et al.* 2002, Pietrzik *et al.* 2004) . Hence, it is possible that ADAMTS4 and APP are both internalized by LRP1 and might interact in endocytic vesicles to generate Aβ4-x. At present, we cannot decide whether APP and ADAMTS4 meet in oligodendrocytes, in the extracellular space, or after internalization in neurons. In the future, this issue could be addressed in co-culture experiments with primary neurons from APP-transgenic mice and primary oligodendrocytes from wild type and ADAMTS4$^{-/-}$ knockout mice. In any case, all three of these possibilities appear to be consistent with our immunohistochemical detection of punctate Aβ4-x-positive deposits in white matter structures of 5xFAD mice [Figure 29] (see below).

The abundance, distribution, and functional role of N-truncated Aβ4-x peptides in the pathogenesis of AD is still largely unclear. Evidence from human studies suggests that N-truncated Aβ peptides and in particular Aβ4-x peptides constitute a large proportion if not the majority of all Aβ peptides in the brains of AD patients. Early protein sequencing studies had demonstrated that only around 10% of Aβ peptides in amyloid plaque cores purified from AD brains displayed an intact N-terminus whereas more than 60% started with the phenylalanine residue in position 4 (Masters et al. 1985). Later studies have confirmed that Aβ4-42 peptides are a major component of insoluble amyloid deposits in the human brain, next to Aβ1-42 and pGlu-Aβ3-42 peptides, but further quantitative studies are clearly needed (Miller et al. 1993, Sergeant et al. 2003, Portelius et al. 2010, Moore et al. 2012, Portelius et al. 2015). By immunohistochemistry using Aβ4-x specific antibodies, we and others have shown that Aβ4-x is mainly located to the highly aggregated core region of amyloid plaques, which also supports an important role in Aβ aggregation and amyloid plaque formation (Cabrera *et al.* 2017, Wirths et al. in press). *In vitro* Aβ4-42 formed soluble oligomers and fibrillar higher molecular weight aggregates more rapidly than full-length Aβ peptides, and exposure of primary rat cortical cultures to aggregated Aβ4-x peptides induced neuron loss with the strongest effect for Aβ4-42. Furthermore, transgenic mice overexpressing Aβ4-42 developed age-dependent behavioral deficits and hippocampal neuron loss (Bouter et al. 2013). However, biochemical studies have consistently shown that N-truncated Aβ species are far less abundant in APP transgenic mouse models (Kawarabayashi et al. 2001, Kalback et al. 2002, Schieb et al. 2011). The ELISA measurements in this thesis project and in our previous study have confirmed that, quantitatively, N-truncated Aβ4-x peptides are a minor Aβ species in the 5xFAD mouse model (Wirths et al. in press). The finding that ADAMTS4 expression is restricted to oligodendrocytes, which likely do not express the APP transgene, provides a convincing explanation for these low Aβ4-x peptide levels. Therefore, AD mouse models like 5xFAD, in which APP transgene expression is directed selectively to neurons, are not an appropriate model to study the impact of Aβ4-x peptides on the amyloid pathology *in vivo*. Nevertheless, immunohistochemical stainings with the Aβ4-x specific antibody PSL-029-2 revealed small, punctate deposits of Aβ4-x peptides in white matter fiber tracts in the 5xFAD / ADAMTS4$^{+/+}$ control mice [Figure 29 A]. These punctate deposits in or surrounding oligodendrocytes were present in addition to Aβ4-x positive amyloid plaque cores, and were largely absent in the 5xFAD / ADAMTS4$^{-/-}$ brain samples. This is an interesting finding that could provide a novel

explanation for demyelination and white matter damage, which is frequently observed in AD cases. Neuropathological, biochemical, and imaging studies have all provided evidence for white matter loss and oligodendrocyte dysfunction in brains of AD patients and mouse models of the disease (Brun & Englund 1986, Roher *et al.* 2002, Song *et al.* 2004, Firbank *et al.* 2007, Huang & Auchus 2007, Desai *et al.* 2009, Bartzokis 2011, Rivera *et al.* 2016). Most intriguingly, diffusion tensor imaging has documented white matter abnormalities already in presymptomatic FAD mutation carriers (Ringman *et al.* 2007). The reasons for the white matter loss in AD are unknown and it has been proposed that oligodendrocyte degeneration occurs mainly secondary to the loss of neurons and axons (so called Wallerian degeneration). However, other studies have shown that Aβ peptides are cytotoxic to oligodendrocytes and that they accumulate in white matter structures (Xu et al. 2001, Mitew et al. 2010). This raises the possibility that N-truncated Aβ4-x peptides produced by oligodendrocytes or in myelinated axons could be uniquely toxic, and that they might contribute to white matter abnormalities in AD, a putative pathogenic mechanism that clearly needs to be investigated further.

In summary, the experiments conducted in this thesis project demonstrated that N-terminally truncated Aβ4-x peptides can be generated by an enzymatic activity and that the secreted metalloprotease ADAMTS4 expressed in oligodendrocytes is partially responsible for the production of these peptides in the mouse brain *in vivo*. In the brains of ADAMTS4$^{-/-}$ knockout mice crossed to the 5xFAD mouse model of AD, Aβ4-40 levels were reduced by about 50% and APPs levels were increased. Surprisingly, in the adult murine brain, ADAMTS4 was exclusively expressed in cells of the oligodendrocyte lineage. Cultured oligodendrocytes were able to produce and secrete a variety of Aβ peptide species including Aβ4-40. In contrast, oligodendrocytes prepared from ADAMTS4$^{-/-}$ knockout mice did not produce Aβ4-40 proving that ADAMTS4 is essential for the generation of Aβ4-x peptides in this cell type. In white matter structures of 5xFAD / ADAMTS4$^{+/+}$ knockout mice, punctate deposits of Aβ4-x peptides were observed, which were reduced in 5xFAD / ADAMTS4$^{-/-}$ knockout mice. Particularly interesting questions for future studies are whether Aβ4-x peptides are specifically produced in myelinated axonal compartments, and whether these peptides might be responsible for axonal damage and white matter degeneration seen in AD patients. However, answering

these questions will require new mouse models that account for a role of oligodendrocytes in the pathogenesis of AD.

7. References

Abbaszade, I., Liu, R. Q., Yang, F. et al. (1999) Cloning and characterization of ADAMTS11, an aggrecanase from the ADAMTS family. *The Journal of biological chemistry,* **274,** 23443-23450.

Abramov, E., Dolev, I., Fogel, H., Ciccotosto, G. D., Ruff, E. and Slutsky, I. (2009) Amyloid-beta as a positive endogenous regulator of release probability at hippocampal synapses. *Nature neuroscience,* **12,** 1567-1576.

Ajmo, J. M., Bailey, L. A., Howell, M. D., Cortez, L. K., Pennypacker, K. R., Mehta, H. N., Morgan, D., Gordon, M. N. and Gottschall, P. E. (2010) Abnormal post-translational and extracellular processing of brevican in plaque-bearing mice over-expressing APPsw. *Journal of neurochemistry,* **113,** 784-795.

Alattia, J. R., Kuraishi, T., Dimitrov, M., Chang, I., Lemaitre, B. and Fraering, P. C. (2011) Mercury is a direct and potent gamma-secretase inhibitor affecting Notch processing and development in Drosophila. *FASEB journal : official publication of the Federation of American Societies for Experimental Biology,* **25,** 2287-2295.

Alexandru, A., Jagla, W., Graubner, S. et al. (2011) Selective hippocampal neurodegeneration in transgenic mice expressing small amounts of truncated Abeta is induced by pyroglutamate-Abeta formation. *The Journal of neuroscience : the official journal of the Society for Neuroscience,* **31,** 12790-12801.

Alzheimer, A. (1907) Über eine eigenartige Erkrankung der Hirnrinde. *Allg Z Psychiat,* **64,** 146-148.

Ando, K., Iijima, K. I., Elliott, J. I., Kirino, Y. and Suzuki, T. (2001) Phosphorylation-dependent regulation of the interaction of amyloid precursor protein with Fe65 affects the production of beta-amyloid. *The Journal of biological chemistry,* **276,** 40353-40361.

Andrew, R. J., Kellett, K. A., Thinakaran, G. and Hooper, N. M. (2016) A Greek Tragedy: The Growing Complexity of Alzheimer Amyloid Precursor Protein Proteolysis. **291,** 19235-19244.

Antonios, G., Borgers, H., Richard, B. C. et al. (2015) Alzheimer therapy with an antibody against N-terminal Abeta 4-X and pyroglutamate Abeta 3-X. *Scientific reports,* **5,** 17338.

Antonios, G., Saiepour, N., Bouter, Y. et al. (2013) N-truncated Abeta starting with position four: early intraneuronal accumulation and rescue of toxicity using NT4X-167, a novel monoclonal antibody. *Acta neuropathologica communications,* **1,** 56.

Apte, S. S. (2009) A disintegrin-like and metalloprotease (reprolysin-type) with thrombospondin type 1 motif (ADAMTS) superfamily: functions and mechanisms. *The Journal of biological chemistry,* **284,** 31493-31497.

Arner, E. C., Pratta, M. A., Trzaskos, J. M., Decicco, C. P. and Tortorella, M. D. (1999) Generation and characterization of aggrecanase. A soluble, cartilage-derived aggrecan-degrading activity. *The Journal of biological chemistry,* **274,** 6594-6601.

Ashe, K. H. and Zahs, K. R. (2010) Probing the biology of Alzheimer's disease in mice. *Neuron,* **66,** 631-645.

Ballard, C., Gauthier, S., Corbett, A., Brayne, C., Aarsland, D. and Jones, E. (2011) Alzheimer's disease. *Lancet (London, England),* **377,** 1019-1031.

Baranger, K., Marchalant, Y., Bonnet, A. E. et al. (2016) MT5-MMP is a new pro-amyloidogenic proteinase that promotes amyloid pathology and cognitive decline in

a transgenic mouse model of Alzheimer's disease. *Cellular and molecular life sciences : CMLS,* **73,** 217-236.

Barao, S., Moechars, D., Lichtenthaler, S. F. and De Strooper, B. (2016) BACE1 Physiological Functions May Limit Its Use as Therapeutic Target for Alzheimer's Disease. *Trends in neurosciences,* **39,** 158-169.

Barnes, J., Dickerson, B. C., Frost, C., Jiskoot, L. C., Wolk, D. and van der Flier, W. M. (2015) Alzheimer's disease first symptoms are age dependent: Evidence from the NACC dataset. *Alzheimer's & dementia : the journal of the Alzheimer's Association,* **11,** 1349-1357.

Bartzokis, G. (2011) Alzheimer's disease as homeostatic responses to age-related myelin breakdown. *Neurobiology of aging,* **32,** 1341-1371.

Bateman, R. J., Aisen, P. S., De Strooper, B. et al. (2011) Autosomal-dominant Alzheimer's disease: a review and proposal for the prevention of Alzheimer's disease. *Alzheimers Res Ther,* **2,** 35.

Baumann, N. and Pham-Dinh, D. (2001) Biology of oligodendrocyte and myelin in the mammalian central nervous system. *Physiological reviews,* **81,** 871-927.

Bayer, T. A. and Wirths, O. (2014) Focusing the amyloid cascade hypothesis on N-truncated Abeta peptides as drug targets against Alzheimer's disease. *Acta neuropathologica*.

Becker-Pauly, C. and Pietrzik, C. U. (2017) The Metalloprotease Meprin beta Is an Alternative beta-Secretase of APP. *Frontiers in molecular neuroscience,* **9,** 159.

Beckett, C., Nalivaeva, N. N., Belyaev, N. D. and Turner, A. J. (2012) Nuclear signalling by membrane protein intracellular domains: the AICD enigma. *Cellular signalling,* **24,** 402-409.

Belyaev, N. D., Kellett, K. A., Beckett, C., Makova, N. Z., Revett, T. J., Nalivaeva, N. N., Hooper, N. M. and Turner, A. J. (2010) The transcriptionally active amyloid precursor protein (APP) intracellular domain is preferentially produced from the 695 isoform of APP in a {beta}-secretase-dependent pathway. *The Journal of biological chemistry,* **285,** 41443-41454.

Benilova, I. and De Strooper, B. (2013) Neuroscience. Promiscuous Alzheimer's amyloid: yet another partner. *Science (New York, N.Y.),* **341,** 1354-1355.

Bettens, K., Sleegers, K. and Van Broeckhoven, C. (2013) Genetic insights in Alzheimer's disease. *The Lancet. Neurology,* **12,** 92-104.

Beyreuther, K. and Masters, C. L. (1991) Amyloid precursor protein (APP) and ßA4 amyloid in the etiology of Alzheimer´s disease: precursor-produkt relationships in the derangement of neuronal function. *Brain Pathology,* **1,** 241-251.

Bibl, M., Gallus, M., Welge, V., Esselmann, H., Wolf, S., Ruther, E. and Wiltfang, J. (2012) Cerebrospinal fluid amyloid-beta 2-42 is decreased in Alzheimer's, but not in frontotemporal dementia. *Journal of neural transmission (Vienna, Austria : 1996),* **119,** 805-813.

Bien, J., Jefferson, T., Causevic, M., Jumpertz, T., Munter, L., Multhaup, G., Weggen, S., Becker-Pauly, C. and Pietrzik, C. U. (2012) The metalloprotease meprin beta generates amino terminal-truncated amyloid beta peptide species. *The Journal of biological chemistry,* **287,** 33304-33313.

Borchelt, D. R., Thinakaran, G., Eckman, C. B. et al. (1996) Familial Alzheimers disease-linked presenilin 1 variants elevate Abeta 1-42/1-40 ratio in vitro and in vivo. *Neuron,* **17,** 1005-1013.

Borg, J. P., Ooi, J., Levy, E. and Margolis, B. (1996) The phosphotyrosine interaction domains of X11 and FE65 bind to distinct sites on the YENPTY motif of amyloid precursor protein. *Molecular and cellular biology,* **16,** 6229-6241.

Bouter, Y., Dietrich, K., Wittnam, J. L. et al. (2013) N-truncated amyloid beta (Abeta) 4-42 forms stable aggregates and induces acute and long-lasting behavioral deficits. *Acta neuropathologica*.

Braak, H., Thal, D. R., Ghebremedhin, E. and Del Tredici, K. (2011) Stages of the pathologic process in Alzheimer disease: age categories from 1 to 100 years. *Journal of neuropathology and experimental neurology,* **70,** 960-969.

Bradshaw, N. J., Trossbach, S. V., Kober, S., Walter, S., Prikulis, I., Weggen, S. and Korth, C. (2017) Disrupted in Schizophrenia 1 regulates the processing of reelin in the perinatal cortex. *Schizophrenia research*.

Brockhaus, M., Grunberg, J., Rohrig, S., Loetscher, H., Wittenburg, N., Baumeister, R., Jacobsen, H. and Haass, C. (1998) Caspase-mediated cleavage is not required for the activity of presenilins in amyloidogenesis and NOTCH signaling. *Neuroreport,* **9,** 1481-1486.

Brun, A. and Englund, E. (1986) A white matter disorder in dementia of the Alzheimer type: a pathoanatomical study. *Annals of neurology,* **19,** 253-262.

Burdick, D., Soreghan, B., Kwon, M., Kosmoski, J., Knauer, M., Henschen, A., Yates, J., Cotman, C. and Glabe, C. (1992) Assembly and aggregation properties of synthetic Alzheimer's A4/beta amyloid peptide analogs. *The Journal of biological chemistry,* **267,** 546-554.

Bursavich, M. G., Harrison, B. A. and Blain, J. F. (2016) Gamma Secretase Modulators: New Alzheimer's Drugs on the Horizon? *J Med Chem*.

Butt, A. M., Ibrahim, M. and Berry, M. (1997) The relationship between developing oligodendrocyte units and maturing axons during myelinogenesis in the anterior medullary velum of neonatal rats. *Journal of neurocytology,* **26,** 327-338.

Cabrera, E., Mathews, P., Mezhericher, E., Beach, T. G., Deng, J., Neubert, T. A., Rostagno, A. and Ghiso, J. (2017) Abeta truncated species: Implications for brain clearance mechanisms and amyloid plaque deposition. *Biochimica et biophysica acta*.

Cacabelos, R., Barquero, M., Garcia, P., Alvarez, X. A. and Varela de Seijas, E. (1991) Cerebrospinal fluid interleukin-1 beta (IL-1 beta) in Alzheimer's disease and neurological disorders. *Methods and findings in experimental and clinical pharmacology,* **13,** 455-458.

Cacquevel, M., Aeschbach, L., Houacine, J. and Fraering, P. C. (2012) Alzheimer's Disease-Linked Mutations in Presenilin-1 Result in a Drastic Loss of Activity in Purified gamma-Secretase Complexes. *PloS one,* **7,** e35133.

Cairns, N. J. (2009) Alzheimer's Disease: Neurodegeneration. *Elsevier Ltd.*

Capell, A., Meyn, L., Fluhrer, R., Teplow, D. B., Walter, J. and Haass, C. (2002) Apical sorting of beta-secretase limits amyloid beta-peptide production. *The Journal of biological chemistry,* **277,** 5637-5643.

Carulli, D., Laabs, T., Geller, H. M. and Fawcett, J. W. (2005) Chondroitin sulfate proteoglycans in neural development and regeneration. *Current opinion in neurobiology,* **15,** 116-120.

Castellano, J. M., Kim, J., Stewart, F. R. et al. (2011) Human apoE Isoforms Differentially Regulate Brain Amyloid-{beta} Peptide Clearance. *Sci Transl Med,* **3,** 89ra57.

Chabrier, M. A., Blurton-Jones, M., Agazaryan, A. A., Nerhus, J. L., Martinez-Coria, H. and Laferla, F. M. (2012) Soluble abeta promotes wild-type tau pathology in vivo. *The*

Journal of neuroscience : the official journal of the Society for Neuroscience, **32,** 17345-17350.

Chasseigneaux, S. and Allinquant, B. (2012) Functions of Abeta, sAPPalpha and sAPPbeta : similarities and differences. *Journal of neurochemistry,* **120 Suppl 1,** 99-108.

Chen, L., Yang, L., Zha, Y. and Cui, L. (2011) Association of serum a disintegrin and metalloproteinase with thrombospodin motif 4 levels with the presence and severity of coronary artery disease. *Coronary artery disease,* **22,** 570-576.

Citron, M., Oltersdorf, T., Haass, C., McConlogue, L., Hung, A. Y., Seubert, P., Vigo, P. C., Lieberburg, I. and Selkoe, D. J. (1992) Mutation of the beta-amyloid precursor protein in familial Alzheimer's disease increases beta-protein production. *Nature,* **360,** 672-674.

Citron, M., Teplow, D. B. and Selkoe, D. J. (1995) Generation of amyloid beta protein from its precursor is sequence specific. *Neuron,* **14,** 661-670.

Citron, M., Westaway, D., Xia, W. et al. (1997) Mutant presenilins of Alzheimer's disease increase production of 42- residue amyloid beta-protein in both transfected cells and transgenic mice. *Nature medicine,* **3,** 67-72.

Cleary, J. P., Walsh, D. M., Hofmeister, J. J., Shankar, G. M., Kuskowski, M. A., Selkoe, D. J. and Ashe, K. H. (2005) Natural oligomers of the amyloid-beta protein specifically disrupt cognitive function. *Nature neuroscience,* **8,** 79-84.

Connor, J. R., Menzies, S. L., St Martin, S. M. and Mufson, E. J. (1990) Cellular distribution of transferrin, ferritin, and iron in normal and aged human brains. *Journal of neuroscience research,* **27,** 595-611.

Corder, E. H., Saunders, A. M., Strittmatter, W. J., Schmechel, D. E., Gaskell, P. C., Small, G. W., Roses, A. D., Haines, J. L. and Pericak, V. M. (1993) Gene dose of apolipoprotein E type 4 allele and the risk of Alzheimer's disease in late onset families [see comments]. *Science (New York, N.Y.),* **261,** 921-923.

Crawford, A. H., Stockley, J. H., Tripathi, R. B., Richardson, W. D. and Franklin, R. J. (2014) Oligodendrocyte progenitors: adult stem cells of the central nervous system? *Experimental neurology,* **260,** 50-55.

Cross, A. K., Haddock, G., Stock, C. J., Allan, S., Surr, J., Bunning, R. A., Buttle, D. J. and Woodroofe, M. N. (2006a) ADAMTS-1 and -4 are up-regulated following transient middle cerebral artery occlusion in the rat and their expression is modulated by TNF in cultured astrocytes. *Brain research,* **1088,** 19-30.

Cross, A. K., Haddock, G., Surr, J., Plumb, J., Bunning, R. A., Buttle, D. J. and Woodroofe, M. N. (2006b) Differential expression of ADAMTS-1, -4, -5 and TIMP-3 in rat spinal cord at different stages of acute experimental autoimmune encephalomyelitis. *Journal of autoimmunity,* **26,** 16-23.

Davies, S. J., Fitch, M. T., Memberg, S. P., Hall, A. K., Raisman, G. and Silver, J. (1997) Regeneration of adult axons in white matter tracts of the central nervous system. *Nature,* **390,** 680-683.

De Felice, F. G., Vieira, M. N., Bomfim, T. R. et al. (2009) Protection of synapses against Alzheimer's-linked toxins: insulin signaling prevents the pathogenic binding of Abeta oligomers. *Proceedings of the National Academy of Sciences of the United States of America,* **106,** 1971-1976.

De Felice, F. G., Wu, D., Lambert, M. P. et al. (2008) Alzheimer's disease-type neuronal tau hyperphosphorylation induced by A beta oligomers. *Neurobiology of aging,* **29,** 1334-1347.

de Groot, R., Bardhan, A., Ramroop, N., Lane, D. A. and Crawley, J. T. (2009) Essential role of the disintegrin-like domain in ADAMTS13 function. *Blood,* **113,** 5609-5616.

De Strooper, B. (2003) Aph-1, Pen-2, and Nicastrin with Presenilin generate an active gamma-Secretase complex. *Neuron,* **38,** 9-12.

De Strooper, B. and Annaert, W. (2000) Proteolytic processing and cell biological functions of the amyloid precursor protein. *Journal of cell science,* **113,** 1857-1870.

De Strooper, B. and Chavez Gutierrez, L. (2015) Learning by failing: ideas and concepts to tackle gamma-secretases in Alzheimer's disease and beyond. *Annu Rev Pharmacol Toxicol,* **55,** 419-437.

De Strooper, B. and Karran, E. (2016) The Cellular Phase of Alzheimer's Disease. *Cell,* **164,** 603-615.

De Strooper, B., Saftig, P., Craessaerts, K., Vanderstichele, H., Guhde, G., Annaert, W., Von Figura, K. and Van Leuven, F. (1998) Deficiency of presenilin-1 inhibits the normal cleavage of amyloid precursor protein. *Nature,* **391,** 387-390.

Deane, R., Sagare, A., Hamm, K., Parisi, M., Lane, S., Finn, M. B., Holtzman, D. M. and Zlokovic, B. V. (2008) apoE isoform-specific disruption of amyloid beta peptide clearance from mouse brain. *The Journal of clinical investigation,* **118,** 4002-4013.

DeBoer, S. R., Dolios, G., Wang, R. and Sisodia, S. S. (2014) Differential release of beta-amyloid from dendrite- versus axon-targeted APP. *The Journal of neuroscience : the official journal of the Society for Neuroscience,* **34,** 12313-12327.

Demircan, K., Gunduz, E., Gunduz, M. et al. (2009) Increased mRNA expression of ADAMTS metalloproteinases in metastatic foci of head and neck cancer. *Head Neck,* **31,** 793-801.

Demircan, K., Topcu, V., Takigawa, T. et al. (2014) ADAMTS4 and ADAMTS5 knockout mice are protected from versican but not aggrecan or brevican proteolysis during spinal cord injury. **2014,** 693746.

Desai, M. K., Mastrangelo, M. A., Ryan, D. A., Sudol, K. L., Narrow, W. C. and Bowers, W. J. (2010) Early oligodendrocyte/myelin pathology in Alzheimer's disease mice constitutes a novel therapeutic target. *The American journal of pathology,* **177,** 1422-1435.

Desai, M. K., Sudol, K. L., Janelsins, M. C., Mastrangelo, M. A., Frazer, M. E. and Bowers, W. J. (2009) Triple-transgenic Alzheimer's disease mice exhibit region-specific abnormalities in brain myelination patterns prior to appearance of amyloid and tau pathology. *Glia,* **57,** 54-65.

Devi, L. and Ohno, M. (2010) Phospho-eIF2alpha level is important for determining abilities of BACE1 reduction to rescue cholinergic neurodegeneration and memory defects in 5XFAD mice. *PloS one,* **5,** e12974.

Dimitrov, M., Alattia, J. R., Lemmin, T. et al. (2013) Alzheimer's disease mutations in APP but not gamma-secretase modulators affect epsilon-cleavage-dependent AICD production. *Nature communications,* **4,** 2246.

Dubey, D., McRae, P. A., Rankin-Gee, E. K., Baranov, E., Wandrey, L., Rogers, S. and Porter, B. E. (2017) Increased metalloproteinase activity in the hippocampus following status epilepticus. *Epilepsy research,* **132,** 50-58.

Dubois, B., Feldman, H. H., Jacova, C. et al. (2007) Research criteria for the diagnosis of Alzheimer's disease: revising the NINCDS-ADRDA criteria. *The Lancet. Neurology,* **6,** 734-746.

Duff, K., Eckman, C., Zehr, C. et al. (1996) Increased amyloid-beta 42(43) in brains of mice expressing mutant presenilin 1. *Nature,* **383,** 710-713.

Dull, T., Zufferey, R., Kelly, M., Mandel, R. J., Nguyen, M., Trono, D. and Naldini, L. (1998) A third-generation lentivirus vector with a conditional packaging system. *J Virol,* **72,** 8463-8471.

Eimer, W. A. and Vassar, R. (2013) Neuron loss in the 5XFAD mouse model of Alzheimer's disease correlates with intraneuronal Abeta42 accumulation and Caspase-3 activation. *Mol Neurodegener,* **8,** 2.

Elder, G. A., Gama Sosa, M. A., De Gasperi, R., Dickstein, D. L. and Hof, P. R. (2010) Presenilin transgenic mice as models of Alzheimer's disease. *Brain Struct Funct,* **214,** 127-143.

Ettle, B., Schlachetzki, J. C. and Winkler, J. (2015) Oligodendroglia and Myelin in Neurodegenerative Diseases: More Than Just Bystanders? *Molecular neurobiology*.

Ferreira, S. T. and Klein, W. L. (2011) The Abeta oligomer hypothesis for synapse failure and memory loss in Alzheimer's disease. *Neurobiology of learning and memory,* **96,** 529-543.

Firbank, M. J., Blamire, A. M., Krishnan, M. S., Teodorczuk, A., English, P., Gholkar, A., Harrison, R. and O'Brien, J. T. (2007) Atrophy is associated with posterior cingulate white matter disruption in dementia with Lewy bodies and Alzheimer's disease. *NeuroImage,* **36,** 1-7.

Flannery, C. R., Zeng, W., Corcoran, C. et al. (2002) Autocatalytic cleavage of ADAMTS-4 (Aggrecanase-1) reveals multiple glycosaminoglycan-binding sites. *The Journal of biological chemistry,* **277,** 42775-42780.

Fox, A. J. S., Bedi, A. and Rodeo, S. A. (2009) The Basic Science of Articular Cartilage: Structure, Composition, and Function. *Sports Health,* **1,** 461-468.

Fox, N. C., Warrington, E. K., Freeborough, P. A., Hartikainen, P., Kennedy, A. M., Stevens, J. M. and Rossor, M. N. (1996) Presymptomatic hippocampal atrophy in Alzheimer's disease. A longitudinal MRI study. *Brain,* **119 (Pt 6),** 2001-2007.

Frantz, C., Stewart, K. M. and Weaver, V. M. (2010) The extracellular matrix at a glance. *Journal of cell science,* **123,** 4195-4200.

Frautschy, S. A., Yang, F., Irrizarry, M., Hyman, B., Saido, T. C., Hsiao, K. and Cole, G. M. (1998) Microglial response to amyloid plaques in APPsw transgenic mice. *The American journal of pathology,* **152,** 307-317.

Fritschi, S. K., Langer, F., Kaeser, S. A. et al. (2014) Highly potent soluble amyloid-beta seeds in human Alzheimer brain but not cerebrospinal fluid. *Brain : a journal of neurology*.

Funfschilling, U., Supplie, L. M., Mahad, D. et al. (2012) Glycolytic oligodendrocytes maintain myelin and long-term axonal integrity. *Nature,* **485,** 517-521.

Gendron, C., Kashiwagi, M., Lim, N. H., Enghild, J. J., Thogersen, I. B., Hughes, C., Caterson, B. and Nagase, H. (2007) Proteolytic activities of human ADAMTS-5: comparative studies with ADAMTS-4. *The Journal of biological chemistry,* **282,** 18294-18306.

Gerber, H., Wu, F., Dimitrov, M., Garcia Osuna, G. M. and Fraering, P. C. (2017) Zinc and Copper Differentially Modulate Amyloid Precursor Protein Processing by gamma-Secretase and Amyloid-beta Peptide Production. *The Journal of biological chemistry,* **292,** 3751-3767.

Girard, S. D., Baranger, K., Gauthier, C. et al. (2013) Evidence for early cognitive impairment related to frontal cortex in the 5XFAD mouse model of Alzheimer's disease. *Journal of Alzheimer's disease : JAD,* **33,** 781-796.

Glabe, C. C. (2005) Amyloid accumulation and pathogensis of Alzheimer's disease: significance of monomeric, oligomeric and fibrillar Abeta. *Sub-cellular biochemistry,* **38,** 167-177.

Glasson, S. S., Askew, R., Sheppard, B. et al. (2005) Deletion of active ADAMTS5 prevents cartilage degradation in a murine model of osteoarthritis. *Nature,* **434,** 644-648.

Glasson, S. S., Askew, R., Sheppard, B. et al. (2004) Characterization of and osteoarthritis susceptibility in ADAMTS-4-knockout mice. *Arthritis and rheumatism,* **50,** 2547-2558.

Glenner, G. G. and Wong, C. W. (1984) Alzheimer's disease: initial report of the purification and characterization of a novel cerebrovascular amyloid protein. *Biochemical and biophysical research communications,* **120,** 885-890.

Goate, A., Chartier, H. M., Mullan, M. et al. (1991) Segregation of a missense mutation in the amyloid precursor protein gene with familial Alzheimer's disease [see comments]. *Nature,* **349,** 704-706.

Goedert, M. and Jakes, R. (2005) Mutations causing neurodegenerative tauopathies. *Biochimica et biophysica acta,* **1739,** 240-250.

Gomis-Ruth, F. X. (2009) Catalytic domain architecture of metzincin metalloproteases. *The Journal of biological chemistry,* **284,** 15353-15357.

Gotz, J., Chen, F., van Dorpe, J. and Nitsch, R. M. (2001) Formation of neurofibrillary tangles in P301l tau transgenic mice induced by Abeta 42 fibrils. *Science (New York, N.Y.),* **293,** 1491-1495.

Gravina, S. A., Ho, L., Eckman, C. B., Long, K. E., Otvos, L., Jr., Younkin, L. H., Suzuki, N. and Younkin, S. G. (1995) Amyloid beta protein (A beta) in Alzheimer's disease brain. Biochemical and immunocytochemical analysis with antibodies specific for forms ending at A beta 40 or A beta 42(43). *The Journal of biological chemistry,* **270,** 7013-7016.

Griffin, W. S., Stanley, L. C., Ling, C., White, L., MacLeod, V., Perrot, L. J., White, C. L., 3rd and Araoz, C. (1989) Brain interleukin 1 and S-100 immunoreactivity are elevated in Down syndrome and Alzheimer disease. *Proceedings of the National Academy of Sciences of the United States of America,* **86,** 7611-7615.

Grundke-Iqbal, I., Iqbal, K., Tung, Y. C., Quinlan, M., Wisniewski, H. M. and Binder, L. I. (1986) Abnormal phosphorylation of the microtubule-associated protein tau (tau) in Alzheimer cytoskeletal pathology. *Proc Natl Acad Sci U S A,* **83,** 4913-4917.

Haass, C., Hung, A. Y. and Selkoe, D. J. (1991) Processing of beta-amyloid precursor protein in microglia and astrocytes favors an internal localization over constitutive secretion. *The Journal of neuroscience : the official journal of the Society for Neuroscience,* **11,** 3783-3793.

Haass, C., Schlossmacher, M. G., Hung, A. Y. et al. (1992) Amyloid beta-peptide is produced by cultured cells during normal metabolism. *Nature,* **359,** 322-325.

Haddock, G., Cross, A. K., Plumb, J., Surr, J., Buttle, D. J., Bunning, R. A. and Woodroofe, M. N. (2006) Expression of ADAMTS-1, -4, -5 and TIMP-3 in normal and multiple sclerosis CNS white matter. *Mult Scler,* **12,** 386-396.

Hahn, S., Bruning, T., Ness, J. et al. (2011) Presenilin-1 but not amyloid precursor protein mutations present in mouse models of Alzheimer's disease attenuate the response of cultured cells to gamma-secretase modulators regardless of their potency and structure. *Journal of neurochemistry,* **116,** 385-395.

Halim, A., Brinkmalm, G., Ruetschi, U., Westman-Brinkmalm, A., Portelius, E., Zetterberg, H., Blennow, K., Larson, G. and Nilsson, J. (2011) Site-specific characterization of threonine, serine, and tyrosine glycosylations of amyloid precursor protein/amyloid beta-peptides in human cerebrospinal fluid. *Proceedings of the National Academy of Sciences of the United States of America,* **108,** 11848-11853.

Hamel, M. G., Ajmo, J. M., Leonardo, C. C., Zuo, F., Sandy, J. D. and Gottschall, P. E. (2008) Multimodal signaling by the ADAMTSs (a disintegrin and metalloproteinase with thrombospondin motifs) promotes neurite extension. *Experimental neurology,* **210,** 428-440.

Hamel, M. G., Mayer, J. and Gottschall, P. E. (2005) Altered production and proteolytic processing of brevican by transforming growth factor beta in cultured astrocytes. *Journal of neurochemistry,* **93,** 1533-1541.

Hampel, H., Schneider, L. S., Giacobini, E. et al. (2015) Advances in the therapy of Alzheimer's disease: targeting amyloid beta and tau and perspectives for the future. *Expert review of neurotherapeutics,* **15,** 83-105.

Hardy, J. (1997) Amyloid, the presenilins and Alzheimer's disease. *Trends in neurosciences,* **20,** 154-159.

Hardy, J. A. and Higgins, G. A. (1992) Alzheimer's disease: the amyloid cascade hypothesis. *Science (New York, N.Y.),* **256,** 184-185.

Hecimovic, S., Wang, J., Dolios, G., Martinez, M., Wang, R. and Goate, A. M. (2004) Mutations in APP have independent effects on Abeta and CTFgamma generation. *Neurobiology of disease,* **17,** 205-218.

Held-Feindt, J., Paredes, E. B., Blomer, U., Seidenbecher, C., Stark, A. M., Mehdorn, H. M. and Mentlein, R. (2006) Matrix-degrading proteases ADAMTS4 and ADAMTS5 (disintegrins and metalloproteinases with thrombospondin motifs 4 and 5) are expressed in human glioblastomas. *International journal of cancer,* **118,** 55-61.

Hendriks, L., Thinakaran, G., Harris, C. L., De Jonghe, C., Martin, J. J., Sisodia, S. S. and Van Broeckhoven, C. (1997) Processing of presenilin 1 in brains of patients with Alzheimer's disease and controls. *Neuroreport,* **8,** 1717-1721.

Heneka, M. T., Kummer, M. P. and Latz, E. (2014) Innate immune activation in neurodegenerative disease. *Nature reviews. Immunology,* **14,** 463-477.

Herculano-Houzel, S. (2014) The glia/neuron ratio: how it varies uniformly across brain structures and species and what that means for brain physiology and evolution. *Glia,* **62,** 1377-1391.

Hills, R., Mazzarella, R., Fok, K. et al. (2007) Identification of an ADAMTS-4 cleavage motif using phage display leads to the development of fluorogenic peptide substrates and reveals matrilin-3 as a novel substrate. *The Journal of biological chemistry,* **282,** 11101-11109.

Hoefgen, S., Dahms, S. O., Oertwig, K. and Than, M. E. (2015) The amyloid precursor protein shows a pH-dependent conformational switch in its E1 domain. *Journal of molecular biology,* **427,** 433-442.

Hongpaisan, J., Sun, M. K. and Alkon, D. L. (2011) PKC epsilon activation prevents synaptic loss, Abeta elevation, and cognitive deficits in Alzheimer's disease transgenic mice. *The Journal of neuroscience : the official journal of the Society for Neuroscience,* **31,** 630-643.

Hook, G., Yu, J., Toneff, T., Kindy, M. and Hook, V. (2014) Brain pyroglutamate amyloid-beta is produced by cathepsin B and is reduced by the cysteine protease inhibitor E64d, representing a potential Alzheimer's disease therapeutic. *Journal of Alzheimer's disease : JAD,* **41,** 129-149.

Hook, V. Y., Kindy, M. and Hook, G. (2008) Inhibitors of cathepsin B improve memory and reduce beta-amyloid in transgenic Alzheimer disease mice expressing the wild-type, but not the Swedish mutant, beta-secretase site of the amyloid precursor protein. *The Journal of biological chemistry,* **283,** 7745-7753.

Horiuchi, M., Maezawa, I., Itoh, A., Wakayama, K., Jin, L. W., Itoh, T. and Decarli, C. (2012) Amyloid beta1-42 oligomer inhibits myelin sheet formation in vitro. *Neurobiology of aging,* **33,** 499-509.

Hou, L., Kang, I., Marchant, R. E. and Zagorski, M. G. (2002) Methionine 35 oxidation reduces fibril assembly of the amyloid abeta-(1-42) peptide of Alzheimer's disease. *The Journal of biological chemistry,* **277,** 40173-40176.

Howell, M. D., Torres-Collado, A. X., Iruela-Arispe, M. L. and Gottschall, P. E. (2012) Selective decline of synaptic protein levels in the frontal cortex of female mice deficient in the extracellular metalloproteinase ADAMTS1. *PloS one,* **7,** e47226.

Huang, J. and Auchus, A. P. (2007) Diffusion tensor imaging of normal appearing white matter and its correlation with cognitive functioning in mild cognitive impairment and Alzheimer's disease. *Annals of the New York Academy of Sciences,* **1097,** 259-264.

Huang, X., Atwood, C. S., Moir, R. D., Hartshorn, M. A., Tanzi, R. E. and Bush, A. I. (2004) Trace metal contamination initiates the apparent auto-aggregation, amyloidosis, and oligomerization of Alzheimer's Abeta peptides. *Journal of biological inorganic chemistry : JBIC : a publication of the Society of Biological Inorganic Chemistry,* **9,** 954-960.

Hurskainen, T. L., Hirohata, S., Seldin, M. F. and Apte, S. S. (1999) ADAM-TS5, ADAM-TS6, and ADAM-TS7, novel members of a new family of zinc metalloproteases. General features and genomic distribution of the ADAM-TS family. *The Journal of biological chemistry,* **274,** 25555-25563.

Hussain, I., Powell, D., Howlett, D. R. et al. (1999) Identification of a novel aspartic protease (Asp 2) as beta-secretase. *Molecular and cellular neurosciences,* **14,** 419-427.

Huttenrauch, M., Walter, S., Kaufmann, M., Weggen, S. and Wirths, O. (2016) Limited Effects of Prolonged Environmental Enrichment on the Pathology of 5XFAD Mice. *Molecular neurobiology*.

Iozzo, R. V. and Murdoch, A. D. (1996) Proteoglycans of the extracellular environment: clues from the gene and protein side offer novel perspectives in molecular diversity and function. *FASEB journal : official publication of the Federation of American Societies for Experimental Biology,* **10,** 598-614.

Irie, K., Murakami, K., Masuda, Y. et al. (2005) Structure of beta-amyloid fibrils and its relevance to their neurotoxicity: implications for the pathogenesis of Alzheimer's disease. *Journal of bioscience and bioengineering,* **99,** 437-447.

Iruela-Arispe, M. L., Vazquez, F. and Ortega, M. A. (1999) Antiangiogenic domains shared by thrombospondins and metallospondins, a new family of angiogenic inhibitors. *Annals of the New York Academy of Sciences,* **886,** 58-66.

Iwatsubo, T., Odaka, A., Suzuki, N., Mizusawa, H., Nukina, N. and Ihara, Y. (1994) Visualization of A beta 42(43) and A beta 40 in senile plaques with end-specific A beta monoclonals: evidence that an initially deposited species is A beta 42(43). *Neuron,* **13,** 45-53.

Iwatsubo, T., Saido, T. C., Mann, D. M., Lee, V. M. and Trojanowski, J. Q. (1996) Full-length amyloid-beta (1-42(43)) and amino-terminally modified and truncated amyloid-beta 42(43) deposit in diffuse plaques. *The American journal of pathology,* **149,** 1823-1830.

Jantaratnotai, N., Ryu, J. K., Kim, S. U. and McLarnon, J. G. (2003) Amyloid beta peptide-induced corpus callosum damage and glial activation in vivo. *Neuroreport,* **14,** 1429-1433.

Jarrett, J. T., Berger, E. P. and Lansbury, P. T., Jr. (1993) The carboxy terminus of the beta amyloid protein is critical for the seeding of amyloid formation: implications for the pathogenesis of Alzheimer's disease. *Biochemistry,* **32,** 4693-4697.

Jawhar, S., Trawicka, A., Jenneckens, C., Bayer, T. A. and Wirths, O. (2012) Motor deficits, neuron loss, and reduced anxiety coinciding with axonal degeneration and intraneuronal Abeta aggregation in the 5XFAD mouse model of Alzheimer's disease. *Neurobiology of aging,* **33,** 196.e129-140.

Jefferson, T., Auf dem Keller, U., Bellac, C. et al. (2013) The substrate degradome of meprin metalloproteases reveals an unexpected proteolytic link between meprin beta and ADAM10. *Cellular and molecular life sciences : CMLS,* **70,** 309-333.

Jefferson, T., Causevic, M., Auf dem Keller, U. et al. (2011) Metalloprotease Meprin {beta} Generates Nontoxic N-terminal Amyloid Precursor Protein Fragments in Vivo. *The Journal of biological chemistry,* **286,** 27741-27750.

Jones, L., Holmans, P. A., Hamshere, M. L. et al. (2010) Genetic evidence implicates the immune system and cholesterol metabolism in the aetiology of Alzheimer's disease. *PloS one,* **5,** e13950.

Jonsson, T., Atwal, J. K., Steinberg, S. et al. (2012) A mutation in APP protects against Alzheimer's disease and age-related cognitive decline. *Nature,* **488,** 96-99.

Jucker, M. (2010) The benefits and limitations of animal models for translational research in neurodegenerative diseases. *Nature medicine,* **16,** 1210-1214.

Jucker, M. and Walker, L. C. (2013) Self-propagation of pathogenic protein aggregates in neurodegenerative diseases. *Nature,* **501,** 45-51.

Jungers, K. A., Le Goff, C., Somerville, R. P. and Apte, S. S. (2005) Adamts9 is widely expressed during mouse embryo development. *Gene expression patterns : GEP,* **5,** 609-617.

Kaether, C., Lammich, S., Edbauer, D., Ertl, M., Rietdorf, J., Capell, A., Steiner, H. and Haass, C. (2002) Presenilin-1 affects trafficking and processing of betaAPP and is targeted in a complex with nicastrin to the plasma membrane. *J Cell Biol,* **158,** 551-561.

Kalback, W., Watson, M. D., Kokjohn, T. A. et al. (2002) APP transgenic mice Tg2576 accumulate Abeta peptides that are distinct from the chemically modified and insoluble peptides deposited in Alzheimer's disease senile plaques. *Biochemistry,* **41,** 922-928.

Kalinin, S., Polak, P. E., Lin, S. X., Sakharkar, A. J., Pandey, S. C. and Feinstein, D. L. (2012) The noradrenaline precursor L-DOPS reduces pathology in a mouse model of Alzheimer's disease. *Neurobiology of aging,* **33,** 1651-1663.

Kang, J., Lemaire, H. G., Unterbeck, A., Salbaum, J. M., Masters, C. L., Grzeschik, K. H., Multhaup, G., Beyreuther, K. and Muller, H. B. (1987) The precursor of Alzheimer's disease amyloid A4 protein resembles a cell-surface receptor. *Nature,* **325,** 733-736.

Karran, E., Mercken, M. and Strooper, B. D. (2011) The amyloid cascade hypothesis for Alzheimer's disease: an appraisal for the development of therapeutics. *Nature reviews. Drug discovery,* **10,** 698-712.

Kawarabayashi, T., Younkin, L. H., Saido, T. C., Shoji, M., Ashe, K. H. and Younkin, S. G. (2001) Age-dependent changes in brain, CSF, and plasma amyloid (beta) protein in the Tg2576 transgenic mouse model of Alzheimer's disease. *The Journal of neuroscience : the official journal of the Society for Neuroscience,* **21,** 372-381.

Kelwick, R., Desanlis, I., Wheeler, G. N. and Edwards, D. R. (2015) The ADAMTS (A Disintegrin and Metalloproteinase with Thrombospondin motifs) family. *Genome biology,* **16,** 113.

Kimoto, S., Okuda, A., Toritsuka, M. et al. (2011) Olanzapine stimulates proliferation but inhibits differentiation in rat oligodendrocyte precursor cell cultures. *Progress in neuro-psychopharmacology & biological psychiatry,* **35,** 1950-1956.

Kitaguchi, N., Takahashi, Y., Tokushima, Y., Shiojiri, S. and Ito, H. (1988) Novel precursor of Alzheimer's disease amyloid protein shows protease inhibitory activity. *Nature,* **331,** 530-532.

Knauer, M. F., Orlando, R. A. and Glabe, C. G. (1996) Cell surface APP751 forms complexes with protease nexin 2 ligands and is internalized via the low density lipoprotein receptor-related protein (LRP). *Brain research,* **740,** 6-14.

Knowles, T. P., Vendruscolo, M. and Dobson, C. M. (2014) The amyloid state and its association with protein misfolding diseases. *Nature reviews. Molecular cell biology,* **15,** 384-396.

Kocherhans, S., Madhusudan, A., Doehner, J., Breu, K. S., Nitsch, R. M., Fritschy, J. M. and Knuesel, I. (2010) Reduced Reelin expression accelerates amyloid-beta plaque formation and tau pathology in transgenic Alzheimer's disease mice. *The Journal of neuroscience : the official journal of the Society for Neuroscience,* **30,** 9228-9240.

Koo, E. H., Park, L. and Selkoe, D. J. (1993) Amyloid beta-protein as a substrate interacts with extracellular matrix to promote neurite outgrowth. *Proceedings of the National Academy of Sciences of the United States of America,* **90,** 4748-4752.

Krabbe, G., Halle, A., Matyash, V. et al. (2013) Functional impairment of microglia coincides with Beta-amyloid deposition in mice with Alzheimer-like pathology. *PloS one,* **8,** e60921.

Krstic, D., Rodriguez, M. and Knuesel, I. (2012) Regulated proteolytic processing of Reelin through interplay of tissue plasminogen activator (tPA), ADAMTS-4, ADAMTS-5, and their modulators. *PloS one,* **7,** e47793.

Kuhn, P. H., Wang, H., Dislich, B., Colombo, A., Zeitschel, U., Ellwart, J. W., Kremmer, E., Rossner, S. and Lichtenthaler, S. F. (2010) ADAM10 is the physiologically relevant, constitutive alpha-secretase of the amyloid precursor protein in primary neurons. *The EMBO journal,* **29,** 3020-3032.

Kumar, S., Chen, M., Li, Y. et al. (2016) Loss of ADAMTS4 reduces high fat diet-induced atherosclerosis and enhances plaque stability in ApoE(-/-) mice. *Scientific reports,* **6,** 31130.

Kumar, S., Rezaei-Ghaleh, N., Terwel, D. et al. (2011) Extracellular phosphorylation of the amyloid beta-peptide promotes formation of toxic aggregates during the pathogenesis of Alzheimer's disease. *The EMBO journal*.

Kummer, M. P. and Heneka, M. T. (2014) Truncated and modified amyloid-beta species. *Alzheimers Res Ther,* **6,** 28.

Kummer, M. P., Hermes, M., Delekarte, A. et al. (2011) Nitration of tyrosine 10 critically enhances amyloid beta aggregation and plaque formation. *Neuron,* **71,** 833-844.

Lacor, P. N., Buniel, M. C., Chang, L. et al. (2004) Synaptic targeting by Alzheimer's-related amyloid beta oligomers. *The Journal of neuroscience : the official journal of the Society for Neuroscience,* **24,** 10191-10200.

LaFerla, F. M. and Green, K. N. (2012) Animal models of Alzheimer disease. *Cold Spring Harbor perspectives in medicine,* **2**.

LaFerla, F. M. and Oddo, S. (2005) Alzheimer's disease: Abeta, tau and synaptic dysfunction. *Trends in molecular medicine,* **11,** 170-176.

Lammich, S., Kojro, E., Postina, R., Gilbert, S., Pfeiffer, R., Jasionowski, M., Haass, C. and Fahrenholz, F. (1999) Constitutive and regulated alpha-secretase cleavage of

Alzheimer's amyloid precursor protein by a disintegrin metalloprotease. *Proceedings of the National Academy of Sciences of the United States of America,* **96,** 3922-3927.

Lark, M. W., Bayne, E. K., Flanagan, J. et al. (1997) Aggrecan degradation in human cartilage. Evidence for both matrix metalloproteinase and aggrecanase activity in normal, osteoarthritic, and rheumatoid joints. *The Journal of clinical investigation,* **100,** 93-106.

Lauren, J., Gimbel, D. A., Nygaard, H. B., Gilbert, J. W. and Strittmatter, S. M. (2009) Cellular prion protein mediates impairment of synaptic plasticity by amyloid-beta oligomers. *Nature,* **457,** 1128-1132.

LeBlanc, A. C., Papadopoulos, M., Belair, C., Chu, W., Crosato, M., Powell, J. and Goodyer, C. G. (1997) Processing of amyloid precursor protein in human primary neuron and astrocyte cultures. *Journal of neurochemistry,* **68,** 1183-1190.

LeBlanc, A. C., Xue, R. and Gambetti, P. (1996) Amyloid precursor protein metabolism in primary cell cultures of neurons, astrocytes, and microglia. *Journal of neurochemistry,* **66,** 2300-2310.

Ledo, J. H., Azevedo, E. P., Clarke, J. R., Ribeiro, F. C., Figueiredo, C. P., Foguel, D., De Felice, F. G. and Ferreira, S. T. (2013) Amyloid-beta oligomers link depressive-like behavior and cognitive deficits in mice. *Molecular psychiatry,* **18,** 1053-1054.

Lee, E. B., Skovronsky, D. M., Abtahian, F., Doms, R. W. and Lee, V. M. (2003) Secretion and intracellular generation of truncated Abeta in beta-site amyloid-beta precursor protein-cleaving enzyme expressing human neurons. *The Journal of biological chemistry,* **278,** 4458-4466.

Lemarchant, S., Dunghana, H., Pomeshchik, Y. et al. (2016a) Anti-inflammatory effects of ADAMTS-4 in a mouse model of ischemic stroke. *Glia,* **64,** 1492-1507.

Lemarchant, S., Pomeshchik, Y., Kidin, I. et al. (2016b) ADAMTS-4 promotes neurodegeneration in a mouse model of amyotrophic lateral sclerosis. *Mol Neurodegener,* **11,** 10.

Lemarchant, S., Pruvost, M., Hebert, M. et al. (2014) tPA promotes ADAMTS-4-induced CSPG degradation, thereby enhancing neuroplasticity following spinal cord injury. *Neurobiology of disease,* **66,** 28-42.

Lemarchant, S., Pruvost, M., Montaner, J., Emery, E., Vivien, D., Kanninen, K. and Koistinaho, J. (2013) ADAMTS proteoglycanases in the physiological and pathological central nervous system. *Journal of neuroinflammation,* **10,** 133.

Lemarchant, S., Wojciechowski, S., Vivien, D. and Koistinaho, J. (2017) ADAMTS-4 in central nervous system pathologies. *Journal of neuroscience research*.

Lepka, K., Volbracht, K., Bill, E. et al. (2017) Iron-sulfur glutaredoxin 2 protects oligodendrocytes against damage induced by nitric oxide release from activated microglia.

Levy-Lahad, E., Wijsman, E. M., Nemens, E., Anderson, L., Goddard, K. A., Weber, J. L., Bird, T. D. and Schellenberg, G. D. (1995) A familial Alzheimer's disease locus on chromosome 1. *Science (New York, N.Y.),* **269,** 970-973.

Levy, C., Brooks, J. M., Chen, J., Su, J. and Fox, M. A. (2015) Cell-specific and developmental expression of lectican-cleaving proteases in mouse hippocampus and neocortex. *J Comp Neurol,* **523,** 629-648.

Lewis, H., Beher, D., Cookson, N. et al. (2006) Quantification of Alzheimer pathology in ageing and dementia: age-related accumulation of amyloid-beta(42) peptide in vascular dementia. *Neuropathol Appl Neurobiol,* **32,** 103-118.

Lichtenthaler, S. F., Haass, C. and Steiner, H. (2011) Regulated intramembrane proteolysis--lessons from amyloid precursor protein processing. *Journal of neurochemistry,* **117,** 779-796.

Liu, B., Moloney, A., Meehan, S. et al. (2011) Iron promotes the toxicity of amyloid beta peptide by impeding its ordered aggregation. *The Journal of biological chemistry,* **286,** 4248-4256.

Longpre, J. M., McCulloch, D. R., Koo, B. H., Alexander, J. P., Apte, S. S. and Leduc, R. (2009) Characterization of proADAMTS5 processing by proprotein convertases. *The international journal of biochemistry & cell biology,* **41,** 1116-1126.

Loy, C. T., Schofield, P. R., Turner, A. M. and Kwok, J. B. (2014) Genetics of dementia. *Lancet (London, England),* **383,** 828-840.

Lue, L. F., Rydel, R., Brigham, E. F. et al. (2001) Inflammatory repertoire of Alzheimer's disease and nondemented elderly microglia in vitro. *Glia,* **35,** 72-79.

Luo, J., Deng, Z. L., Luo, X. et al. (2007) A protocol for rapid generation of recombinant adenoviruses using the AdEasy system. *Nat Protoc,* **2,** 1236-1247.

Lyons, B., Friedrich, M., Raftery, M. and Truscott, R. (2016) Amyloid Plaque in the Human Brain Can Decompose from Abeta(1-40/1-42) by Spontaneous Nonenzymatic Processes. *Anal Chem,* **88,** 2675-2684.

Mahley, R. W. and Rall, S. C., Jr. (2000) Apolipoprotein E: far more than a lipid transport protein. *Annual review of genomics and human genetics,* **1,** 507-537.

Maloney, J. A., Bainbridge, T., Gustafson, A. et al. (2014) Molecular mechanisms of Alzheimer disease protection by the A673T allele of amyloid precursor protein. *The Journal of biological chemistry,* **289,** 30990-31000.

Mann, D. M., Iwatsubo, T., Ihara, Y. et al. (1996) Predominant deposition of amyloid-beta 42(43) in plaques in cases of Alzheimer's disease and hereditary cerebral hemorrhage associated with mutations in the amyloid precursor protein gene. *The American journal of pathology,* **148,** 1257-1266.

Martiskainen, H., Herukka, S. K., Stancakova, A., Paananen, J., Soininen, H., Kuusisto, J., Laakso, M. and Hiltunen, M. (2017) Decreased plasma beta-amyloid in the Alzheimer's disease APP A673T variant carriers. *Annals of neurology*.

Masters, C. L., Simms, G., Weinman, N. A., Multhaup, G., McDonald, B. L. and Beyreuther, K. (1985) Amyloid plaque core protein in Alzheimer disease and Down syndrome. *Proceedings of the National Academy of Sciences of the United States of America,* **82,** 4245-4249.

Matthews, R. T., Gary, S. C., Zerillo, C., Pratta, M., Solomon, K., Arner, E. C. and Hockfield, S. (2000) Brain-enriched hyaluronan binding (BEHAB)/brevican cleavage in a glioma cell line is mediated by a disintegrin and metalloproteinase with thrombospondin motifs (ADAMTS) family member. *The Journal of biological chemistry,* **275,** 22695-22703.

Mattson, M. P. (2004) Pathways towards and away from Alzheimer's disease. *Nature,* **430,** 631-639.

Mawuenyega, K. G., Sigurdson, W., Ovod, V., Munsell, L., Kasten, T., Morris, J. C., Yarasheski, K. E. and Bateman, R. J. (2010) Decreased Clearance of CNS {beta}-Amyloid in Alzheimer's Disease. *Science (New York, N.Y.)*.

Mayer, J., Hamel, M. G. and Gottschall, P. E. (2005) Evidence for proteolytic cleavage of brevican by the ADAMTSs in the dentate gyrus after excitotoxic lesion of the mouse entorhinal cortex. *BMC Neurosci,* **6,** 52.

McKhann, G. M., Knopman, D. S., Chertkow, H. et al. (2011) The diagnosis of dementia due to Alzheimer's disease: recommendations from the National Institute on Aging-

Alzheimer's Association workgroups on diagnostic guidelines for Alzheimer's disease. *Alzheimer's & dementia : the journal of the Alzheimer's Association,* **7,** 263-269.

Meyer-Luehmann, M. and Prinz, M. (2015) Myeloid cells in Alzheimer's disease: culprits, victims or innocent bystanders? *Trends in neurosciences,* **38,** 659-668.

Miguel, R. F., Pollak, A. and Lubec, G. (2005) Metalloproteinase ADAMTS-1 but not ADAMTS-5 is manifold overexpressed in neurodegenerative disorders as Down syndrome, Alzheimer's and Pick's disease. *Brain research. Molecular brain research,* **133,** 1-5.

Miller, D. L., Papayannopoulos, I. A., Styles, J., Bobin, S. A., Lin, Y. Y., Biemann, K. and Iqbal, K. (1993) Peptide compositions of the cerebrovascular and senile plaque core amyloid deposits of Alzheimer's disease. *Archives of biochemistry and biophysics,* **301,** 41-52.

Miller, R. H. (1996) Oligodendrocyte origins. *Trends in neurosciences,* **19,** 92-96.

Mimata, Y., Kamataki, A., Oikawa, S., Murakami, K., Uzuki, M., Shimamura, T. and Sawai, T. (2012) Interleukin-6 upregulates expression of ADAMTS-4 in fibroblast-like synoviocytes from patients with rheumatoid arthritis. *International journal of rheumatic diseases,* **15,** 36-44.

Minobe, K., Ono, R., Matsumine, A. et al. (2010) Expression of ADAMTS4 in Ewing's sarcoma. *Int J Oncol,* **37,** 569-581.

Mitew, S., Kirkcaldie, M. T., Halliday, G. M., Shepherd, C. E., Vickers, J. C. and Dickson, T. C. (2010) Focal demyelination in Alzheimer's disease and transgenic mouse models. *Acta neuropathologica,* **119,** 567-577.

Mongiat, M., Andreuzzi, E., Tarticchio, G. and Paulitti, A. (2016) Extracellular Matrix, a Hard Player in Angiogenesis. *International journal of molecular sciences,* **17**.

Montoliu-Gaya, L. and Villegas, S. (2015) Protein structures in Alzheimer's disease: The basis for rationale therapeutic design. *Archives of biochemistry and biophysics,* **588,** 1-14.

Moore, B. D., Chakrabarty, P., Levites, Y. et al. (2012) Overlapping profiles of Abeta peptides in the Alzheimer's disease and pathological aging brains. *Alzheimers Res Ther,* **4,** 18.

Morley, J. E. and Farr, S. A. (2014) The role of amyloid-beta in the regulation of memory. *Biochemical pharmacology,* **88,** 479-485.

Mullan, M., Crawford, F., Axelman, K., Houlden, H., Lilius, L., Winblad, B. and Lannfelt, L. (1992) A pathogenic mutation for probable Alzheimer's disease in the APP gene at the N-terminus of beta-amyloid. *Nat Genet,* **1,** 345-347.

Murphy, G. (2011) Tissue inhibitors of metalloproteinases. *Genome biology,* **12,** 233.

Murrell, J., Farlow, M., Ghetti, B. and Benson, M. D. (1991) A mutation in the amyloid precursor protein associated with hereditary Alzheimer's disease. *Science (New York, N.Y.),* **254,** 97-99.

Musiek, E. S. and Holtzman, D. M. (2015) Three dimensions of the amyloid hypothesis: time, space and 'wingmen'. *Nature neuroscience,* **18,** 800-806.

Naito, S., Shiomi, T., Okada, A. et al. (2007) Expression of ADAMTS4 (aggrecanase-1) in human osteoarthritic cartilage. *Pathology international,* **57,** 703-711.

Nakada, M., Miyamori, H., Kita, D., Takahashi, T., Yamashita, J., Sato, H., Miura, R., Yamaguchi, Y. and Okada, Y. (2005) Human glioblastomas overexpress ADAMTS-5 that degrades brevican. *Acta neuropathologica,* **110,** 239-246.

Nakamura, H., Fujii, Y., Inoki, I., Sugimoto, K., Tanzawa, K., Matsuki, H., Miura, R., Yamaguchi, Y. and Okada, Y. (2000) Brevican is degraded by matrix metalloproteinases and aggrecanase-1 (ADAMTS4) at different sites. *The Journal of biological chemistry,* **275,** 38885-38890.

Naslund, J., Haroutunian, V., Mohs, R., Davis, K. L., Davies, P., Greengard, P. and Buxbaum, J. D. (2000) Correlation between elevated levels of amyloid beta-peptide in the brain and cognitive decline. *Jama,* **283,** 1571-1577.

Nhan, H. S., Chiang, K. and Koo, E. H. (2015) The multifaceted nature of amyloid precursor protein and its proteolytic fragments: friends and foes. *Acta neuropathologica,* **129,** 1-19.

Nickerson, D. A., Taylor, S. L., Fullerton, S. M., Weiss, K. M., Clark, A. G., Stengard, J. H., Salomaa, V., Boerwinkle, E. and Sing, C. F. (2000) Sequence diversity and large-scale typing of SNPs in the human apolipoprotein E gene. *Genome research,* **10,** 1532-1545.

Nicolas, M. and Hassan, B. A. (2014) Amyloid precursor protein and neural development. *Development,* **141,** 2543-2548.

Nielsen, H. M., Mulder, S. D., Belien, J. A., Musters, R. J., Eikelenboom, P. and Veerhuis, R. (2010) Astrocytic A beta 1-42 uptake is determined by A beta-aggregation state and the presence of amyloid-associated proteins. *Glia,* **58,** 1235-1246.

Nussbaum, J. M., Schilling, S., Cynis, H. et al. (2012) Prion-like behaviour and tau-dependent cytotoxicity of pyroglutamylated amyloid-beta. *Nature,* **485,** 651-655.

Oakley, H., Cole, S. L., Logan, S. et al. (2006) Intraneuronal beta-amyloid aggregates, neurodegeneration, and neuron loss in transgenic mice with five familial Alzheimer's disease mutations: potential factors in amyloid plaque formation. *The Journal of neuroscience : the official journal of the Society for Neuroscience,* **26,** 10129-10140.

Oberstein, T. J., Spitzer, P., Klafki, H. W. et al. (2015) Astrocytes and microglia but not neurons preferentially generate N-terminally truncated Abeta peptides. *Neurobiology of disease,* **73,** 24-35.

Ohno, M., Cole, S. L., Yasvoina, M., Zhao, J., Citron, M., Berry, R., Disterhoft, J. F. and Vassar, R. (2007) BACE1 gene deletion prevents neuron loss and memory deficits in 5XFAD APP/PS1 transgenic mice. *Neurobiology of disease,* **26,** 134-145.

Palacios, G., Palacios, J. M., Mengod, G. and Frey, P. (1992) Beta-amyloid precursor protein localization in the Golgi apparatus in neurons and oligodendrocytes. An immunocytochemical structural and ultrastructural study in normal and axotomized neurons. *Brain research. Molecular brain research,* **15,** 195-206.

Paresce, D. M., Ghosh, R. N. and Maxfield, F. R. (1996) Microglial cells internalize aggregates of the Alzheimer's disease amyloid beta-protein via a scavenger receptor. *Neuron,* **17,** 553-565.

Pehlivan, S., Fedakar, R., Eren, B. et al. (2016) ADAMTS4, 5, 9, and 15 expressions in the autopsied brain of patients with Alzheimer's disease: a preliminary immunohistochemistry study. *Klinik Psikofarmakoloji Bulteni-Bulletin of Clinical Psychopharmacology,* **26,** 7.

Pelvig, D. P., Pakkenberg, H., Stark, A. K. and Pakkenberg, B. (2008) Neocortical glial cell numbers in human brains. *Neurobiology of aging,* **29,** 1754-1762.

Pietrzik, C. U., Busse, T., Merriam, D. E., Weggen, S. and Koo, E. H. (2002) The cytoplasmic domain of the LDL receptor-related protein regulates multiple steps in APP processing. *The EMBO journal,* **21,** 5691-5700.

Pietrzik, C. U., Yoon, I. S., Jaeger, S., Busse, T., Weggen, S. and Koo, E. H. (2004) FE65 constitutes the functional link between the low-density lipoprotein receptor-related protein and the amyloid precursor protein. *The Journal of neuroscience : the official journal of the Society for Neuroscience,* **24,** 4259-4265.

Pike, C. J., Overman, M. J. and Cotman, C. W. (1995) Amino-terminal deletions enhance aggregation of beta-amyloid peptides in vitro. *The Journal of biological chemistry,* **270,** 23895-23898.

Pohlkamp, T., Wasser, C. R. and Herz, J. (2017) Functional Roles of the Interaction of APP and Lipoprotein Receptors. *Frontiers in molecular neuroscience,* **10,** 54.

Ponte, P., Gonzalez-DeWhitt, P., Schilling, J. et al. (1988) A new A4 amyloid mRNA contains a domain homologous to serine proteinase inhibitors. *Nature,* **331,** 530-532.

Portelius, E., Bogdanovic, N., Gustavsson, M. K., Volkmann, I., Brinkmalm, G., Zetterberg, H., Winblad, B. and Blennow, K. (2010) Mass spectrometric characterization of brain amyloid beta isoform signatures in familial and sporadic Alzheimer's disease. *Acta neuropathologica,* **120,** 185-193.

Portelius, E., Lashley, T., Westerlund, A., Persson, R., Fox, N. C., Blennow, K., Revesz, T. and Zetterberg, H. (2015) Brain amyloid-beta fragment signatures in pathological ageing and Alzheimer's disease by hybrid immunoprecipitation mass spectrometry. *Neuro-degenerative diseases,* **15,** 50-57.

Porter, S., Scott, S. D., Sassoon, E. M., Williams, M. R., Jones, J. L., Girling, A. C., Ball, R. Y. and Edwards, D. R. (2004) Dysregulated expression of adamalysin-thrombospondin genes in human breast carcinoma. *Clinical cancer research : an official journal of the American Association for Cancer Research,* **10,** 2429-2440.

Pruvost, M., Lepine, M., Leonetti, C. et al. (2017) ADAMTS-4 in oligodendrocytes contributes to myelination with an impact on motor function. *Glia*.

Rao, N., Ke, Z., Liu, H., Ho, C. J., Kumar, S., Xiang, W., Zhu, Y. and Ge, R. (2013) ADAMTS4 and its proteolytic fragments differentially affect melanoma growth and angiogenesis in mice. *International journal of cancer,* **133,** 294-306.

Reinert, J., Richard, B. C., Klafki, H. W. et al. (2016) Deposition of C-terminally truncated Abeta species Abeta37 and Abeta39 in Alzheimer's disease and transgenic mouse models. *Acta neuropathologica communications,* **4,** 24.

Ren, P., Zhang, L., Xu, G., Palmero, L. C., Albini, P. T., Coselli, J. S., Shen, Y. H. and LeMaire, S. A. (2013) ADAMTS-1 and ADAMTS-4 levels are elevated in thoracic aortic aneurysms and dissections. *The Annals of thoracic surgery,* **95,** 570-577.

Richard, B. C., Kurdakova, A., Baches, S., Bayer, T. A., Weggen, S. and Wirths, O. (2015) Gene Dosage Dependent Aggravation of the Neurological Phenotype in the 5XFAD Mouse Model of Alzheimer's Disease. *Journal of Alzheimer's disease : JAD,* **45,** 1223-1236.

Rijal Upadhaya, A., Kosterin, I., Kumar, S., von Arnim, C. A., Yamaguchi, H., Fandrich, M., Walter, J. and Thal, D. R. (2014) Biochemical stages of amyloid-beta peptide aggregation and accumulation in the human brain and their association with symptomatic and pathologically preclinical Alzheimer's disease. *Brain : a journal of neurology,* **137,** 887-903.

Ringman, J. M., O'Neill, J., Geschwind, D. et al. (2007) Diffusion tensor imaging in preclinical and presymptomatic carriers of familial Alzheimer's disease mutations. *Brain : a journal of neurology,* **130,** 1767-1776.

Rivera, A., Vanzuli, I., Arellano, J. J. and Butt, A. (2016) Decreased Regenerative Capacity of Oligodendrocyte Progenitor Cells (NG2-Glia) in the Ageing Brain: A Vicious Cycle of Synaptic Dysfunction, Myelin Loss and Neuronal Disruption? *Current Alzheimer research,* **13,** 413-418.

Robakis, N. K. (2011) Mechanisms of AD neurodegeneration may be independent of Abeta and its derivatives. *Neurobiology of aging,* **32,** 372-379.

Roher, A. E., Weiss, N., Kokjohn, T. A. et al. (2002) Increased A beta peptides and reduced cholesterol and myelin proteins characterize white matter degeneration in Alzheimer's disease. *Biochemistry,* **41,** 11080-11090.

Rossor, M. N., Fox, N. C., Freeborough, P. A. and Harvey, R. J. (1996) Clinical features of sporadic and familial Alzheimer's disease. *Neurodegeneration,* **5,** 393-397.

Rovelet-Lecrux, A., Hannequin, D., Raux, G. et al. (2006) APP locus duplication causes autosomal dominant early-onset Alzheimer disease with cerebral amyloid angiopathy. *Nat Genet,* **38,** 24-26.

Rozario, T. and DeSimone, D. W. (2010) The extracellular matrix in development and morphogenesis: a dynamic view. *Developmental biology,* **341,** 126-140.

Russo, C., Violani, E., Salis, S. et al. (2002) Pyroglutamate-modified amyloid beta-peptides--AbetaN3(pE)--strongly affect cultured neuron and astrocyte survival. *Journal of neurochemistry,* **82,** 1480-1489.

Sacitharan, P. K., Snelling, S. J. and Edwards, J. R. (2012) Aging mechanisms in arthritic disease. *Discovery medicine,* **14,** 345-352.

Sacks, C. A., Avorn, J. and Kesselheim, A. S. (2017) The Failure of Solanezumab - How the FDA Saved Taxpayers Billions. *The New England journal of medicine,* **376,** 1706-1708.

Sagi, S. A., Lessard, C. B., Winden, K. D., Maruyama, H., Koo, J. C., Weggen, S., Kukar, T. L., Golde, T. E. and Koo, E. H. (2011) Substrate sequence influences gamma-secretase modulator activity, role of the transmembrane domain of the amyloid precursor protein. *The Journal of biological chemistry,* **286,** 39794-39803.

Saido, T. and Leissring, M. A. (2012) Proteolytic degradation of amyloid beta-protein. *Cold Spring Harbor perspectives in medicine,* **2,** a006379.

Saito, T., Suemoto, T., Brouwers, N. et al. (2011) Potent amyloidogenicity and pathogenicity of Abeta43. *Nature neuroscience,* **14,** 1023-1032.

Sandy, J. D., Westling, J., Kenagy, R. D. et al. (2001) Versican V1 proteolysis in human aorta in vivo occurs at the Glu441-Ala442 bond, a site that is cleaved by recombinant ADAMTS-1 and ADAMTS-4. *The Journal of biological chemistry,* **276,** 13372-13378.

Satoh, K., Suzuki, N. and Yokota, H. (2000) ADAMTS-4 (a disintegrin and metalloproteinase with thrombospondin motifs) is transcriptionally induced in beta-amyloid treated rat astrocytes. *Neuroscience letters,* **289,** 177-180.

Schellenberg, G. D., Bird, T. D., Wijsman, E. M. et al. (1992) Genetic linkage evidence for a familial Alzheimer's disease locus on chromosome 14. *Science (New York, N.Y.),* **258,** 668-671.

Schellenberg, G. D. and Montine, T. J. (2012) The genetics and neuropathology of Alzheimer's disease. *Acta Neuropathol,* **124,** 305-323.

Scheuner, D., Eckman, C., Jensen, M. et al. (1996) Secreted amyloid beta-protein similar to that in the senile plaques of Alzheimers disease is increased in vivo by the presenilin 1 and 2 and APP mutations linked to familial Alzheimers disease. *Nature medicine,* **2,** 864-869.

Schieb, H., Kratzin, H., Jahn, O., Mobius, W., Rabe, S., Staufenbiel, M., Wiltfang, J. and Klafki, H. W. (2011) Beta-amyloid peptide variants in brains and cerebrospinal fluid from amyloid precursor protein (APP) transgenic mice: comparison with human Alzheimer amyloid. *The Journal of biological chemistry,* **286,** 33747-33758.

Schilling, S., Lauber, T., Schaupp, M., Manhart, S., Scheel, E., Bohm, G. and Demuth, H. U. (2006) On the seeding and oligomerization of pGlu-amyloid peptides (in vitro). *Biochemistry,* **45,** 12393-12399.

Schonherr, C., Bien, J., Isbert, S. et al. (2016) Generation of aggregation prone N-terminally truncated amyloid beta peptides by meprin beta depends on the sequence specificity at the cleavage site. *Mol Neurodegener,* **11,** 19.

Selkoe, D. J. (1991) The molecular pathology of Alzheimer's disease. *Neuron,* **6,** 487-498.

Selkoe, D. J. and Hardy, J. (2016) The amyloid hypothesis of Alzheimer's disease at 25 years. *EMBO Mol Med*.

Selkoe, D. J., Podlisny, M. B., Joachim, C. L., Vickers, E. A., Lee, G., Fritz, L. C. and Oltersdorf, T. (1988) Beta-amyloid precursor protein of Alzheimer disease occurs as 110- to 135-kilodalton membrane-associated proteins in neural and nonneural tissues. *Proceedings of the National Academy of Sciences of the United States of America,* **85,** 7341-7345.

Serano, R. D., Pegram, C. N. and Bigner, D. D. (1980) Tumorigenic cell culture lines from a spontaneous VM/Dk murine astrocytoma (SMA). *Acta neuropathologica,* **51,** 53-64.

Sergeant, N., Bombois, S., Ghestem, A. et al. (2003) Truncated beta-amyloid peptide species in pre-clinical Alzheimer's disease as new targets for the vaccination approach. *Journal of neurochemistry,* **85,** 1581-1591.

Sevalle, J., Amoyel, A., Robert, P., Fournie-Zaluski, M. C., Roques, B. and Checler, F. (2009) Aminopeptidase A contributes to the N-terminal truncation of amyloid beta-peptide. *Journal of neurochemistry,* **109,** 248-256.

Sevigny, J., Chiao, P., Bussiere, T. et al. (2016) The antibody aducanumab reduces Abeta plaques in Alzheimer's disease. *Nature,* **537,** 50-56.

Sharma, K., Schmitt, S., Bergner, C. G. et al. (2015) Cell type- and brain region-resolved mouse brain proteome. *Nature neuroscience,* **18,** 1819-1831.

Sherrington, R., Rogaev, E. I., Liang, Y. et al. (1995) Cloning of a gene bearing missense mutations in early- onset familial Alzheimer's disease. *Nature,* **375,** 754-760.

Sinha, S. and Lieberburg, I. (1999) Cellular mechanisms of beta-amyloid production and secretion. *Proceedings of the National Academy of Sciences of the United States of America,* **96,** 11049-11053.

Sisodia, S. S. (1992) Beta-amyloid precursor protein cleavage by a membrane-bound protease. *Proceedings of the National Academy of Sciences of the United States of America,* **89,** 6075-6079.

Skaper, S. D., Evans, N. A., Evans, N. A., Rosin, C., Facci, L. and Richardson, J. C. (2009) Oligodendrocytes are a novel source of amyloid peptide generation. *Neurochem Res,* **34,** 2243-2250.

Smolen, J. S. and Steiner, G. (2003) Therapeutic strategies for rheumatoid arthritis. *Nature reviews. Drug discovery,* **2,** 473-488.

Song, R. H., Tortorella, M. D., Malfait, A. M., Alston, J. T., Yang, Z., Arner, E. C. and Griggs, D. W. (2007) Aggrecan degradation in human articular cartilage explants is mediated by both ADAMTS-4 and ADAMTS-5. *Arthritis and rheumatism,* **56,** 575-585.

Song, S. K., Kim, J. H., Lin, S. J., Brendza, R. P. and Holtzman, D. M. (2004) Diffusion tensor imaging detects age-dependent white matter changes in a transgenic mouse model with amyloid deposition. *Neurobiology of disease,* **15,** 640-647.

Soriano, S., Kang, D. E., Fu, M., Pestell, R., Chevallier, N., Zheng, H. and Koo, E. H. (2001) Presenilin 1 Negatively Regulates beta-Catenin/T Cell Factor/Lymphoid Enhancer Factor-1 Signaling Independently of beta-Amyloid Precursor Protein and Notch Processing. *J Cell Biol,* **152,** 785-794.

Spires, T. L., Meyer-Luehmann, M., Stern, E. A., McLean, P. J., Skoch, J., Nguyen, P. T., Bacskai, B. J. and Hyman, B. T. (2005) Dendritic spine abnormalities in amyloid

precursor protein transgenic mice demonstrated by gene transfer and intravital multiphoton microscopy. *The Journal of neuroscience : the official journal of the Society for Neuroscience,* **25,** 7278-7287.

Sprinkle, T. J. (1989) 2',3'-cyclic nucleotide 3'-phosphodiesterase, an oligodendrocyte-Schwann cell and myelin-associated enzyme of the nervous system. *Critical reviews in neurobiology,* **4,** 235-301.

Stalder, M., Deller, T., Staufenbiel, M. and Jucker, M. (2001) 3D-Reconstruction of microglia and amyloid in APP23 transgenic mice: no evidence of intracellular amyloid. *Neurobiology of aging,* **22,** 427-434.

Stanton, H., Melrose, J., Little, C. B. and Fosang, A. J. (2011) Proteoglycan degradation by the ADAMTS family of proteinases. *Biochimica et biophysica acta,* **1812,** 1616-1629.

Stanton, H., Rogerson, F. M., East, C. J. et al. (2005) ADAMTS5 is the major aggrecanase in mouse cartilage in vivo and in vitro. *Nature,* **434,** 648-652.

Sun, B., Zhou, Y., Halabisky, B. et al. (2008) Cystatin C-cathepsin B axis regulates amyloid beta levels and associated neuronal deficits in an animal model of Alzheimer's disease. *Neuron,* **60,** 247-257.

Suzuki, N., Cheung, T. T., Cai, X. D., Odaka, A., Otvos, L. J., Eckman, C., Golde, T. E. and Younkin, S. G. (1994) An increased percentage of long amyloid beta protein secreted by familial amyloid beta protein precursor (beta APP717) mutants. *Science (New York, N.Y.),* **264,** 1336-1340.

Takami, M., Nagashima, Y., Sano, Y., Ishihara, S., Morishima-Kawashima, M., Funamoto, S. and Ihara, Y. (2009) {gamma}-Secretase: Successive Tripeptide and Tetrapeptide Release from the Transmembrane Domain of {beta}-Carboxyl Terminal Fragment. *The Journal of neuroscience : the official journal of the Society for Neuroscience,* **29,** 13042-13052.

Takeda, K., Araki, W., Akiyama, H. and Tabira, T. (2004) Amino-truncated amyloid beta-peptide (Abeta5-40/42) produced from caspase-cleaved amyloid precursor protein is deposited in Alzheimer's disease brain. *FASEB journal : official publication of the Federation of American Societies for Experimental Biology,* **18,** 1755-1757.

Tauchi, R., Imagama, S., Natori, T., Ohgomori, T., Muramoto, A., Shinjo, R., Matsuyama, Y., Ishiguro, N. and Kadomatsu, K. (2012) The endogenous proteoglycan-degrading enzyme ADAMTS-4 promotes functional recovery after spinal cord injury. *Journal of neuroinflammation,* **9,** 53.

Thal, D. R., Walter, J., Saido, T. C. and Fandrich, M. (2015) Neuropathology and biochemistry of Abeta and its aggregates in Alzheimer's disease. *Acta neuropathologica,* **129,** 167-182.

Tognatta, R. and Miller, R. H. (2016) Contribution of the oligodendrocyte lineage to CNS repair and neurodegenerative pathologies. *Neuropharmacology*.

Tomic, J. L., Pensalfini, A., Head, E. and Glabe, C. G. (2009) Soluble fibrillar oligomer levels are elevated in Alzheimer's disease brain and correlate with cognitive dysfunction. *Neurobiology of disease,* **35,** 352-358.

Tortorella, M. D., Malfait, F., Barve, R. A., Shieh, H. S. and Malfait, A. M. (2009) A review of the ADAMTS family, pharmaceutical targets of the future. *Curr Pharm Des,* **15,** 2359-2374.

Troeberg, L. and Nagase, H. (2012) Proteases involved in cartilage matrix degradation in osteoarthritis. *Biochimica et biophysica acta,* **1824,** 133-145.

Uhl, M., Aulwurm, S., Wischhusen, J. et al. (2004) SD-208, a novel transforming growth factor beta receptor I kinase inhibitor, inhibits growth and invasiveness and enhances

immunogenicity of murine and human glioma cells in vitro and in vivo. *Cancer research,* **64,** 7954-7961.

Ulery, P. G., Beers, J., Mikhailenko, I., Tanzi, R. E., Rebeck, G. W., Hyman, B. T. and Strickland, D. K. (2000) Modulation of beta-amyloid precursor protein processing by the low density lipoprotein receptor-related protein (LRP). Evidence that LRP contributes to the pathogenesis of Alzheimer's disease. *The Journal of biological chemistry,* **275,** 7410-7415.

Valenzuela, J. C., Heise, C., Franken, G., Singh, J., Schweitzer, B., Seidenbecher, C. I. and Frischknecht, R. (2014) Hyaluronan-based extracellular matrix under conditions of homeostatic plasticity. *Philos Trans R Soc Lond B Biol Sci,* **369**.

Van Dam, D. and De Deyn, P. P. (2011) Animal models in the drug discovery pipeline for Alzheimer's disease. *British journal of pharmacology,* **164,** 1285-1300.

Vassar, R., Bennett, B. D., Babu-Khan, S. et al. (1999) Beta-secretase cleavage of Alzheimer's amyloid precursor protein by the transmembrane aspartic protease BACE. *Science (New York, N.Y.),* **286,** 735-741.

Verghese, P. B., Castellano, J. M. and Holtzman, D. M. (2011) Apolipoprotein E in Alzheimer's disease and other neurological disorders. *The Lancet. Neurology,* **10,** 241-252.

Verma, P. and Dalal, K. (2011) ADAMTS-4 and ADAMTS-5: key enzymes in osteoarthritis. *J Cell Biochem,* **112,** 3507-3514.

Villemagne, V. L., Pike, K. E., Chetelat, G. et al. (2011) Longitudinal assessment of Abeta and cognition in aging and Alzheimer disease. *Annals of neurology,* **69,** 181-192.

Wagsater, D., Bjork, H., Zhu, C., Bjorkegren, J., Valen, G., Hamsten, A. and Eriksson, P. (2008) ADAMTS-4 and -8 are inflammatory regulated enzymes expressed in macrophage-rich areas of human atherosclerotic plaques. *Atherosclerosis,* **196,** 514-522.

Wagstaff, L., Kelwick, R., Decock, J. and Edwards, D. R. (2011) The roles of ADAMTS metalloproteinases in tumorigenesis and metastasis. *Frontiers in bioscience (Landmark edition),* **16,** 1861-1872.

Walsh, D. M., Klyubin, I., Fadeeva, J. V., Cullen, W. K., Anwyl, R., Wolfe, M. S., Rowan, M. J. and Selkoe, D. J. (2002) Naturally secreted oligomers of amyloid beta protein potently inhibit hippocampal long-term potentiation in vivo. *Nature,* **416,** 535-539.

Walsh, D. M. and Selkoe, D. J. (2007) A beta oligomers - a decade of discovery. *Journal of neurochemistry,* **101,** 1172-1184.

Walsh, D. M. and Teplow, D. B. (2012) Alzheimer's disease and the amyloid beta-protein. *Progress in molecular biology and translational science,* **107,** 101-124.

Walter, J., Capell, A., Hung, A. Y., Langen, H., Schnolzer, M., Thinakaran, G., Sisodia, S. S., Selkoe, D. J. and Haass, C. (1997) Ectodomain phosphorylation of beta-amyloid precursor protein at two distinct cellular locations. *J Biol Chem,* **272,** 1896-1903.

Wang, P., Tortorella, M., England, K., Malfait, A. M., Thomas, G., Arner, E. C. and Pei, D. (2004) Proprotein convertase furin interacts with and cleaves pro-ADAMTS4 (Aggrecanase-1) in the trans-Golgi network. *The Journal of biological chemistry,* **279,** 15434-15440.

Weber, C. and Noels, H. (2011) Atherosclerosis: current pathogenesis and therapeutic options. *Nature medicine,* **17,** 1410-1422.

Webster, S. J., Bachstetter, A. D., Nelson, P. T., Schmitt, F. A. and Van Eldik, L. J. (2014) Using mice to model Alzheimer's dementia: an overview of the clinical disease and the preclinical behavioral changes in 10 mouse models. *Frontiers in genetics,* **5,** 88.

Weggen, S. and Beher, D. (2012) Molecular consequences of amyloid precursor protein and presenilin mutations causing autosomal-dominant Alzheimer's disease. *Alzheimers Res Ther,* **4,** 9.

Weggen, S., Eriksen, J. L., Das, P. et al. (2001) A subset of NSAIDs lower amyloidogenic Abeta42 independently of cyclooxygenase activity. *Nature,* **414,** 212-216.

Weidemann, A., Konig, G., Bunke, D., Fischer, P., Salbaum, J. M., Masters, C. L. and Beyreuther, K. (1989) Identification, biogenesis, and localization of precursors of Alzheimer's disease A4 amyloid protein. *Cell,* **57,** 115-126.

Willem, M., Tahirovic, S., Busche, M. A. et al. (2015) eta-Secretase processing of APP inhibits neuronal activity in the hippocampus. *Nature,* **526,** 443-447.

Wiltfang, J., Esselmann, H., Cupers, P. et al. (2001) Elevation of beta-amyloid peptide 2-42 in sporadic and familial Alzheimer's disease and its generation in PS1 knockout cells. *The Journal of biological chemistry,* **276,** 42645-42657.

Wirths, O. and Bayer, T. A. (2012) Intraneuronal Abeta accumulation and neurodegeneration: lessons from transgenic models. *Life sciences,* **91,** 1148-1152.

Wirths, O., Multhaup, G., Czech, C., Feldmann, N., Blanchard, V., Tremp, G., Beyreuther, K., Pradier, L. and Bayer, T. A. (2002) Intraneuronal APP/A beta trafficking and plaque formation in beta-amyloid precursor protein and presenilin-1 transgenic mice. *Brain pathology (Zurich, Switzerland),* **12,** 275-286.

Wirths, O., Walter, S., Kraus, I. et al. (in press) N-truncated Aβ4-x peptides in sporadic Alzheimer's disease cases and transgenic Alzheimer mouse models. *Alzheimer's Research & Therapy*.

Wisniewski, K. E., Wisniewski, H. M. and Wen, G. Y. (1985) Occurrence of neuropathological changes and dementia of Alzheimer's disease in Down's syndrome. *Ann Neurol,* **17,** 278-282.

Wittnam, J. L., Portelius, E., Zetterberg, H. et al. (2012) Pyroglutamate amyloid beta (Abeta) aggravates behavioral deficits in transgenic amyloid mouse model for Alzheimer disease. *The Journal of biological chemistry,* **287,** 8154-8162.

Wolfe, M. S., Xia, W., Moore, C. L., Leatherwood, D. D., Ostaszewski, B., Rahmati, T., Donkor, I. O. and Selkoe, D. J. (1999) Peptidomimetic probes and molecular modeling suggest that Alzheimer's gamma-secretase is an intramembrane-cleaving aspartyl protease. *Biochemistry,* **38,** 4720-4727.

Xu, J., Chen, S., Ahmed, S. H., Chen, H., Ku, G., Goldberg, M. P. and Hsu, C. Y. (2001) Amyloid-beta peptides are cytotoxic to oligodendrocytes. *The Journal of neuroscience : the official journal of the Society for Neuroscience,* **21,** Rc118.

Yamamoto, K., Owen, K., Parker, A. E., Scilabra, S. D., Dudhia, J., Strickland, D. K., Troeberg, L. and Nagase, H. (2014) Low density lipoprotein receptor-related protein 1 (LRP1)-mediated endocytic clearance of a disintegrin and metalloproteinase with thrombospondin motifs-4 (ADAMTS-4): functional differences of non-catalytic domains of ADAMTS-4 and ADAMTS-5 in LRP1 binding. *The Journal of biological chemistry,* **289,** 6462-6474.

Yamamoto, K., Troeberg, L., Scilabra, S. D., Pelosi, M., Murphy, C. L., Strickland, D. K. and Nagase, H. (2013) LRP-1-mediated endocytosis regulates extracellular activity of ADAMTS-5 in articular cartilage. *FASEB journal : official publication of the Federation of American Societies for Experimental Biology,* **27,** 511-521.

Yuan, W., Matthews, R. T., Sandy, J. D. and Gottschall, P. E. (2002) Association between protease-specific proteolytic cleavage of brevican and synaptic loss in the dentate gyrus of kainate-treated rats. *Neuroscience,* **114,** 1091-1101.

Zha, Y., Chen, Y., Xu, F., Zhang, J., Li, T., Zhao, C. and Cui, L. (2010) Elevated level of ADAMTS4 in plasma and peripheral monocytes from patients with acute coronary syndrome. *Clinical research in cardiology : official journal of the German Cardiac Society,* **99,** 781-786.

Zhang, Y., Chen, K., Sloan, S. A., Bennett, M. L., Scholze, A. R., O'Keeffe, S., Phatnani, H. P. and Guarnieri, P. (2014) An RNA-sequencing transcriptome and splicing database of glia, neurons, and vascular cells of the cerebral cortex. **34,** 11929-11947.

Zhang, Z., Song, M., Liu, X. et al. (2015) Delta-secretase cleaves amyloid precursor protein and regulates the pathogenesis in Alzheimer's disease. *Nature communications,* **6,** 8762.

Zhao, W. Q., De Felice, F. G., Fernandez, S., Chen, H., Lambert, M. P., Quon, M. J., Krafft, G. A. and Klein, W. L. (2008) Amyloid beta oligomers induce impairment of neuronal insulin receptors. *FASEB journal : official publication of the Federation of American Societies for Experimental Biology,* **22,** 246-260.

Zimmermann, D. R. and Dours-Zimmermann, M. T. (2008) Extracellular matrix of the central nervous system: from neglect to challenge. *Histochemistry and cell biology,* **130,** 635-653.

Acknowledgements

First of all, I would like to thank Prof. Dr. Sascha Weggen for giving me the opportunity to perform my PhD thesis in his laboratory and for supporting me during the course of my project.

I wish to thank Prof. Dr. Lutz Schmitt for agreeing to be my mentor and second supervisor.

I want to express my gratitude to the whole Institute of Neuropathology for the pleasant working atmosphere and help with all of my questions. Especially all current and former members of my working group: Maxi Faust, Parul Goel, Thorsten Jumpertz, Vanessa Kurth, Sandra Lehmann, Isabella Ogorek, and Julia Seegel.

Furthermore, I thank our collaborative partners: Dr. Oliver Wirths for handling the transgenic mice and performing immunostainings as well as providing me with Aβ peptides and antibodies, Dr. Patrick Fraering, Hermeto Gerber, and Mitko Dimitrov for the Aβ immunoprecipitation and mass spectrometry analyses, and Dr. Carsten Berndt and Klaudia Lepka for teaching me how to prepare OPC cultures and providing me with samples and supplies.

Finally, special thanks to my whole family and friends for constant encouragement and caring support.